PNL-4530
Vol. 2 of 2
UC-70

A Systems Study of the Feasibility of High-Level Nuclear Waste Fractionation for Thermal Stress Control in a Geologic Repository

Appendices

R. W. McKee
H. K. Elder
R. F. McCallum
D. J. Silviera
J. L. Swanson
L. E. Wiles

June 1983

Prepared for the U.S. Department of Energy
under Contract DE-AC06-76RLO 1830

Pacific Northwest Laboratory
Operated for the U.S. Department of Energy
by Battelle Memorial Institute

Battelle

PNL-4530

DISCLAIMER

This report was prepared as an account of work sponsored by an agency of the United States Government. Neither the United States Government nor any agency thereof, nor any of their employees, makes any warranty, express or implied, or assumes any legal liability or responsibility for the accuracy, completeness, or usefulness of any information, apparatus, product, or process disclosed, or represents that its use would not infringe privately owned rights. Reference herein to any specific commercial product, process, or service by trade name, trademark, manufacturer, or otherwise, does not necessarily constitute or imply its endorsement, recommendation, or favoring by the United States Government or any agency thereof. The views and opinions of authors expressed herein do not necessarily state or reflect those of the United States Government or any agency thereof.

PACIFIC NORTHWEST LABORATORY
operated by
BATTELLE
for the
UNITED STATES DEPARTMENT OF ENERGY
under Contract DE-AC06-76RLO 1830

Printed in the United States of America
Available from
National Technical Information Service
United States Department of Commerce
5285 Port Royal Road
Springfield, Virginia 22161

NTIS Price Codes
Microfiche A01

Printed Copy

Pages	Price Codes
001-025	A02
026-050	A03
051-075	A04
076-100	A05
101-125	A06
126-150	A07
151-175	A08
176-200	A09
201-225	A010
226-250	A011
251-275	A012
276-300	A013

3 3679 00059 0325

PNL-4530
Vol. 2 of 2
UC-70

A SYSTEMS STUDY OF THE FEASIBILITY OF HIGH-LEVEL NUCLEAR WASTE FRACTIONATION FOR THERMAL STRESS CONTROL IN A GEOLOGIC REPOSITORY

APPENDICES

R. W. McKee
H. K. Elder
R. F. McCallum
D. J. Silviera
J. L. Swanson
L. E. Wiles

June 1983

Prepared for
the U.S. Department of Energy
Under Contract DE-AC06-76RLO 1830

Pacific Northwest Laboratory
Richland, Washington 99352

REPORT CONTENTS OUTLINE

CONTENTS

FIGURES

TABLES

APPENDIX A

THERMAL ANALYSIS SUPPLEMENT

This appendix contains additional details of the thermal analysis procedures described in Chapter 3, Volume 1 of this report. This work is subdivided into six sections: Section A.1 provides details on the assumptions and calculational procedures used; Section A.2 describes the results of sensitivity analyses carried out to check the validity of key assumptions; Section A.3 provides supplementary details for the reference basalt case; Section A.4 provides supplementary details for the parametric analyses; Section A.5 presents details of the salt repository calculations; and Section A.6 presents details of the horizontal borehole calculations.

A.1 ASSUMPTIONS AND PROCEDURES

The physical dimensions of the repository and waste package are described by the near-field and very-near-field models. The "infinite-field" is an extension of the near-field to an infinite canister and room pitch. Basic dimensions defining the repository and waste package design were taken from Westinghouse (1981a) for a repository in basalt and from Westinghouse (1981b) for a repository in salt.

A.1.1 Near-Field Description

Because of symmetry in the room and pillar construction of the repository, only a quarter section of the region of influence of a single canister needed to be considered for the near-field model. All vertical boundaries around the modeled section were adiabatic. The top and bottom boundaries of the near-field region were isothermal, allowing passage of geothermal energy. The top and bottom boundaries were 200 m from the corridor floor, far enough to assure that they remained isothermal throughout the simulation period.

Significant dimensions of the near-field are shown in Figure A.1 for a repository in basalt. The canister pitch, P, is the distance between adjacent canisters along the corridor centerline. The corridor pitch (or room pitch), which is the distance between adjacent corridors, is 23.5 m.

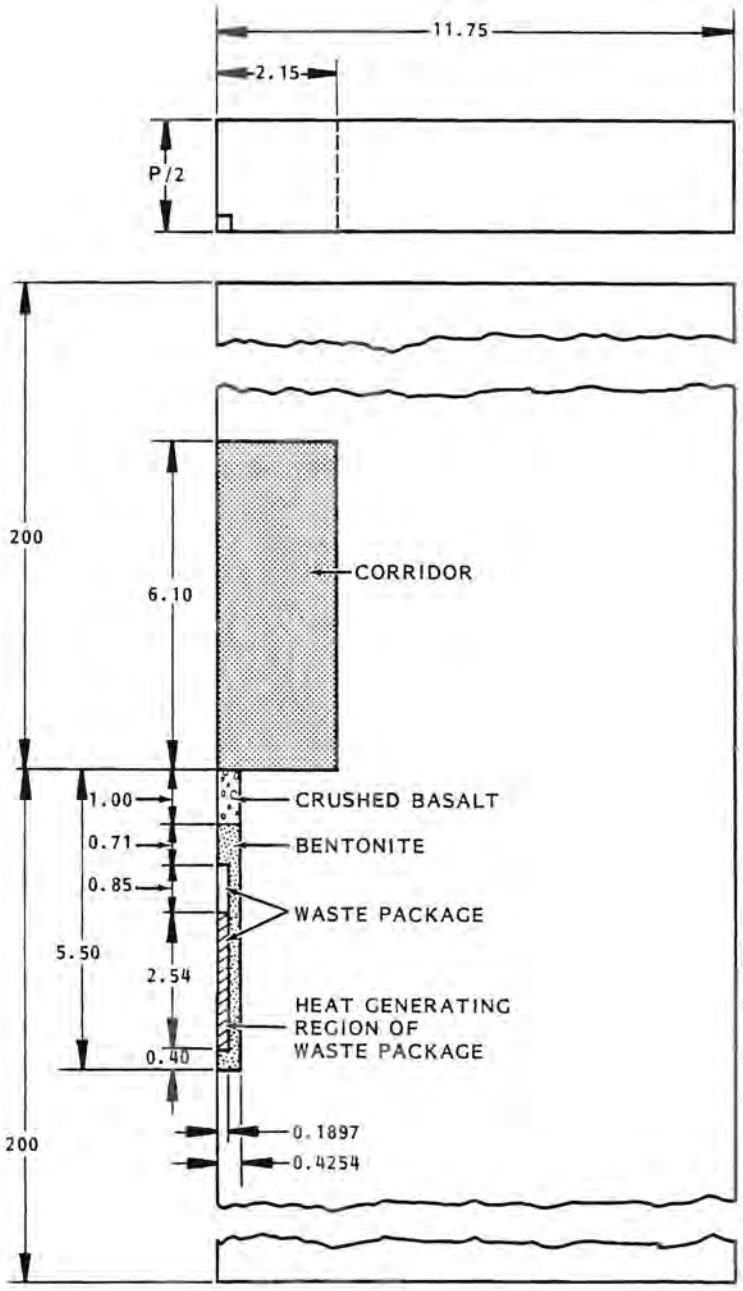

FIGURE A.1. Near-Field Geometry for HLW Emplacement in Basalt (dimensions in meters)

The details of the waste package were substantially distorted in the near-field model. Because the near-field is modeled in Cartesian coordinates, the quadrant of the waste package was represented by a square region that preserved the volume in the transformation. To an observer at a moderate distance, the waste package would appear as a homogeneous source due to the high conductivity of the canister and overpack. Thus, the volume of material including the waste glass, canister, overpack, liner, and air volumes was merged together. This homogenized waste package was used to define the waste package dimensions and material properties in the near-field. As indicated in Figure A.1, only the bottom 3/4 (approximately) of the waste package was defined to be heat generating.

The near-field grid is given in Table A.1. The I, J, and K are indices of the finite-difference cells in the x-, y-, and z-directions, respectively. The horizontal x-direction is perpendicular to the centerline of the corridor. The horizontal v-direction is parallel to the centerline of the corridor. The grid in Table A.1 is defined for a canister pitch of 3.6 m, which applied to the reference HLW repository in basalt. This grid data typified the detail of grids written for other values of canister pitch. The symmetry in the I and J directions is beneficial to selecting temperatures for the very-near-field solution.

A.1.2 Very-Near-Field Description

The very-near-field solution employed a detailed one-dimensional (radical) grid representing the waste package and surrounding host rock. A cross section of the region is shown in Figure A.2. This particular cross section applies to the reference HLW package in basalt, with a canister diameter of 0.304 m (1 ft). For other canister diameters, the annular dimensions of the waste package components remained constant. The radial dimensions of a waste package for a repository in salt are very similar. The differences for salt are that the air gap between the canister and overpack was specified as 1.3 cm, the overpack thickness was 6.0 cm and the crushed backfill annular space was 2.25 cm. For a 1-ft-diameter canister in salt, the hole diameter was 52 cm.

In basalt the emplacement hole designs for HLW, aged-HLW, and FHLW included a preformed bentonite and crushed basalt backfill having an annular

TABLE A.1. Near-Field Grid (dimensions in meters)

Perpendicular to Corridor			Parallel to Corridor			Vertical		
I	Δx	$\Sigma\Delta x$	J	Δy	$\Sigma\Delta y$	K	Δz	$\Sigma\Delta z$
1	--	--	1	--	--			
2	0.1897	0.1897	2	0.1897	0.1897			
3	0.2657	0.4254	3	0.2357	0.4254			
4	0.2246	0.6500	4	0.2246	0.6500	27	--	--
5	0.3000	0.9500	5	0.3000	0.9500	26	80	400
6	0.45	1.40	6	0.45	1.40	25	50.0	320.0
7	0.75	2.15	7	0.20	1.60	24	30.0	270.0
8	1.10	3.25	8	0.20	1.80	23	17.0	240.0
9	1.75	5.00	9	--	--	22	10.0	223.0
10	2.50	7.50				21	4.5	213.0
11	4.25	11.75				20	2.4	208.5
12	--	--				19	2.1	206.1
						18	2.5	204.0
						17	1.5	201.5
						16	1.0	200.0
						15	0.71	199.00
						14	0.85	198.29
						13	0.82	197.44
						12	0.80	196.62
						11	0.92	195.82
						10	0.4	194.9
						9	1.0	194.5
						8	2.0	193.5
						7	4.5	191.5
						6	10.0	187.0
						5	17	177
						4	30	160
						3	50	130
						2	80	80
						1	--	--

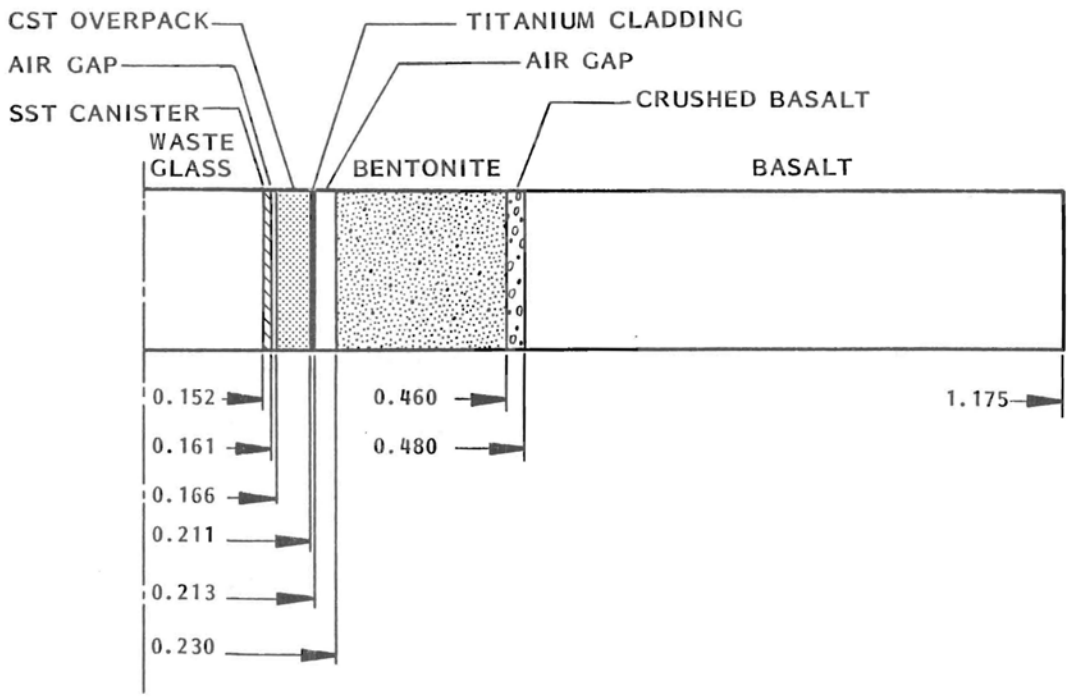

FIGURE A.2. Very-Near-Field Geometry for HLW Emplacement in Basalt (dimensions in meters)

thickness of 0.230 m (9.0 in.). For Cs/Sr in basalt and for all the waste forms in salt, the bentonite and titanium liner were not included. For those cases the annular space between the outside surface of the waste package and the borehole wall, a distance of 2 cm, was filled with a finely crushed host rock. The grid for the very-near-field is given in Table A.2. The outer radius of the grid is 1.175 m, and this corresponds to the location of the nodes in cells I=2, J=5, and I=5, J=2 from the near-field grid, Table A.1. It was those nodal temperatures, at a value of K=12, that were used as a boundary temperature for the very-near-field solution.

A.1.3 Infinite-Field Description

The infinite field model was written to define the minimum temperatures that would occur for a given waste package design; that is, an increase in canister pitch or room pitch would not result in lower temperatures because the waste package was placed in an effectively infinite media.

TABLE A.2. Very-Near-Field Grid (dimensions in meters)

Material	I	Δr	ΣΔr
--	1	--	--
Waste Glass	2	0.02	0.02
Waste Glass	3	0.03	0.05
Waste Glass	4	0.04	0.09
Waste Glass	5	0.03	0.12
Waste Glass	6	0.0200	0.1400
Waste Glass	7	0.0120	0.1520
SST Canister	8	0.0095	0.1610
Air Gap	9	0.0050	0.1665
CST Overpack	10	0.02225	0.18875
CST Overpack	11	0.02225	0.2110
Titanium Liner	12	0.0025	0.2135
Air Gap	13	0.0165	0.2300
Bentonite	14	0.0200	0.2500
Bentonite	15	0.0300	0.2800
Bentonite	16	0.065	0.345
Bentonite	17	0.065	0.410
Bentonite	18	0.030	0.440
Bentonite	19	0.020	0.460
Crushed Basalt	20	0.020	0.480
Undisturbed Basalt	21	0.02	0.50
Undisturbed Basalt	22	0.03	0.53
Undisturbed Basalt	23	0.05	0.58
Undisturbed Basalt	24	0.08	0.66
Undisturbed Basalt	25	0.12	0.78
Undisturbed Basalt	26	0.16	0.040
Undisturbed Basalt	27	0.235	1.175
--	28	--	--

The infinite-field model was based on a two-dimensional, cylindrical geometry. Significant features of the model are shown in Figure A.3. The grid is given in Table A.3. This grid was written for the reference HLW in basalt. Changes were required to accommodate other conditions; in particular, those cases which did not require the bentonite backfill.

One notable distortion in the infinite-field model was the simulation of the corridor. It was modeled as a closed cylindrical room above the waste package rather than a long, rectangular room. Since the peak waste package

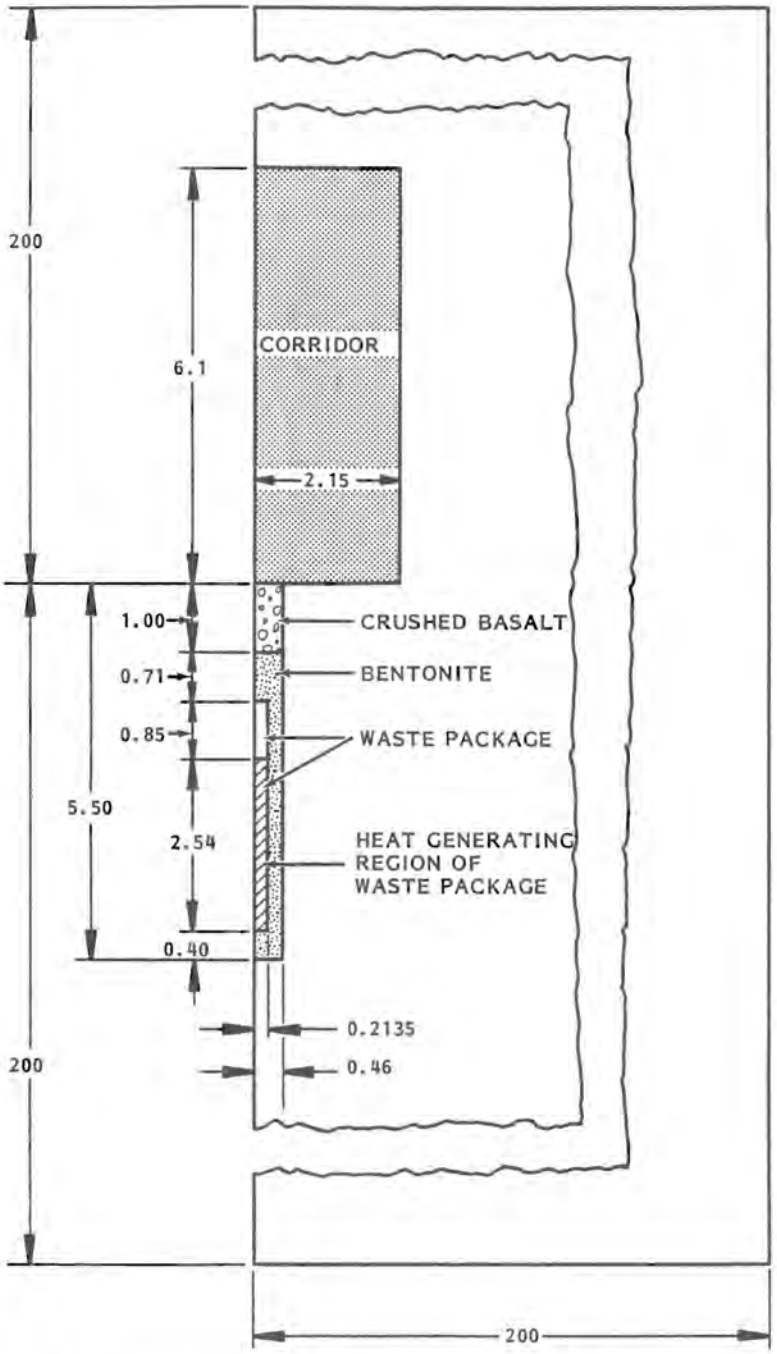

FIGURE A.3. Infinite-Field Geometry for HLW Emplacement in Basalt (dimensions in meters)

TABLE A.3. Infinite-Field Grid (dimensions in meters)

Radial			Vertical		
I	Δr	$\Sigma \Delta r$	K	Δz	$\Sigma \Delta z$
1					
2	0.2135	0.2135			
3	0.2465	0.4600			
4	0.34	0.80	27		
5	0.50	1.30	26	80	400
6	0.85	2.15	25	50.0	320.0
7	1.35	3.50	24	30.0	270.0
8	2.50	6.00	23	17.0	240.0
9	4.00	10.0	22	10.0	223.0
10	6.00	16.00	21	4.5	213.0
11	9	25	20	2.4	208.5
12	15	40	19	2.1	206.1
13	25	65	18	2.5	204.0
14	45	110	17	1.5	201.5
15	90	200	16	1.0	200.0
16	--	--	15	0.71	199.0
			14	0.85	198.29
			13	0.82	197.44
			12	0.80	196.62
			11	0.92	195.82
			10	0.4	194.9
			9	1.0	194.5
			8	2.0	193.5
			7	4.5	191.5
			6	10.0	187.0
			5	17	177
			4	30	160
			3	50	130
			2	80	80
			1	--	--

temperatures were not strongly dependent on the corridor thermal model, this provided an acceptable, simplified means to model the corridor in the axisymmetric geometry.

Another notable point is that the infinite-field model not only models the canister pitch as infinite, but the room pitch is also infinite. Thus, the temperatures predicted by the infinite-field model are lower than those that would be predicted by the near-field model if the canister pitch were increased to a very large value while the room pitch remained constant. This effect was acceptable, however, because the infinite-field analysis was performed only to place a lower bound on temperatures. The infinite-field model provided a very economical means for obtaining such results because it was two-dimensional. The alternative, which was to use the near-field model to effect an infinite canister pitch, would have required an additional 324 computational cells for each cell added in the direction parallel to the corridor. Extending the near-field model to a very large pitch would have been more costly than use of the infinite-field model and may have caused some troubles with computer memory capacity.

A.1.4 Material Properties

The materials described for the heat transfer model generally fall into one of two categories: earth materials and waste package materials. The thermal properties required for the heat transfer analysis are given in this section.

The earth materials required in the analysis were basalt and salt. Crushed basalt and crushed salt were also required as backfills. The thermal properties are given in Table A.4. The thermal conductivities are all temperature dependent. The equations used to calculate the thermal conductivities are

TABLE A.4. Thermal Properties of Earth Materials

Material	Thermal Conductivity, W/m-°C	Density, kg/m^3	Specific Heat, J/kg °C
Basalt	$0.76 + 0.0039 \times T$	2900	940
Crushed Basalt	$0.17 + 0.011 \times T$	1510	940
Salt	$5\ (300/(T + 273))^{1.14}$	2130	920
Crushed Salt	$0.70 - 0.0007 \times T$	1110	920

given in the table. The thermal conductivity of basalt fit data provided by Altenhofen (1981). The thermal conductivity of salt was reported by Sweet (1980). For each of these equations, the temperature was required in °C.

The effective thermal conductivity of the crushed materials was based on a model of conduction and radiation heat transfer through packed, equal-size spheres. The method used to estimate the effective conductivity was similar to that described by Crane and Vachon (1977).

The waste package materials included the waste glass, stainless steel canister, carbon steel overpack, titanium liner, and the bentonite backfill. In addition, assembly gaps for air were included. The thermal properties of these materials are given in Table A.5. All temperature-dependent property equations require a temperature in °C. The effective conductivity across the gap requires a gap thickness, Δx, in meters. The waste glass properties were obtained from Taylor, Groot, Shoemaker (1979).

The thermal properties assigned in Table A.5 are generally accepted, except for the properties of bentonite. In particular, the conductivity of bentonite is not well-established. Reported values have ranged from 0.33 W/m-°C (Westinghouse 1981a) to 1.26 W/m-°C (Altenhofen 1981). Higher values can be achieved, depending on the water content and secondary constituents. While a lower value is conservative, it is also unrealistic. It places such prohibitive thermal constraints on the waste package that its use would most certainly not be tolerated. Therefore, based on available data, a value of 0.75 W/m-°C was considered achievable and was used in this analysis.

The effective conductivity of the air gaps was written to include components due to radiation and conduction. In Table A.5 the first term in the equation for the effective conductivity of the gap is the radiation component. The coefficient was calculated from:

$$\frac{4\sigma}{\frac{1}{\varepsilon_{SST}} + \frac{1}{\varepsilon_{CST}} - 1} = 1.5 \times 10^{-7}$$

TABLE A.5. Thermal Properties of Waste Package Materials

Material	Thermal Conductivity, W/m-°C	Density, kg/m^3	Specific Heat, J/kg °C
Waste Glass	$0.885 + 0.00043 \times T$	Density x Specific Heat $= 1.8 \times 10^6 + 4.0 \times 10^3 \times T$ J/m^3 °C	
Stainless Steel	16.4	7823	460
Carbon Steel	45.0	7855	460
Titanium	17.1	4921	836
Bentonite	0.75	2100	840
Air Gap	$1.5 \times 10^7 \times (T + 273)^3 \times \Delta x + 0.024 + 6.9 \times 10^{-5} \times T$	1.2	1000
Merged Homogeneous Waste Package	10	Density x Specific Heat $= 2.7 \times 10^6$ J/m^3 °C	

where σ is the Stefan-Boltzman constant: 5.67×10^{-8} W/m°-K^4. The emissivities of both stainless steel and carbon steel were defined to be 0.8. The second term in the equation for the effective conductivity of the gap is an approximation for the thermal conductivity of air.

The thermal properties of the individual components of the waste package were applied only in the very-near-field model. In the near-field model the waste package was treated as a homogeneous waste package. These thermal properties are also given in Table A.5. The thermal properties were derived by evaluating appropriate weighted averages. Subsequent analysis verified that the thermal response of the waste package, as predicted from the very-near-field model, was not strongly dependent on the thermal properties assigned to the homogeneous waste package, thus offering a significant simplification.

A.1.5 Repository Operational Scenario

The calculations were made assuming the repository was loaded instantaneously, a condition that yields symmetry and permits a thermal solution of the near-field with one quadrant of a waste package. The initial ambient temperature distribution was determined from the geothermal gradient and an assigned temperature at repository depth. The waste package was assumed to be at the ambient temperature to begin the simulation. The canisters were loaded on a uniform pitch in vertical boreholes along the centerline of the corridor. The minimum pitch was set at 2-1/2 times the borehole diameter.

Following the loading of the repository, the corridor was assumed to be unventilated. In the basalt cases, the corridor remained open throughout the simulation period. For the salt cases, the corridor was backfilled with crushed salt after 5 years. The corridor backfill was added instantaneously at the existing corridor temperature.

A.1.6 Computational Procedure

The computational procedure for each simulation required the solution for both the near-field, or an infinite-field, and the very-near-field. These solutions were developed sequentially as follows: One time step was executed in the near-field. Then, selected temperatures from the near-field were used to define a boundary temperature for the very-near-field. Next, one identical

time step was executed for the very-near-field transient simulation. Then, for the next time step, this procedure was repeated. The simulation continued sequentially in this fashion until the temperature in the host rock and the waste package components had peaked. In the very-near-field model, temperatures were interpolated between node points so that peak temperatures were taken from the inside annular boundary of the component. Therefore, the reported peak temperatures are the actual computed peak temperatures. For example, the peak temperature of the canister occurs at the inside surface of the canister, not in the middle of the computational cell representing the canister.

A.2 SENSITIVITY ANALYSIS OF SELECTED ASSUMPTIONS

A number of the modeling assumptions used in this study were the subject of brief sensitivity analyses. This was done to evaluate the discrepancies incurred in the predicted peak temperatures of the waste package and host rock as a result of these assumptions. Potential discrepancies were acceptable, for the most part, because of the comparative nature of the results; that is, each parametric case was subject to similar discrepancy. The comparison between cases was, therefore, not particularly sensitive to the discrepancy.

A.2.1 Very-Near-Field Simulation

The peak temperatures of the waste package components and the host rock were obtained by coupling a selected temperature from the near-field as a boundary condition for a 1-D radial very-near-field model. This conservative approximation of the very-near-field as a 1-D radial heat transfer problem had the most impact on the temperature solution of all the assumptions discussed in this section. The potential discrepancy associated with the use of the 1-D model was tolerated because the alternative was a full 3-D model that coupled the near-field and very-near-field with an array of selected temperatures. Such a model was used in the study by McCallum (1982), but would have been too costly for the number of calculations required in this study.

For the 1-D approximation to be accurate the waste package must appear to be an infinitely long cylinder with uniform heat generation, a condition that is approached as an observer moves closer to the waste package at its

mid-plane. On the other hand, as an observer moves away from the waste package, the heat generation would, at some point, approximate a point source. In practice, the point of coupling of the near-field and very-near-field lies between these two conditions. The point of coupling cannot be moved closer to the waste package in the near-field without affecting the accuracy of the predicted temperature used for the boundary condition in the very-near-field. The reduced accuracy occurs because of the distortion of the waste package in the near-field model. As the point of coupling is moved away from the waste package, the 1-D radial approximation of the very-near-field is increasingly less accurate because the heat transfer includes a spherical component. Thus, it is necessary to select the coupling temperature at some reasonable distance from the waste package.

Two semi-quantitative measures of the effect of the 1-D approximation on the predicted temperatures were available. The first was a comparison of the results for the conditions given in McCallum (1982) for HLW emplacement in salt. Using the present model with a 1-D very-near-field, the peak temperatures of the waste package components and host rock were about 30°C higher than those given in McCallum. The difference was not entirely attributable to the difference in the very-near-field model. For example, the corridor model used in the present analysis was thermally less conductive, which contributed to higher waste package temperatures. The second measure of the effect of the 1-D approximation of the very-near-field dealt with the bulk waste package temperature. In the near-field model, the homogenized waste package was characterized by the temperature at the mid-plane of the heat-generating region. In the very-near-field model, the thermal energy of the components of the waste package was integrated to develop a comparative bulk waste package temperature. For the reference HLW conditions for a repository in basalt, the bulk waste package temperature from the near-field model was 249°C, at 5 years after emplacement. The integrated bulk waste package temperature from the very-near-field model was 267°C. This difference is typical of the results for the other cases. The lower temperature from the near-field model resulted, in part, because the model permits heat transfer in three dimensions.

These comparisons indicated that the application of the 1-D very-near-field model introduces a moderate discrepancy. Since each parametric case generally incurred similar accuracy, the comparison of the results was not significantly influenced by the assumption. Also, it should be noted that the assumption was conservative, resulting in somewhat higher temperatures than would be predicted by a more elaborate multidimensional model.

A.2.2 Corridor Heat Transfer

In this analysis the heat transfer in the corridor was based on the temperature-dependent thermal conductivity of air at atmospheric pressure. At 100°C the conductivity of air is about 0.03 W/m-°C. In reality, the heat transfer in the corridor will be controlled by radiation and convection. The effective thermal conductivity will be considerably higher than that for air. To measure the effect of this modeling assumption on the results of the thermal analysis, the reference case for HLW emplacement in basalt was evaluated using an artificial corridor conductivity of 10.0 W/m-°C, certainly an upper bound. This decreased the peak temperatures in the waste package components and host rock by about 7°C. The peak temperatures are compared in Table A.6.

TABLE A.6. Peak Temperatures (in °C) of Waste Package Components for Different Values of Corridor Thermal Conductivity (reference HLW in basalt)

Component	Thermal Conductivity (W/m-°C) ~0.3 (air)	10.0
Waste Glass	295	289
Canister	265	259
Titanium	253	246
Bentonite	243	235
Basalt	187	178

Considering the apparent small impact of this effect, a more rigorous corridor heat transfer model including convection and radiation was not justified. In consideration of the number of parametric computations required, the potential discrepancy was considered acceptable.

A second modeling assumption for the corridor dealt with the backfill closure of the corridor for the reference cases in salt. For a repository in salt the corridor may have to be backfilled relatively soon after emplacement due to deformation of the salt. In this analysis the backfill was to occur 5 years after emplacement. The reference cases in salt were analyzed without taking this into account. Rather than repeating all of the computations, a single case was executed to determine the impact on the results. It was found that due to the higher thermal conductivity of the backfill, relative to air, the temperatures of the waste package components increased only slightly from their values at the time of backfill. The result was that there was very little difference in the peak temperatures of the waste glass between the cases of no backfill and backfill at 5 years after emplacement. This occurred because the peak temperature in the waste glass had nearly been obtained at the time of backfill. The maximum difference was 5°C in the salt, which was the last material to reach a peak temperature. Because the salt reaches a peak temperature several years after backfill, the presence of the backfill has more time to influence this temperature. The results are compared in Table A.7.

TABLE A.7. Peak Temperatures (in °C) of Waste Package Components With and Without Corridor Closure (reference HLW in salt)

Component	Corridor Open	Corridor Closed at 5 Years After Emplacement
Waste Glass	330	328
Canister 274	269	
Titanium 249	244	
Salt 232	227	

The discrepancy incurred by not backfilling the corridor was not uniformly distributed between the various reference cases. For the aged-HLW the peak temperatures occur later than for HLW, while for FHLW the peak temperatures occur earlier. Thus, the aged-HLW cases were affected most by not backfilling, while the FHLW cases were affected the least. Nevertheless, the total discrepancy was not considered to be significant to the results of this study and the reference cases were not repeated to correct for the corridor backfill.

A.2.3 Homogenized Waste Package Conductivity

In the near-field model the waste package components were homogenized into a single material. This homogenized waste package comprised four computational cells. The lower three cells were defined to be heat generating. The four cells of the waste package were assigned a thermal conductivity of 10.0 W/m-°C. This value was an approximation, at best. Because of the air gaps and the low conductivity of the waste glass, the waste package will, in practice, exhibit some anisotropy in its apparent thermal conductivity. However, because of the high thermal resistance of the surroundings, an observer at some distance from the waste package could not distinguish this detail. Therefore, the assignment of a constant homogeneous value of conductivity was appropriate in the near-field model.

An analysis was done to define the sensitivity of the results to the value of thermal conductivity assigned to the homogeneous waste package. A value of 1.0 W/m-°C was used for comparison. This value is approximately the conductivity of the waste glass and possibly represents a lower bound. For the reference case of HLW emplacement in salt, the lower thermal conductivity of the homogenized waste package resulted in peak temperatures in the waste package components that were about 2°C greater than for the higher value of conductivity. Thus, the results apparently were not significantly affected by the choice of thermal conductivity of the homogenized waste package. The temperatures are compared in Table A.8. The canister pitch used to obtain these results was 2.48 m.

TABLE A.8. Peak Temperatures (in °C) of Waste Package Components for Different Values of Thermal Conductivity of the Homogenized Waste Package (reference HLW in salt)

	Thermal Conductivity (W/m-°C)	
Component	1.0	10.0
Waste Glass	353	352
Canister	300	298
Titanium	279	277
Salt	261	259

A.2.4 Canister Active Length

In this analysis the active length, or fill level, of the canister was defined to be 8.0 ft (2.44 m). In Westinghouse (1981b) the active length was defined to be 2.63 m. A longer active length effectively distributes a given amount of heat over a greater volume, resulting in lower temperatures.

For the reference case of HLW emplacement in a repository in salt, the active length of 2.63 m resulted in temperatures that were lower by 11°C in the waste glass and 4°C in the salt, as compared to the results for an active length of 2.44 m. The results are compared in Table A.9. The results were obtained for a canister pitch of 2.48 m.

TABLE A.9. Peak Temperatures (in °C) of Waste Package Components for Different Values of Canister Active Length (reference HLW in salt)

Component	Active Length (m)	
	2.44	2.63
Waste Glass	352	341
Canister	298	291
Titanium	277	271
Salt	259	255

A.3 SUPPLEMENTARY REFERENCE BASALT CASE RESULTS

The results of the analysis of the reference cases in basalt are presented in this section. Reference case results were developed for each waste form. The design conditions for the reference cases are presented in Section 3.2 of Chapter 3 (Volume 1). Fundamental reference design parameters include a canister diameter of 1 ft and a canister pitch of 3.6 m. For the HLW, aged-HLW, and FHLW, the initial canister heat load was 1 kW. The waste package design for these three waste forms included a bentonite backfill. For Cs/Sr, the initial canister heat load was 2.0 kW, and there was no bentonite backfill.

Figures A.4 through A.7 are temperature histories showing the maximum temperature in the respective components as a function of time. Figures A.8 through A.11 show the radial temperature profiles through the waste package and

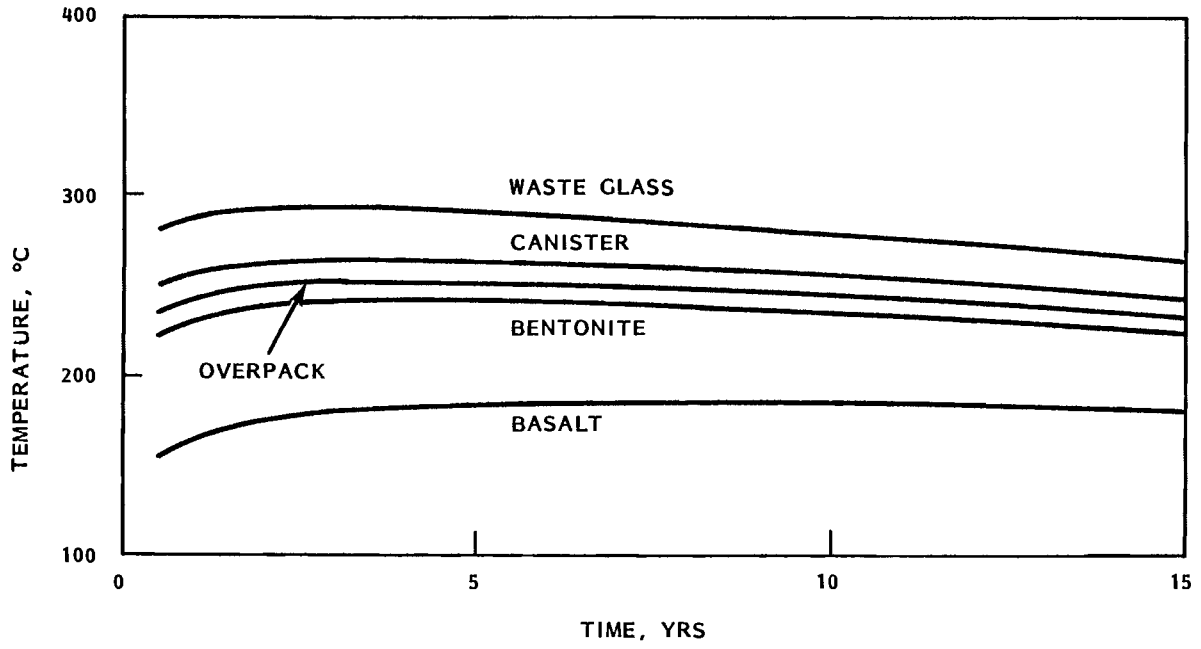

FIGURE A.4. Temperature Histories for Reference HLW Cases in Basalt

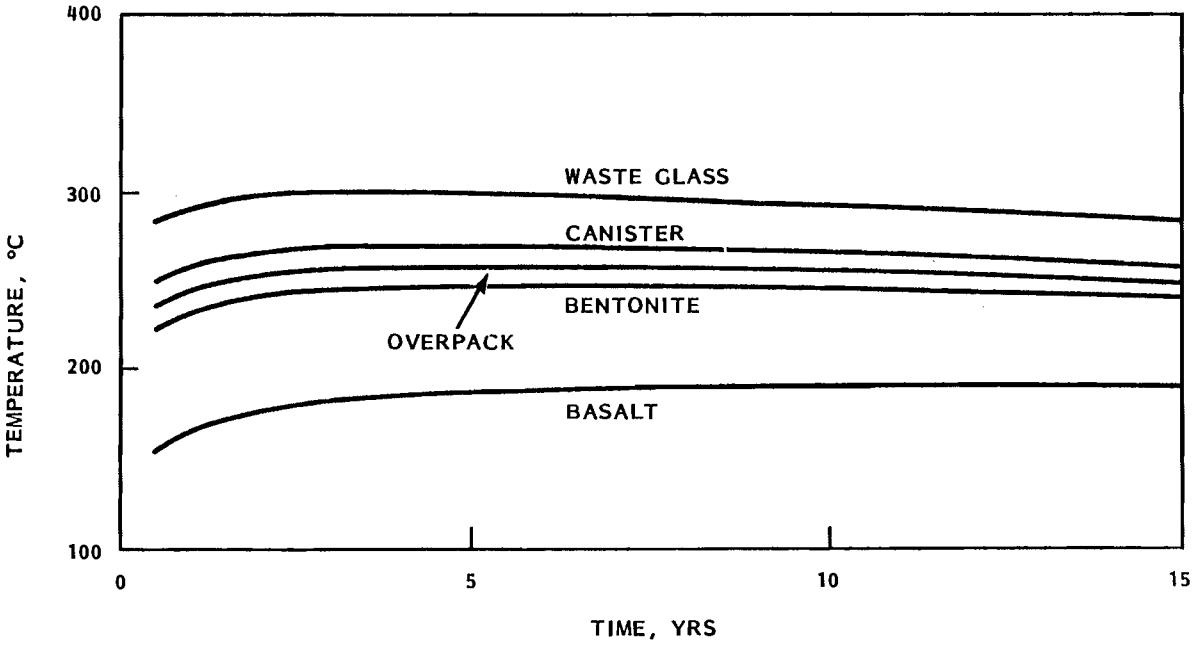

FIGURE A.5. Temperature Histories for Reference Aged-HLW Cases in Basalt

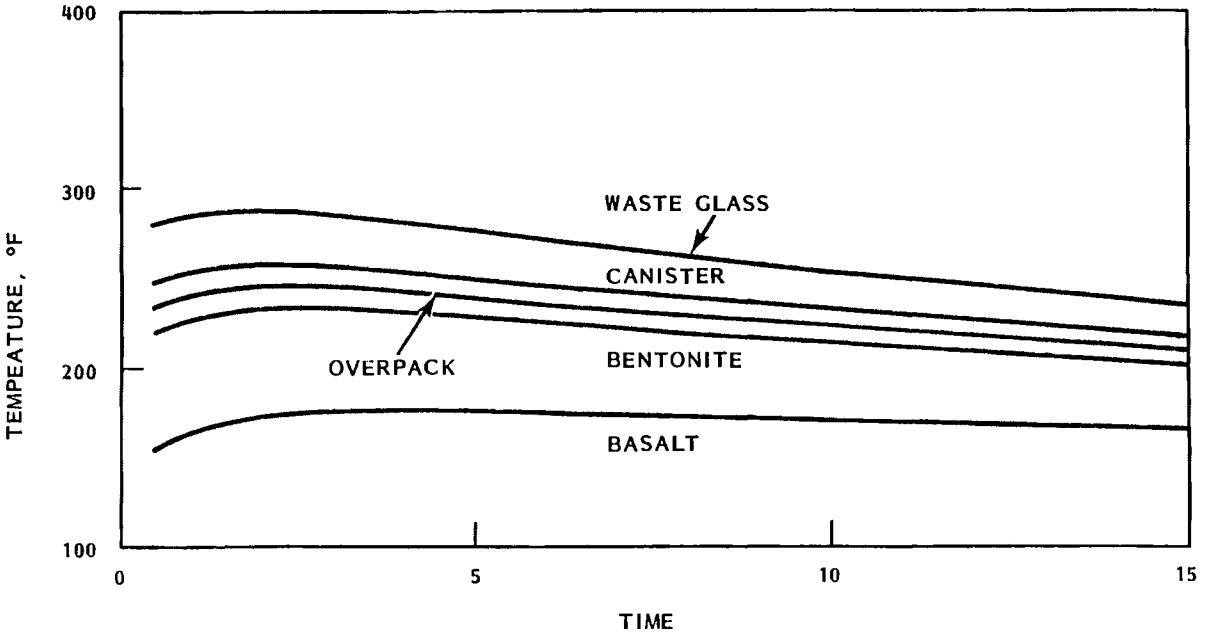

FIGURE A.6. Temperature Histories for Reference FHLW Cases in Basalt

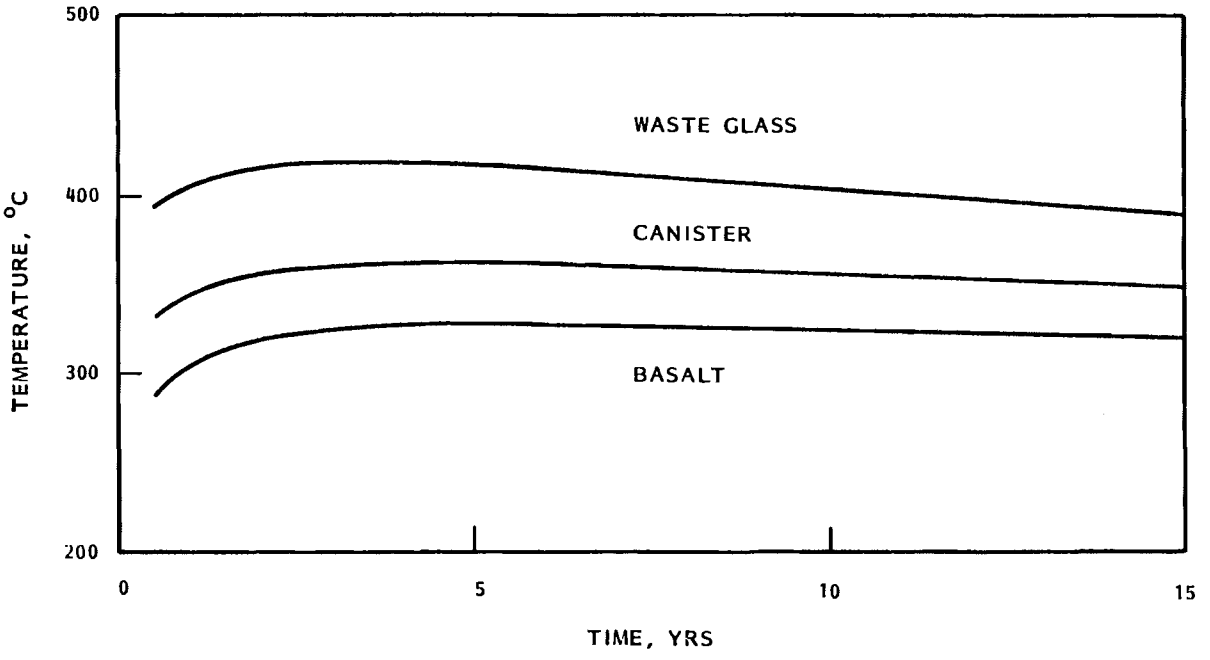

FIGURE A.7. Temperature Histories for Reference Cs/Sr Cases in Basalt

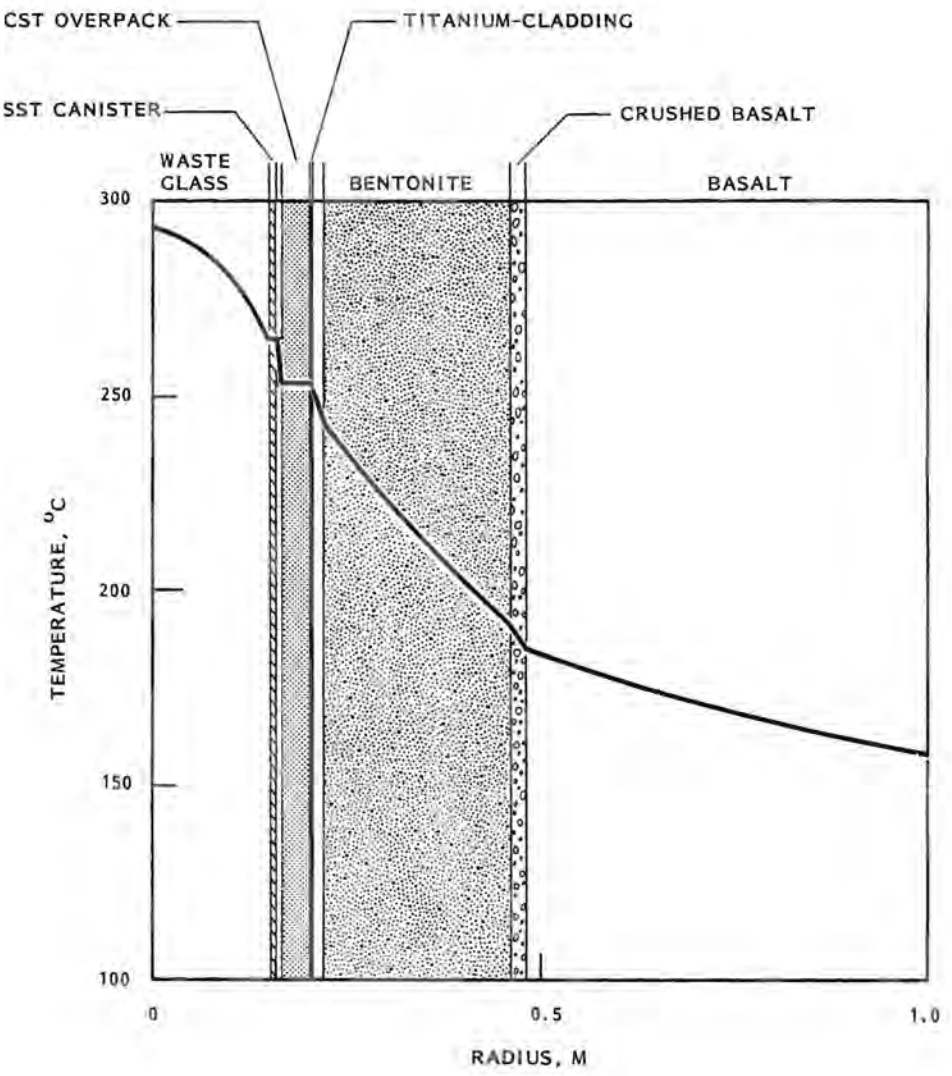

FIGURE A.8. Radial Temperature Profiles for Reference HLW Cases in Basalt

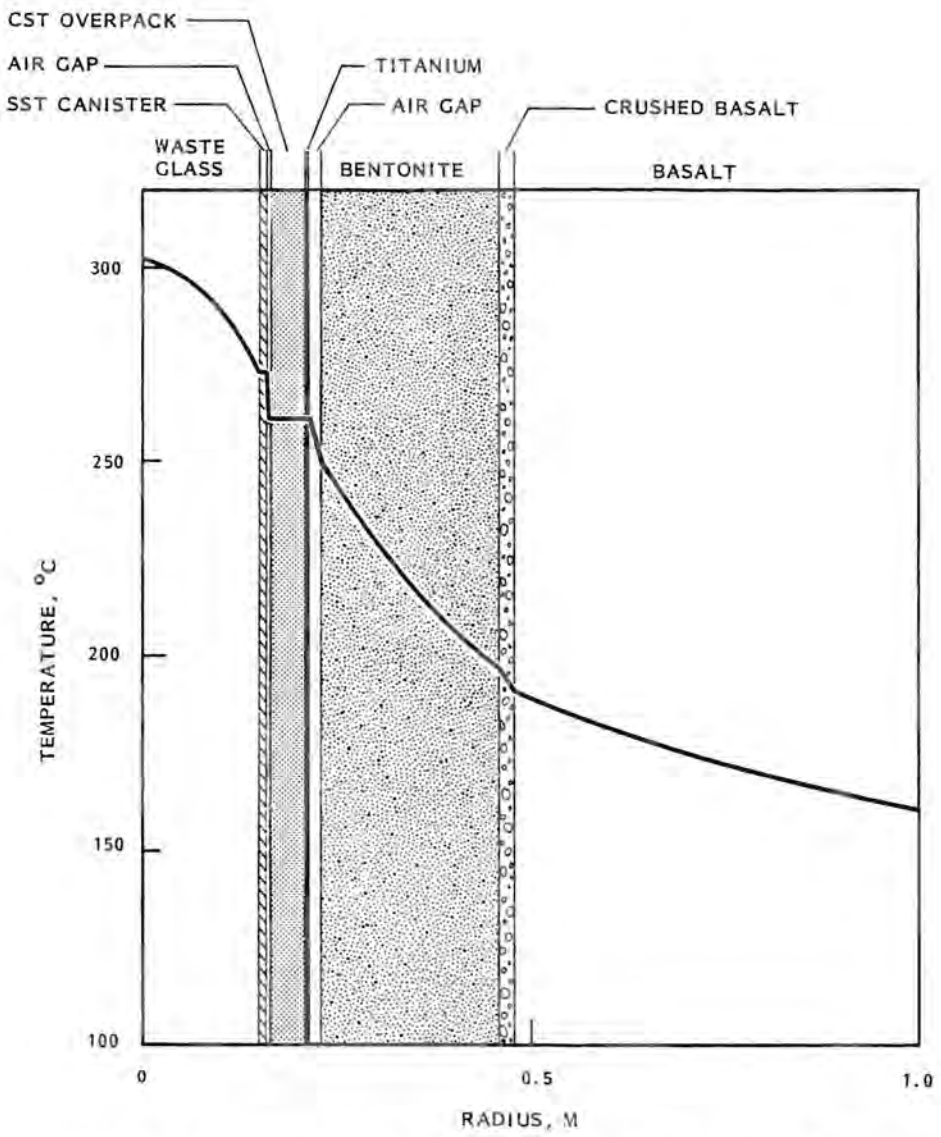

FIGURE A.9. Radial Temperature Profiles for Reference Aged-HLW Cases in Basalt

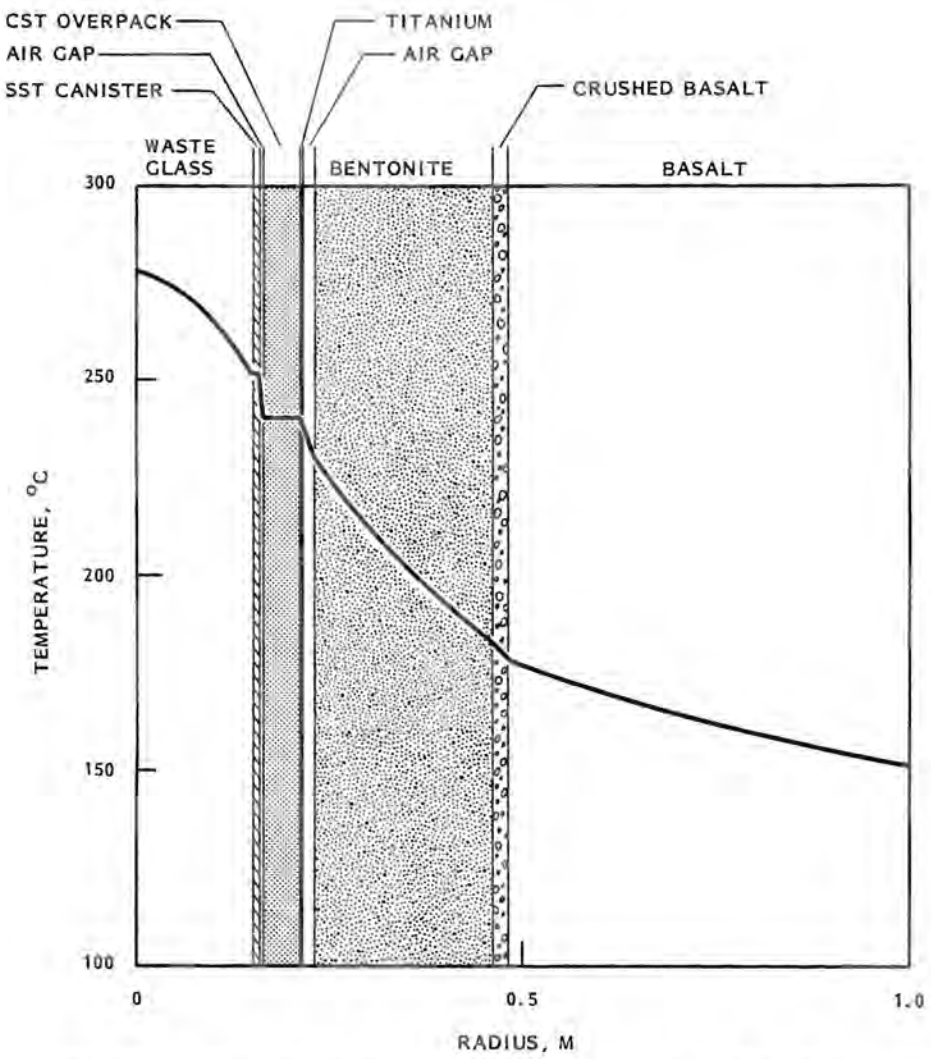

FIGURE A.10. Radial Temperature Profiles for Reference FHLW Cases in Basalt

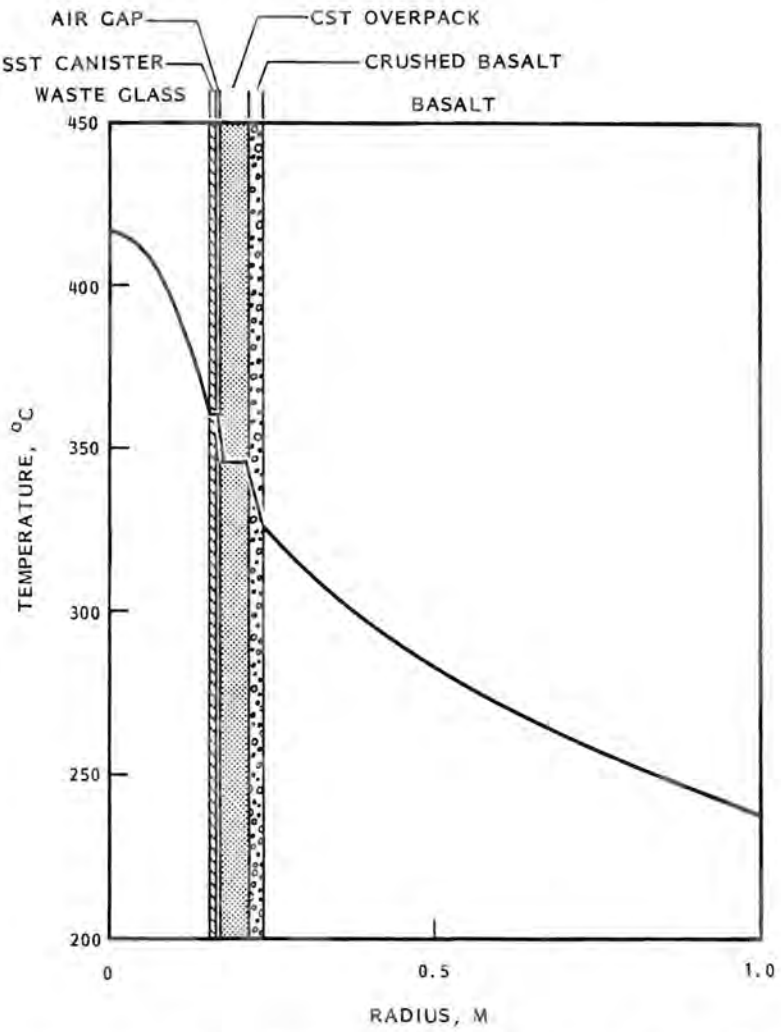

FIGURE A.11. Radial Temperature Profiles for Reference Cs/Sr Cases in Basalt

host rock. These results were taken at the simulation time of 5 years after emplacement. These temperature profiles identify the components that result in the largest temperature drops. Figures A.12 through A.15 show the peak temperature that occurs in a given component as a function of the initial canister heat load. The slightly negative curvature results because of the increase in thermal conductivity of the basalt with an increase in temperature. Also, the effective thermal conductivity through the waste package components generally increases with temperature. Figure A.16 shows the isotherms that develop in

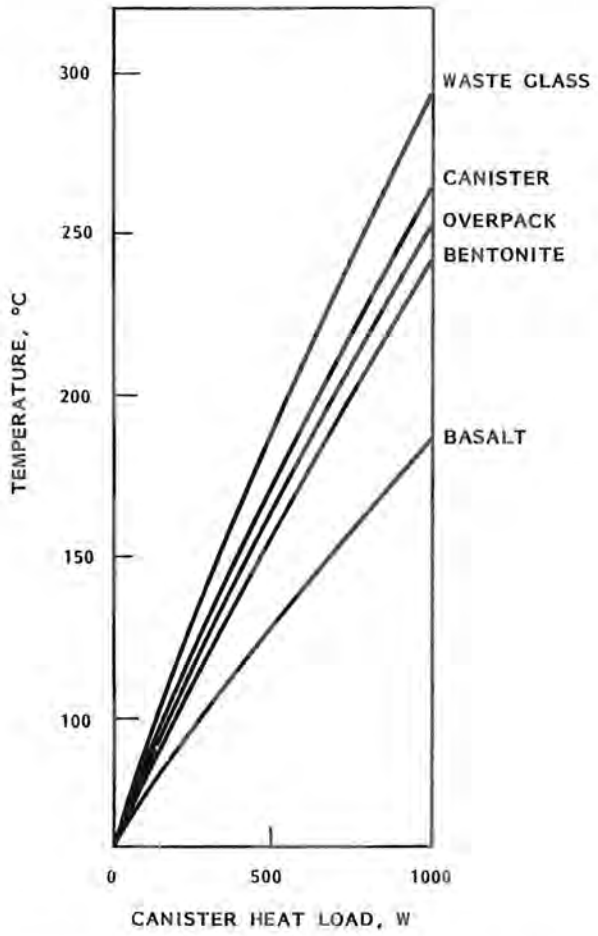

FIGURE A.12. Peak Component Temperatures Versus Initial Canister Heat Load for Reference HLW Cases in Basalt

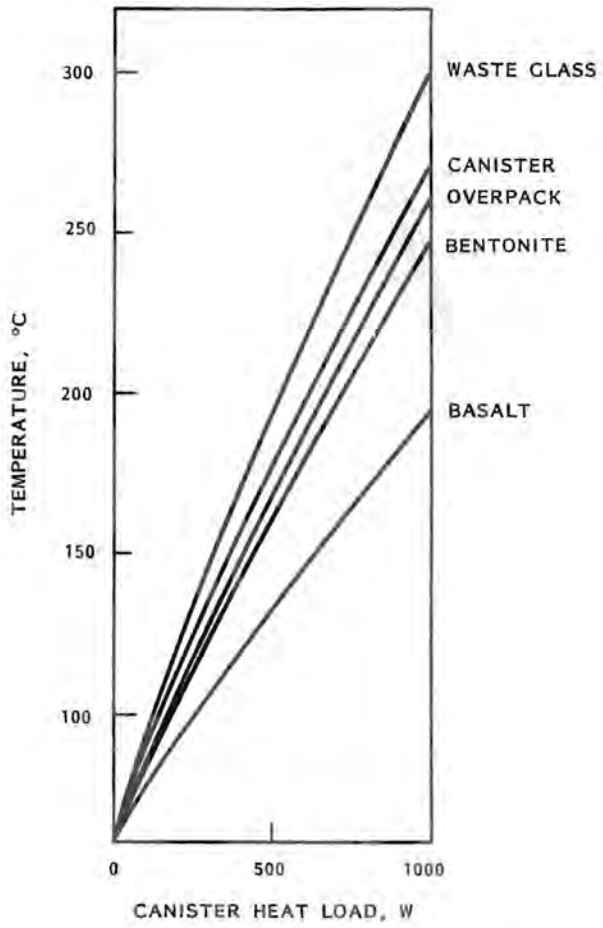

FIGURE A.13. Peak Component Temperatures Versus Initial Canister Heat Load for Reference Aged-HLW Cases in Basalt

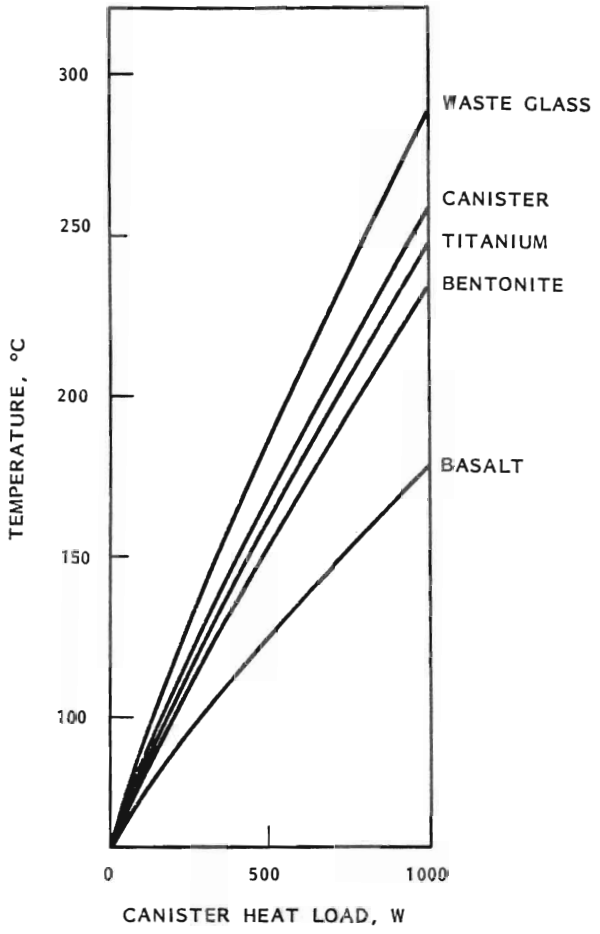

FIGURE A.14. Peak Component Temperatures Versus Initial Canister Heat Load for Reference FHLW Cases in Basalt

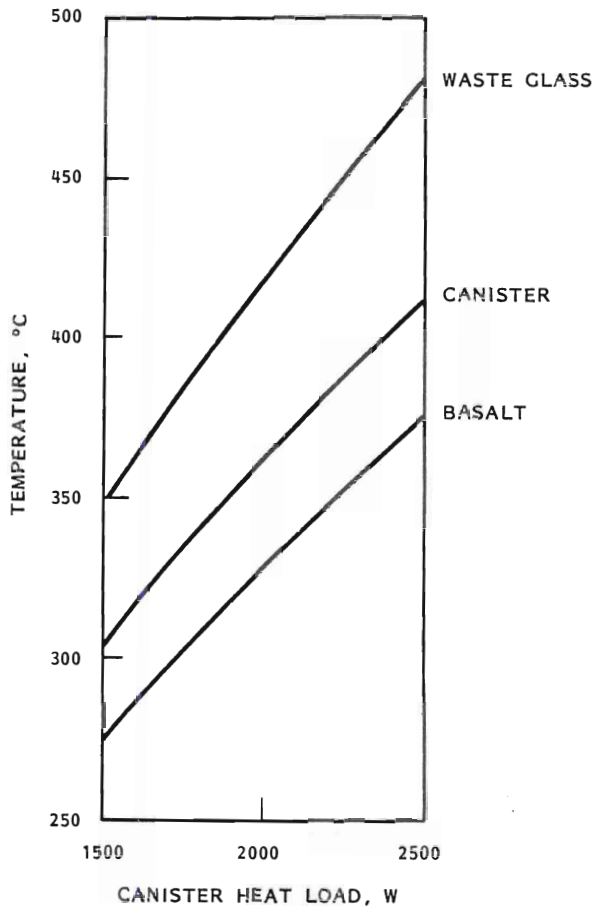

FIGURE A.15. Peak Component Temperatures Versus Initial Canister Heat Load for Reference Cs/Sr Cases in Basalt

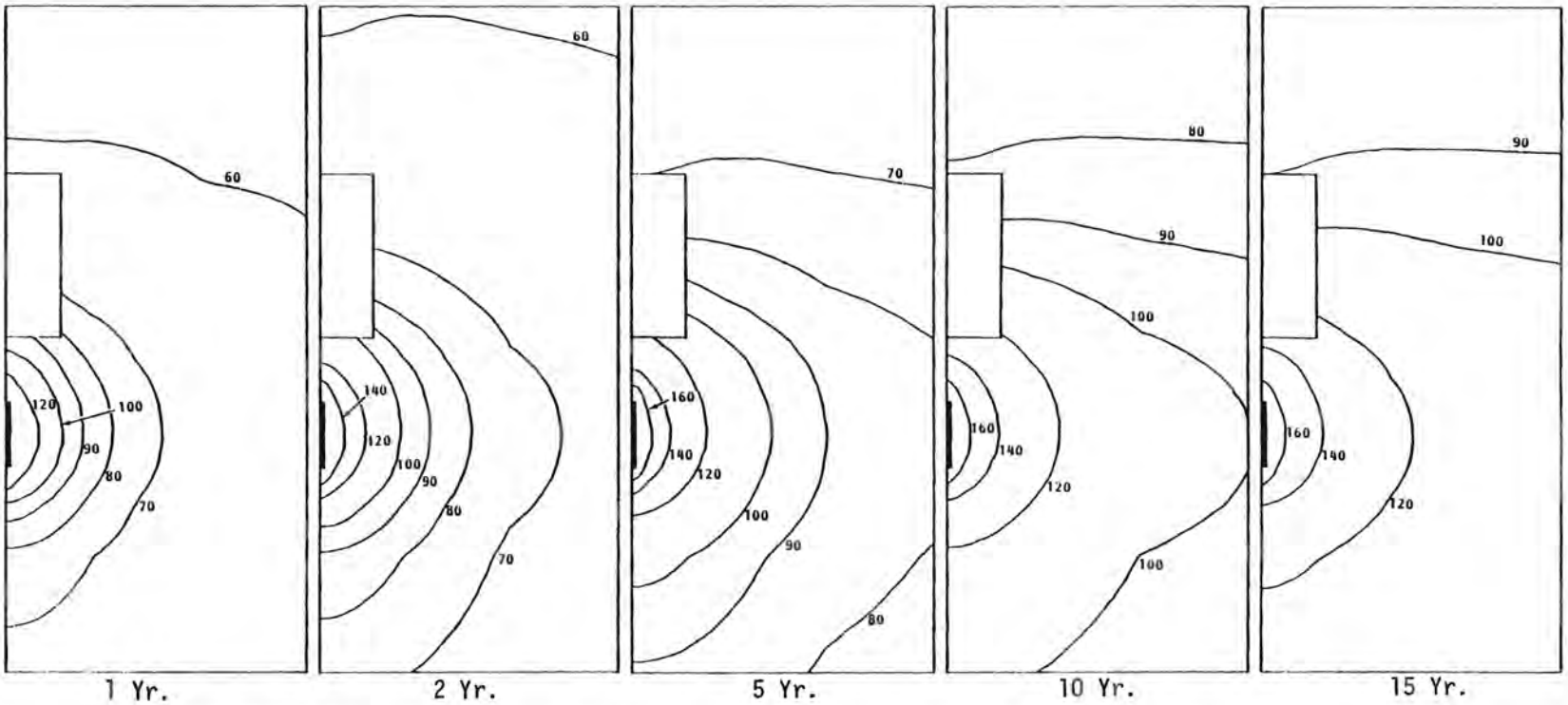

FIGURE A.16. Near-Field Isotherms for Reference HLW Emplacement in Basalt (temperatures in °C)

the near-field for the reference HLW case. Since the interest in this study was directed to the thermal performance of the waste package, similar isotherm plots for the other cases were not presented.

A.4 SUPPLEMENTARY PARAMETRIC ANALYSIS RESULTS

In this section the results are presented for the parametric thermal analysis of waste packages emplaced in a repository in basalt. These results were instrumental in formulating the results presented in Section 3.3 of Chapter 3 (Volume 1).

The parametric analysis was performed for the HLW and Cs/Sr wastes. The results for the HLW were considered to be applicable to the aged-HLW and FHLW as well. For each waste type, several canister diameters were evaluated. For HLW, the canister diameters were 0.5, 1.0, 1.7 and 2.5 ft. For Cs/Sr waste, the canister diameters were 1.0, 1.7, and 2.5 ft.

The parametric analysis performed for each canister diameter consisted of a transient thermal simulation for an array of values of the initial canister heat load and the canister pitch. In each case the minimum pitch was defined to be 2-1/2 times the required borehole diameter while the maximum pitch was, effectively, infinity. A range of canister heat loads was chosen so that for the most severe thermal conditions the maximum allowable waste package component temperatures were slightly exceeded. Thus, a complete mapping of expected peak temperatures as a function of an array of design parameters was obtained.

For each diameter, plots were drawn of the maximum component temperature versus canister heat load for each value of canister pitch. These results are presented in Figures A.17 through A.23. Notice that for the HLW cases (Figures A.17 through A.20) the waste package component maximum temperatures are not strongly sensitive to a change in canister pitch. This results because of the low conductivity of the bentonite. For the Cs/Sr cases, an increase in canister pitch allows a much larger increase in canister heat load to obtain the peak component temperatures. This sensitivity to the canister pitch for the Cs/Sr cases is due to the fact that bentonite was not included in those designs.

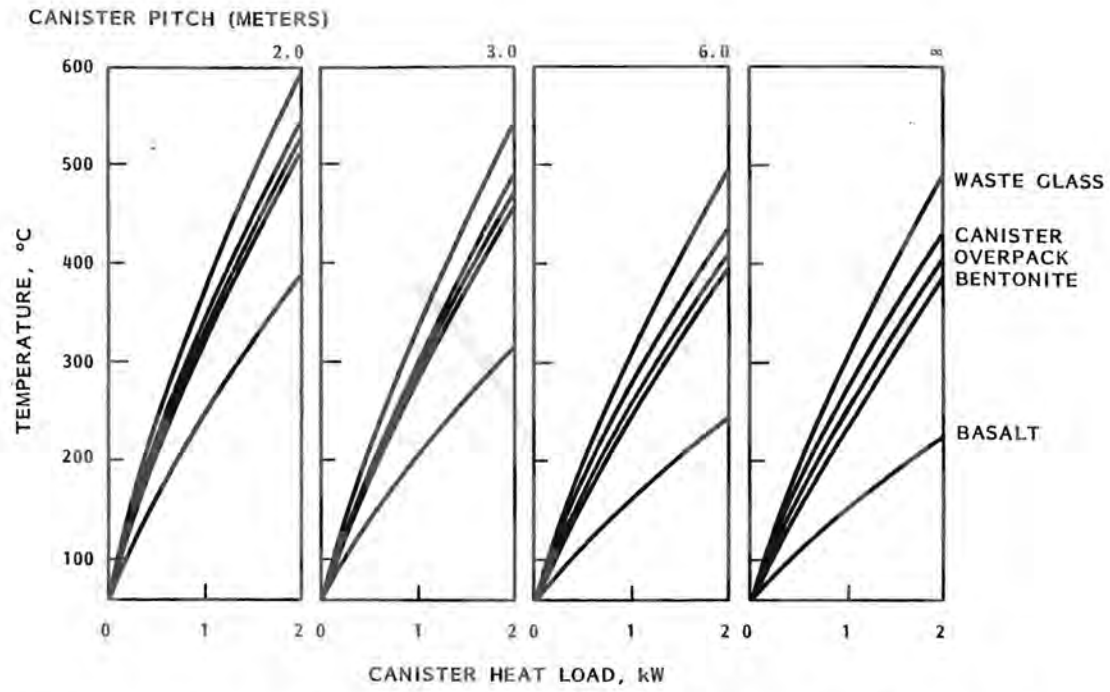

FIGURE A.17. Peak Component Temperatures Versus Initial Canister Heat Load for Selected Canister Pitch (HLW in basalt, canister diameter = 0.5 ft)

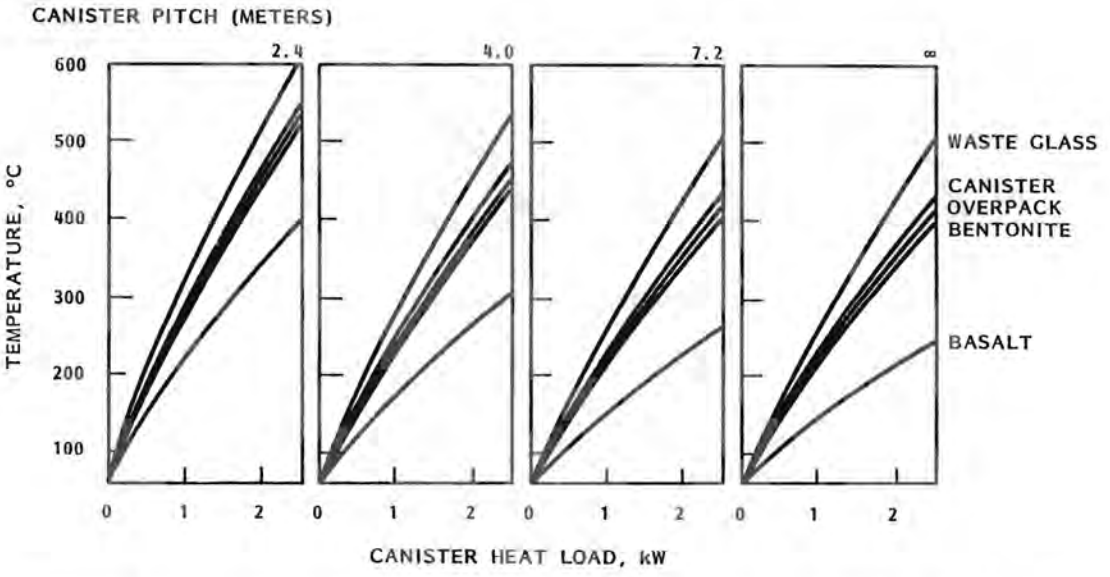

FIGURE A.18. Peak Component Temperatures Versus Initial Canister Heat Load for Selected Canister Pitch (HLW in basalt, canister diameter = 1.0 ft)

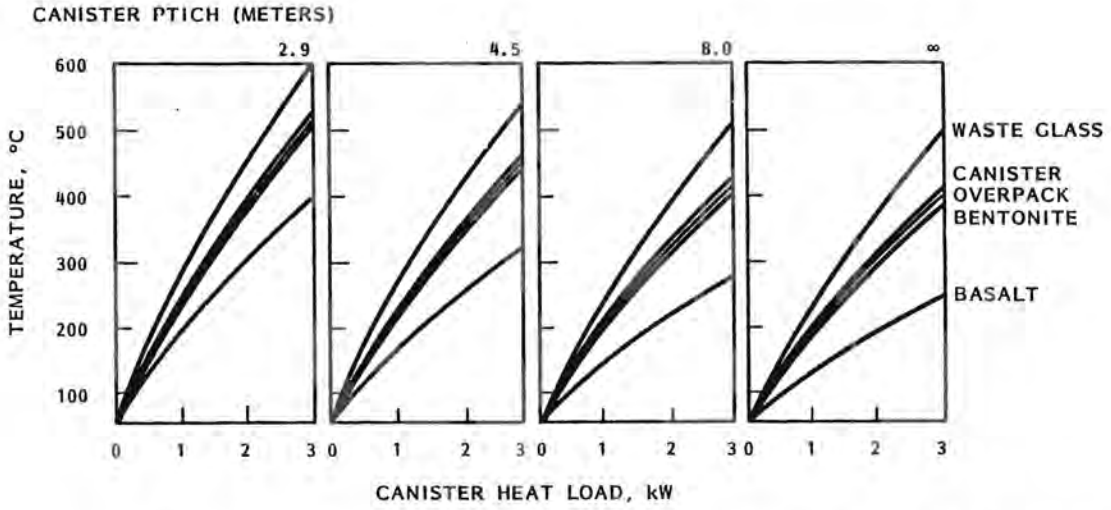

FIGURE A.19. Peak Component Temperatures Versus Initial Canister Heat Load for Selected Canister Pitch (HLW in basalt, canister diameter = 1.7 ft)

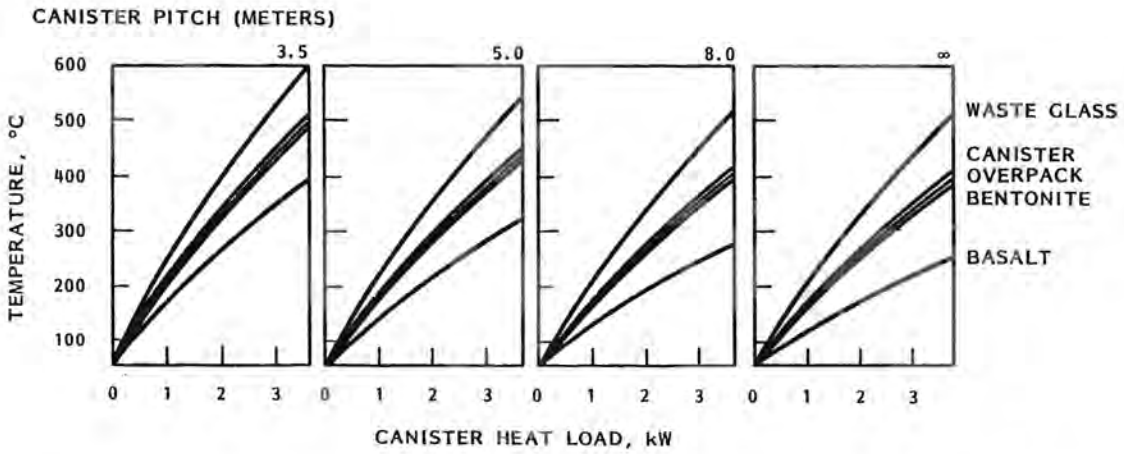

FIGURE A.20. Peak Component Temperatures Versus Initial Canister Heat Load for Selected Canister Pitch (HLW in basalt, canister diameter = 2.5 ft)

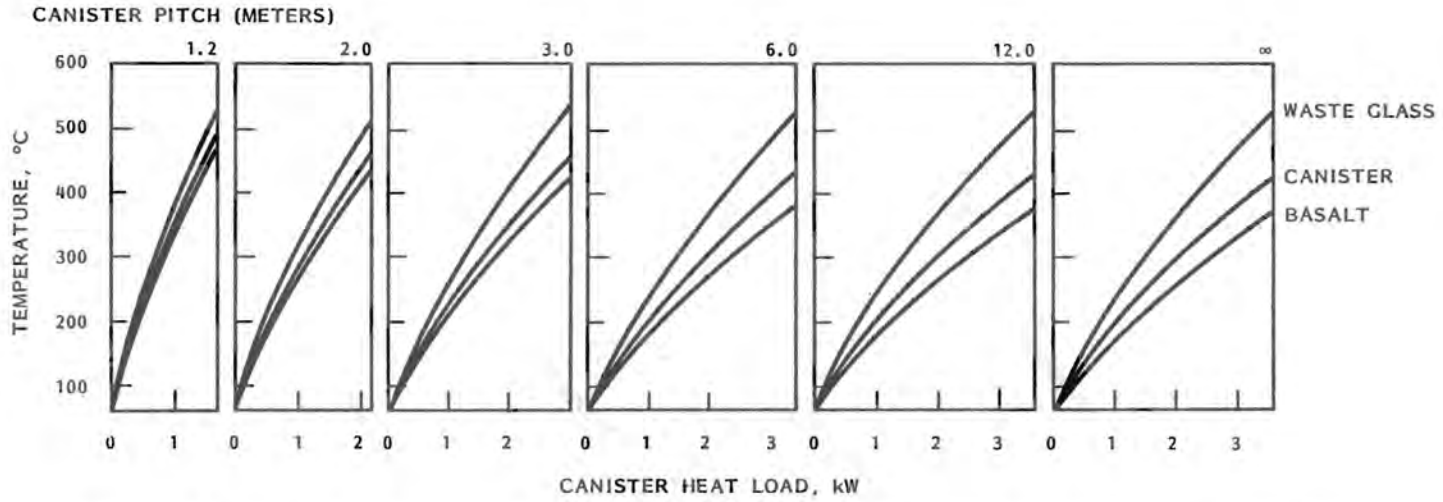

FIGURE A.21. Peak Component Temperatures Versus Initial Canister Heat Load for Selected Canister Pitch (Cs/Sr in basalt, canister diameter = 1.0 ft)

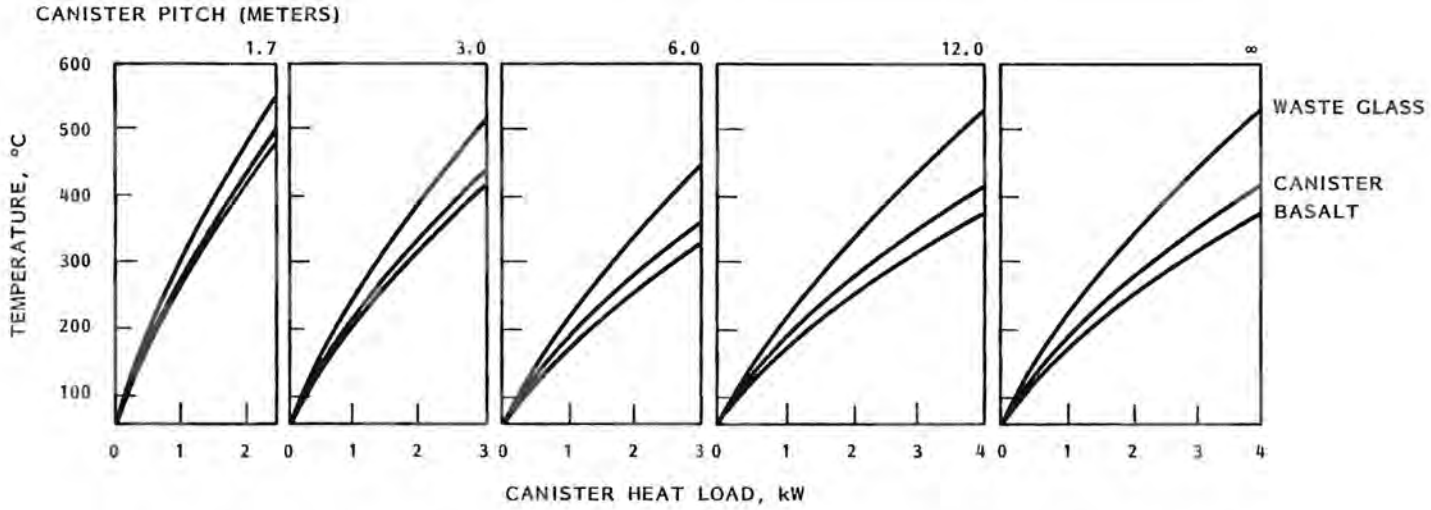

FIGURE A.22. Peak Component Temperatures Versus Initial Canister Heat Load for Selected Canister Pitch (Cs/Sr in basalt, canister diameter = 1.7 ft)

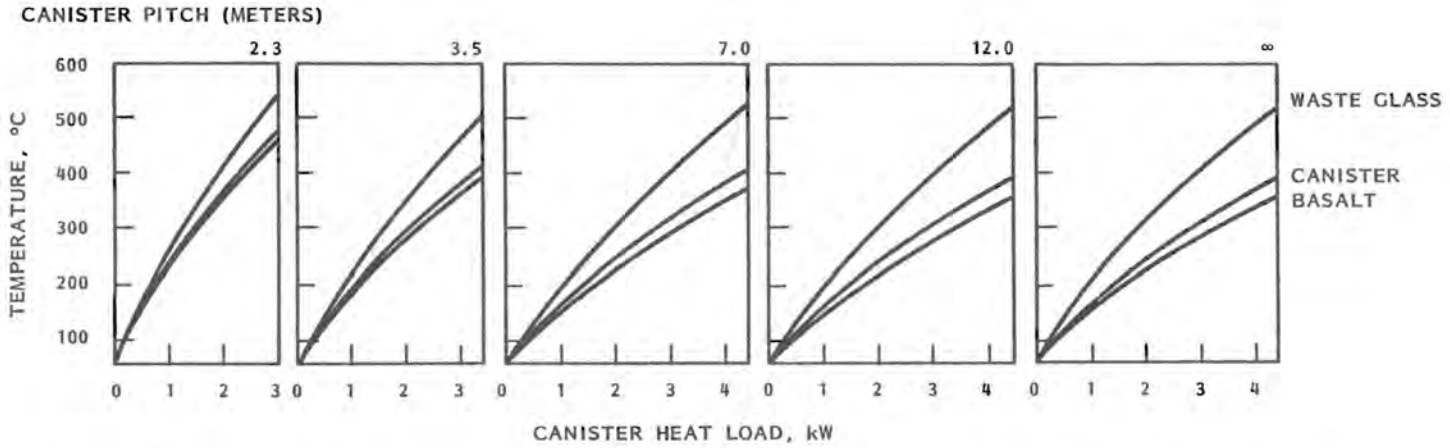

FIGURE A.23. Peak Component Temperatures Versus Initial Canister Heat Load for Selected Canister Pitch (Cs/Sr in basalt canister diameter = 2.5 ft)

The results of Figures A.17 through A.23 were used to develop Figures A.24 through A.30. For HLW, the heat loads that yielded selection temperatures in the bentonite were interpolated from Figures A.17 through A.20. These heat loads were plotted versus canister pitch in Figures A.24 through A.27. Smooth curves connecting the plotted points representing a given temperature were drawn, thereby producing selected isotherms for bentonite. In other words, the isotherm plots define the canister heat load and canister pitch that will yield a selected peak temperature in the bentonite. For the Cs/Sr cases, the same method was used to plot isotherms for selected temperatures in the basalt. These results are shown in Figures A.28 through A.30.

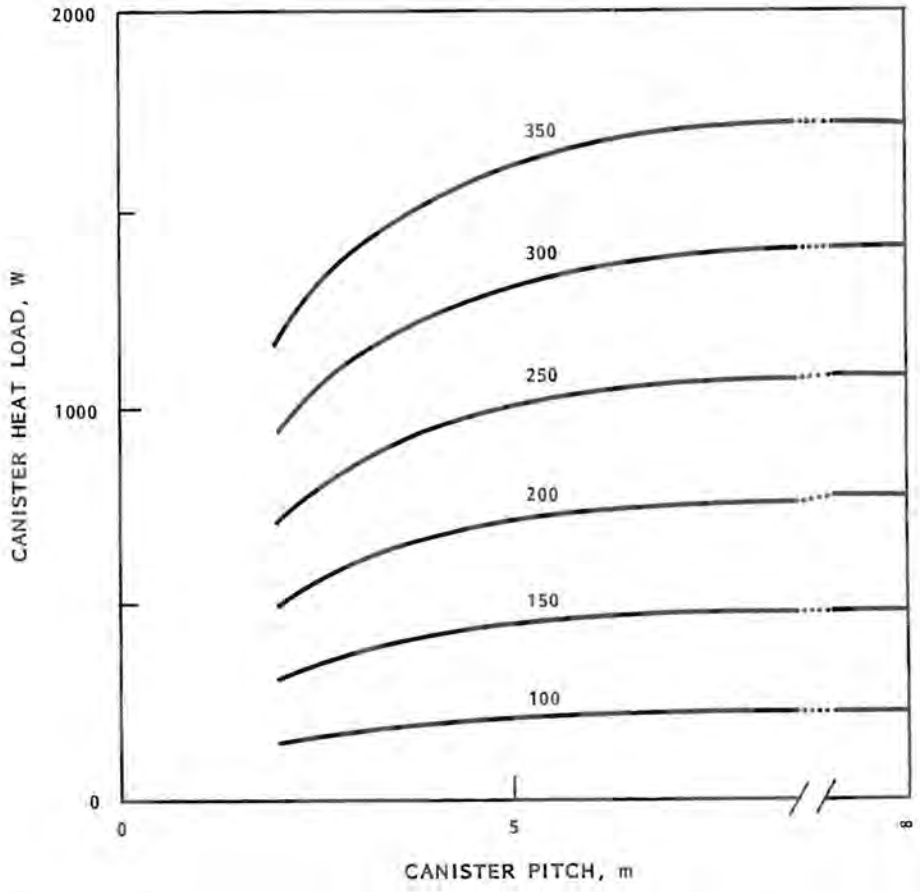

FIGURE A.24. Initial Canister Heat Load Versus Canister Pitch to Achieve Selected Peak Temperatures (in °C) in Bentonite (HLW in basalt, canister diameter = 0.5 ft)

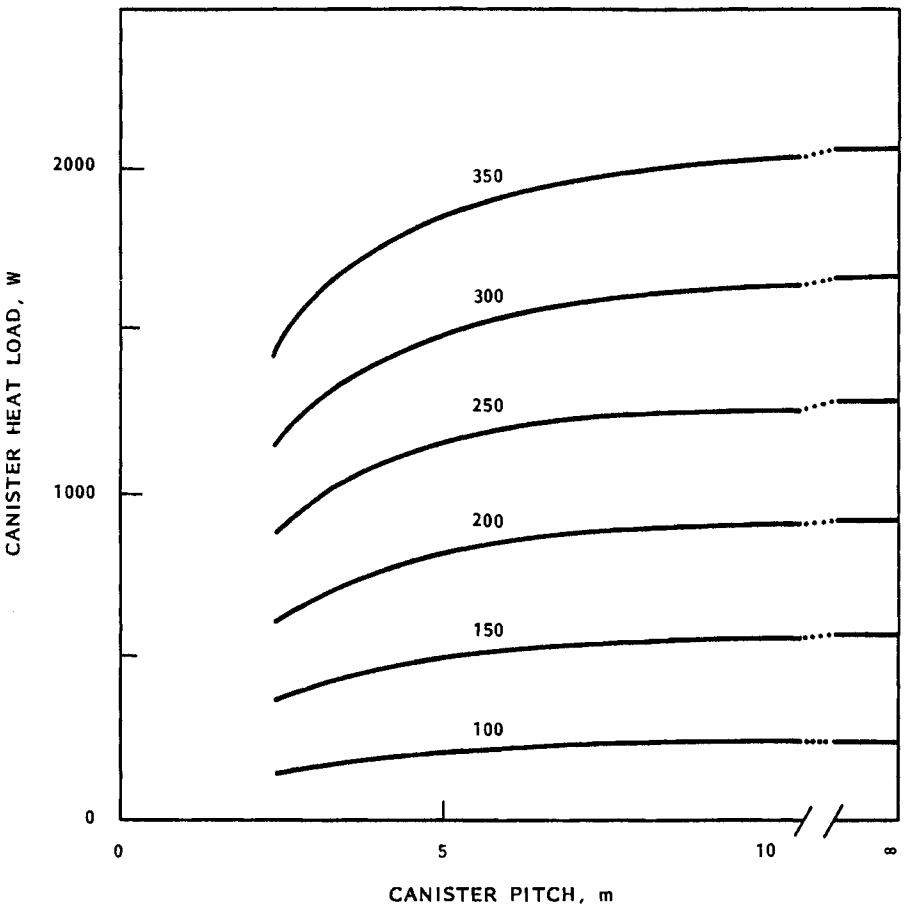

FIGURE A.25. Initial Canister Heat Load Versus Canister Pitch to Achieve Selected Peak Temperatures (in °C) in Bentonite (HLW in basalt, canister diameter = 1.0 ft)

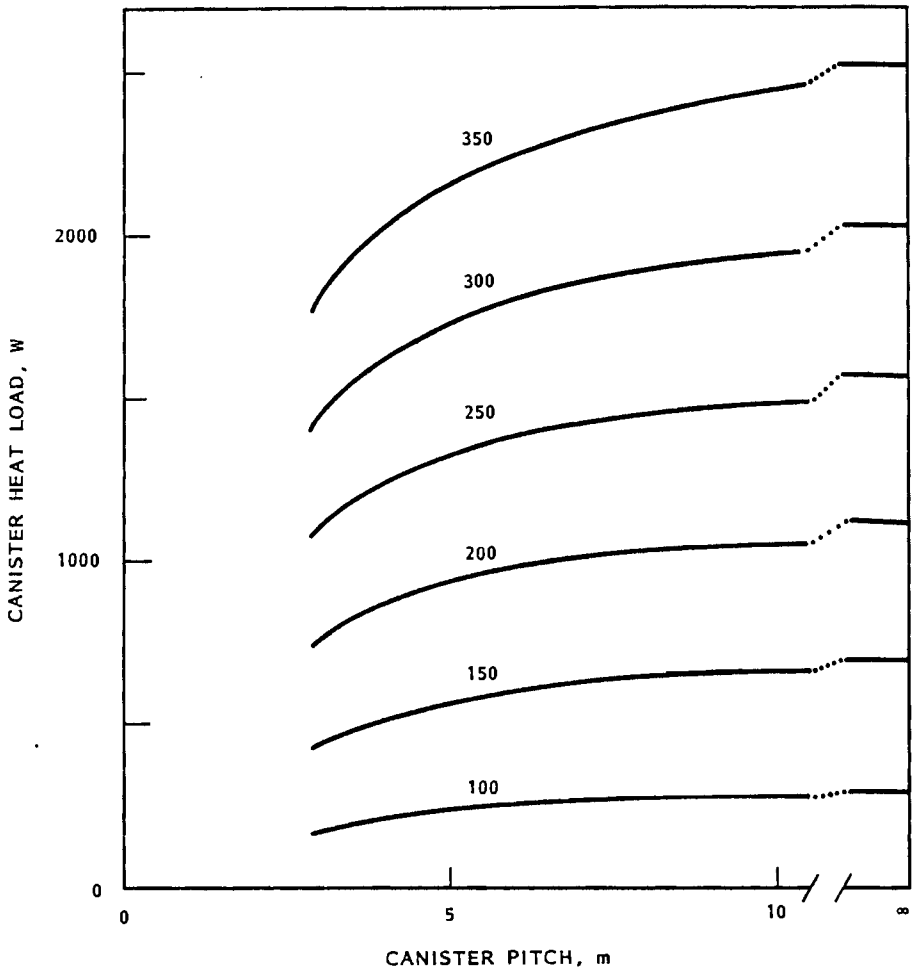

FIGURE A.26. Initial Canister Heat Load Versus Canister Pitch to Achieve Selected Peak Temperatures (in °C) in Bentonite (HLW in basalt, canister diameter = 1.7 ft)

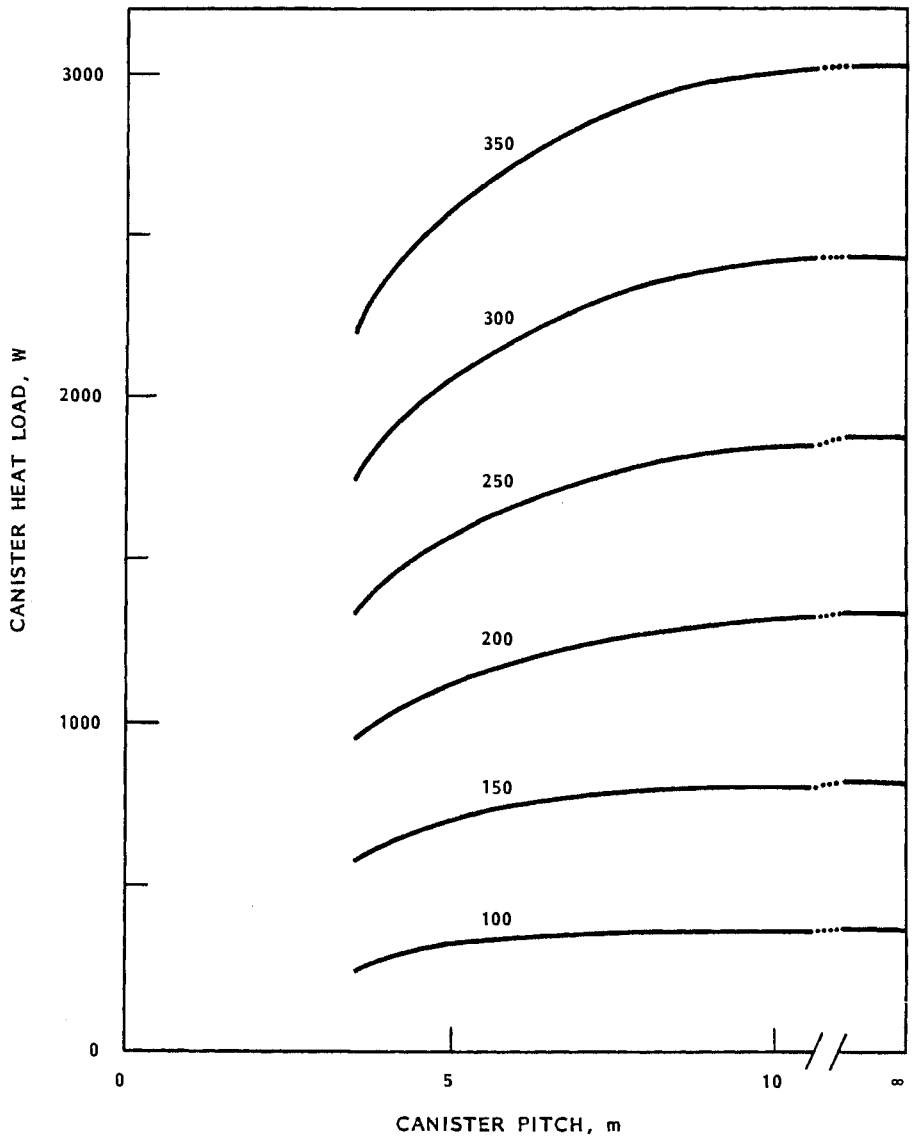

FIGURE A.27. Initial Canister Heat Load Versus Canister Pitch to Achieve Selected Peak Temperatures (in °C) in Bentonite (HLW in basalt, canister diameter = 2.5 ft)

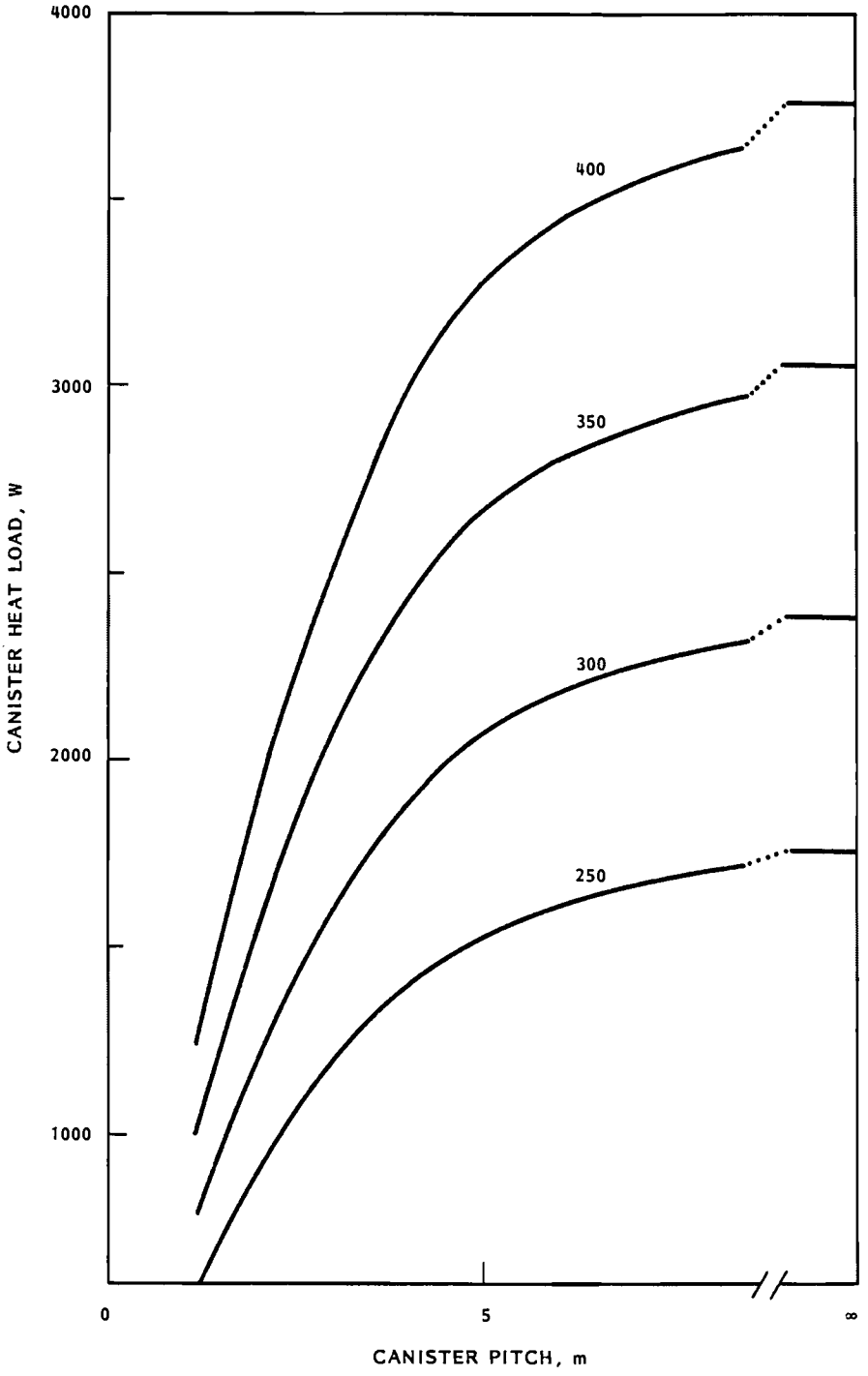

FIGURE A.28. Initial Canister Heat Load Versus Canister Pitch to Achieve Selected Peak Temperatures (in °C) in Basalt (Cs/Sr in basalt, canister diameter = 1.0 ft)

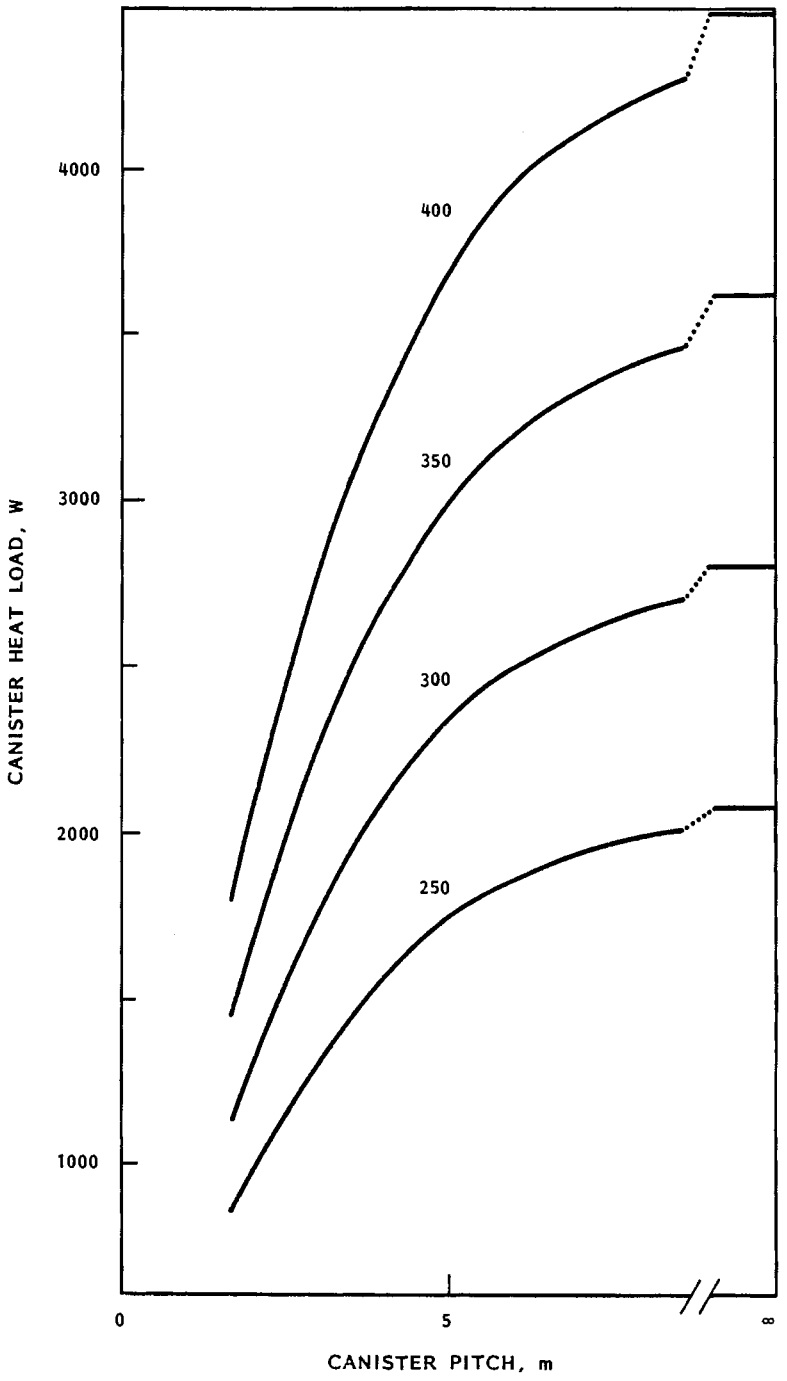

FIGURE A.29. Initial Canister Heat Load Versus Canister Pitch to Achieve Selected Peak Temperatures (in °C) in Basalt (Cs/Sr in basalt, canister diameter = 1.7 ft)

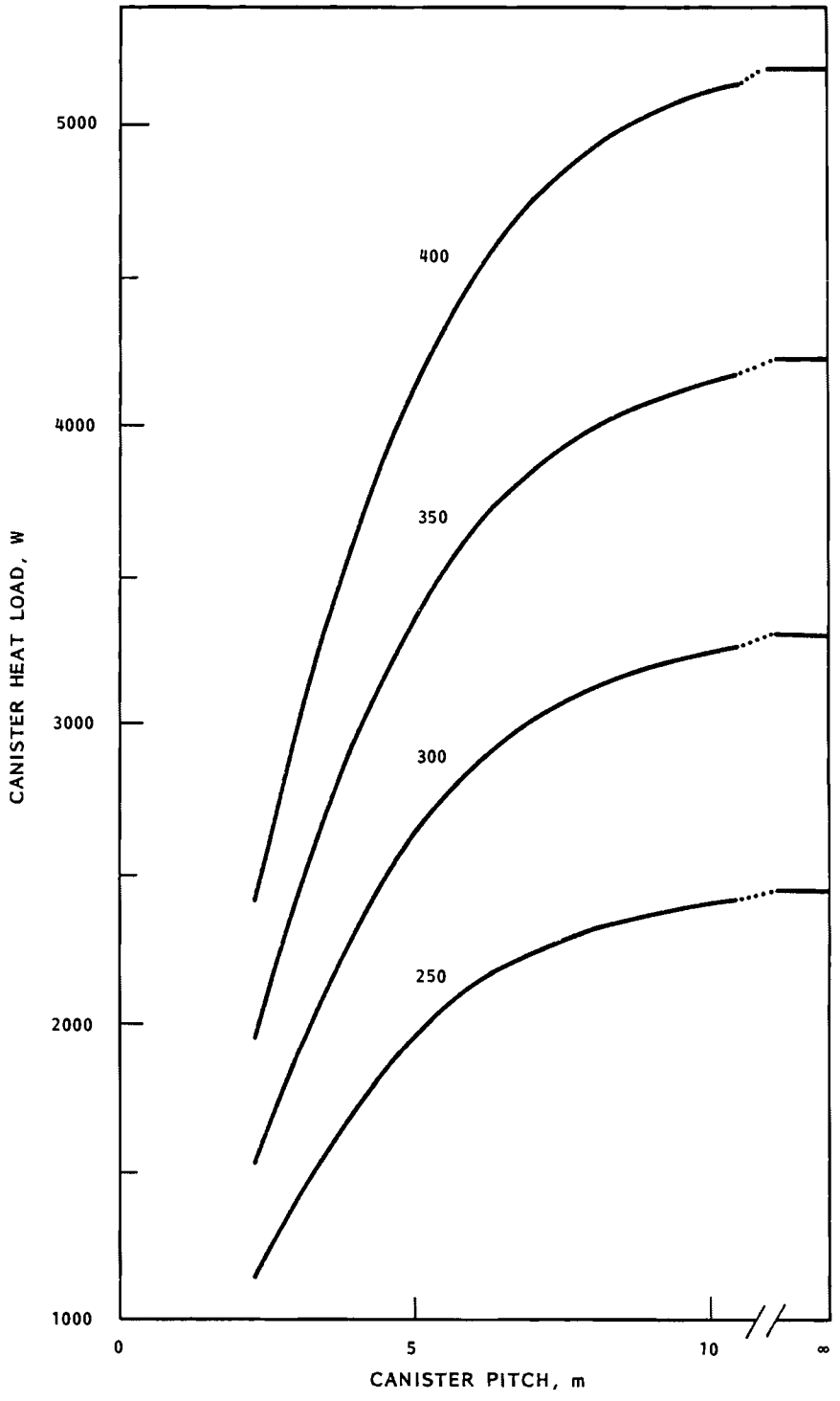

FIGURE A.30. Initial Canister Heat Load Versus Canister Pitch to Achieve Selected Peak Temperatures (in °C) in Basalt (Cs/Sr in basalt, canister diameter = 2.5 ft)

A.5 SALT REPOSITORY CALCULATIONS

The results of the analysis of the reference cases in salt are presented in this section. Reference case results were developed for each waste form. The design conditions for the reference cases were developed for each waste form. The design conditions for the reference cases are presented in Section 3.4 of Chapter 3 (Volume 1). Fundamental reference design parameters include a canister diameter of 1 ft, a canister pitch of 2.84 m, and an initial canister heat load of 2.21 kW. Also, for all of the cases in salt, the bentonite was not included. According to Table 3.8 in Chapter 3, for a 1-ft-diameter canister, only the HLW and possibly the Cs/Sr can be loaded to a concentration that yields this reference case heat load. Nevertheless, the use of a single heat load facilitates comparison of the results for the reference cases.

For HLW emplacement in salt, Westinghouse (1981b) specified the canister pitch as 2.48 m and reported a peak salt temperature of 233°C at 23 years after emplacement. In the Westinghouse analysis, with HLW and a canister pitch of 2.48 m, the peak salt temperature was found to be 259.5°C at 13.7 years after emplacement. For the most part, the basic repository models used by Westinghouse are similar to the models used here. However, one item in particular may effect a part of the difference in results. The Westinghouse analysis was performed with the corridor backfilled at the time of emplacement, while the results reported for the present work involve no backfill. This results in an order of magnitude difference in the effective conductivity of the corridor. The corridor model is discussed in Section A.2.2. Another item, the active length of the canister, is discussed in Section A.2.4. The longer active length used by Westinghouse results in lower temperatures. Also, a portion of the difference in reported results may be due to grid resolution. The finer mesh grid used in the present analysis provides more accurate results and results in higher temperatures in the waste package. At any rate, the canister pitch was increased to 2.84 m, which yielded a peak temperature of 249°C in the titanium, the material that actually limits the design. This canister pitch was then used for the analysis of all four waste forms.

The peak temperature in each component of the waste package as a function of time is shown in Figures A.31 through A.34. For the HLW the temperature

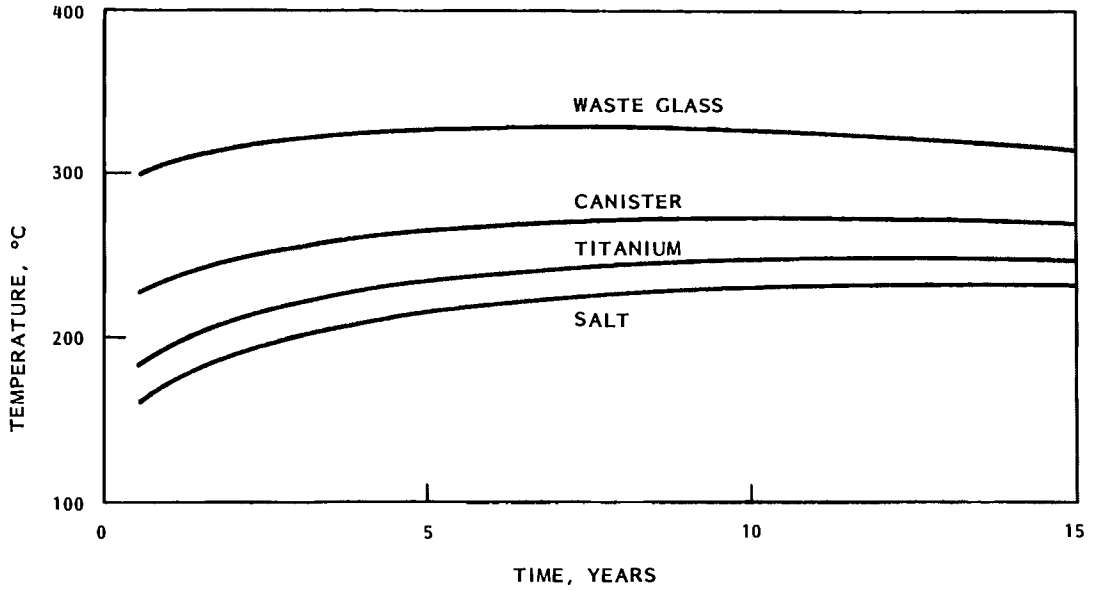

FIGURE A.31. Temperature Histories for Reference HLW Cases in Salt

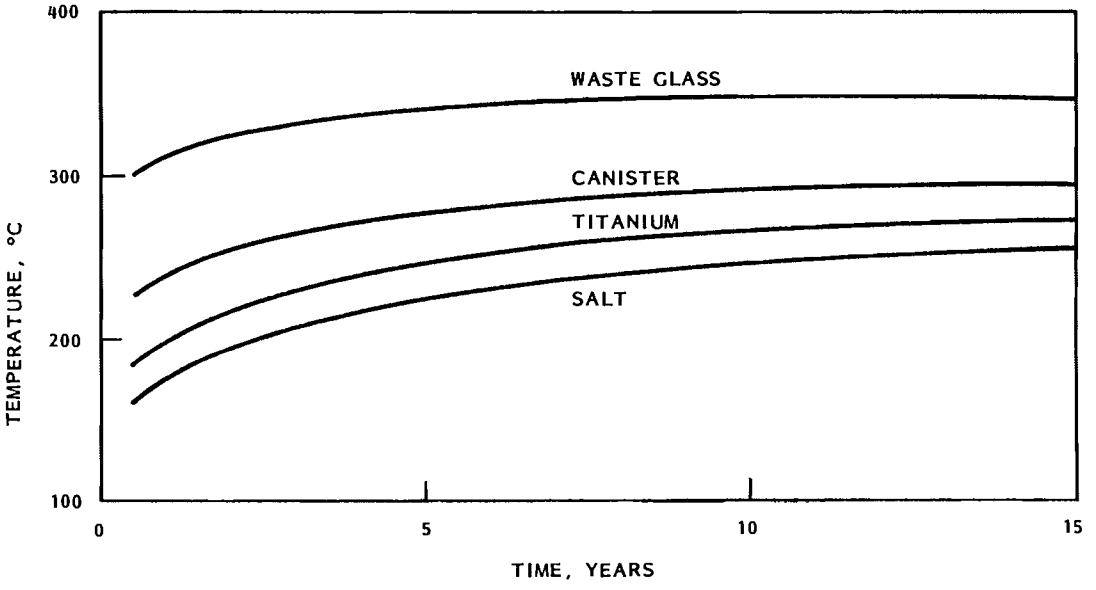

FIGURE A.32. Temperature Histories for Reference Aged-HLW Cases in Salt

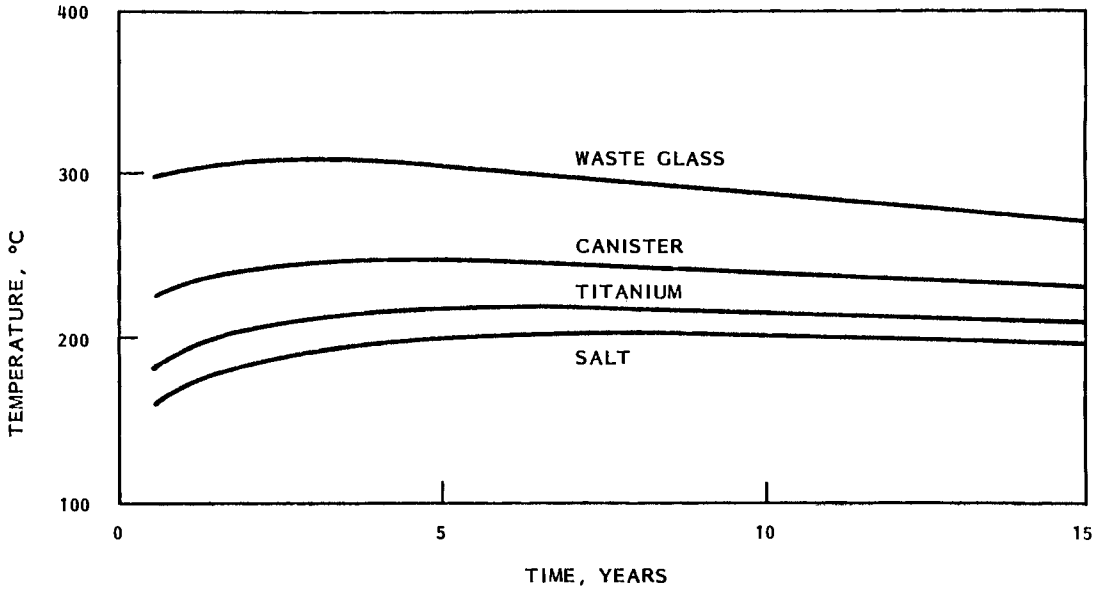

FIGURE A.33. Temperature Histories for Reference FHLW Cases in Salt

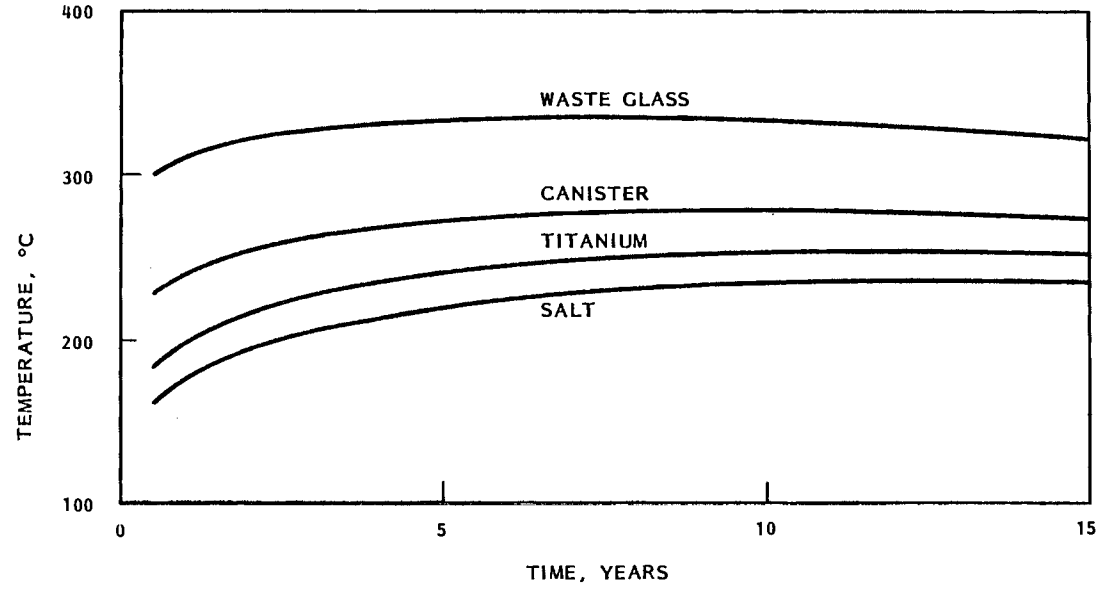

FIGURE A.34. Temperature Histories for Reference Cs/Sr Cases in Salt

limit of 250°C in the titanium is approximately met. This is also true for the Cs/Sr. However, the aged-HLW and FHLW show considerably different thermal responses. The aged-HLW has a peak titanium temperature of 274°C at 17.3 years after emplacement. The FHLW has a peak titanium temperature of 218°C at 6.6 years after emplacement. Unlike the reference cases for basalt, these results demonstrate a stronger dependence on the waste form and the rate of heat-output decay. The greater conductivity of the salt, coupled with the elimination of the bentonite, causes the temperatures to peak at a later time. This gives the unique characteristics of each decay curve more time to become established. The temperatures obtained after 1 year are nearly equal for all the cases, then the results begin to exhibit their unique qualities.

Radial temperature profiles are shown in Figures A.35 through A.38. Each profile represents the thermal solution 5 years after the waste package emplacement. The assembly air gap contributes significantly to elevated temperatures in the glass. However, the low conductivity of the waste glass itself results in a large temperature rise across the glass. The dependence of the peak temperature on the initial heat load is shown in Figures A.39 through A.42. The slight positive curvatures are indicative of the temperature dependence on conductivity. While the conductivity of the waste glass and air gaps increases with temperature, the conductivity of salt decreases with temperature. The result is that higher temperatures are required in the waste package to effect the required heat transfer into the salt.

In basalt, the results for aged-HLW and FHLW were approximated in the parametric study by the results for HLW when it was shown that the reference cases produced similar thermal results. However, a parametric study for salt would require three separate simulations. (The thermal behavior of the emplacement of Cs/Sr could be approximated by the results for HLW.)

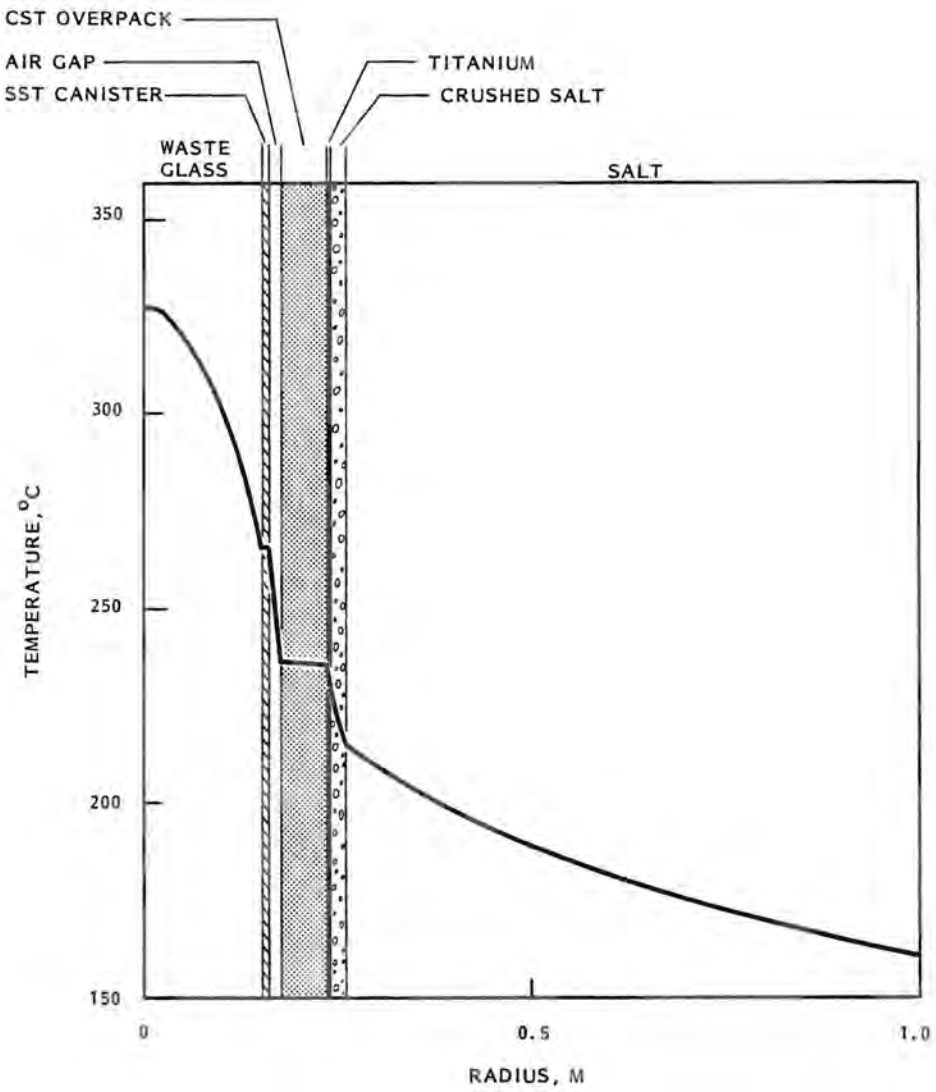

FIGURE A.35. Radial Temperature Profiles for Reference HLW Cases in Salt

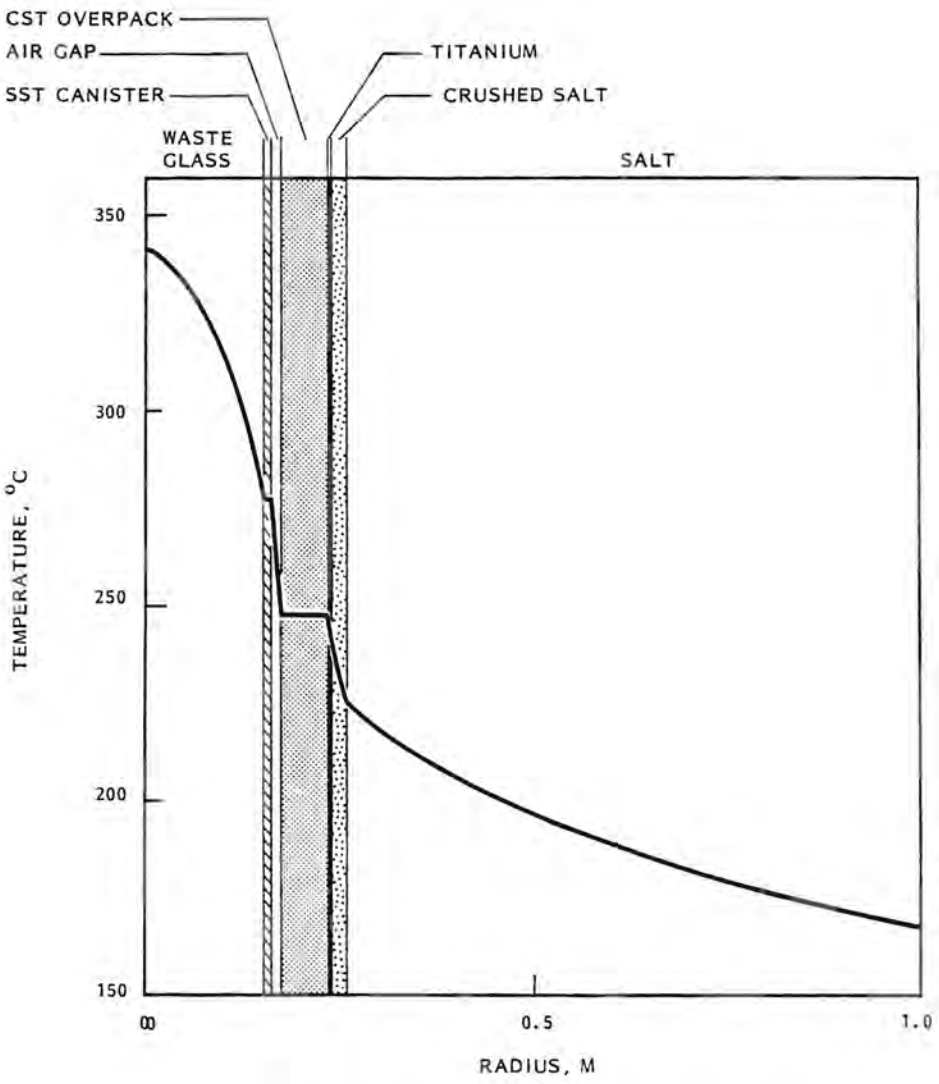

FIGURE A.36. Radial Temperature Profiles for Reference Aged-HLW Cases in Salt

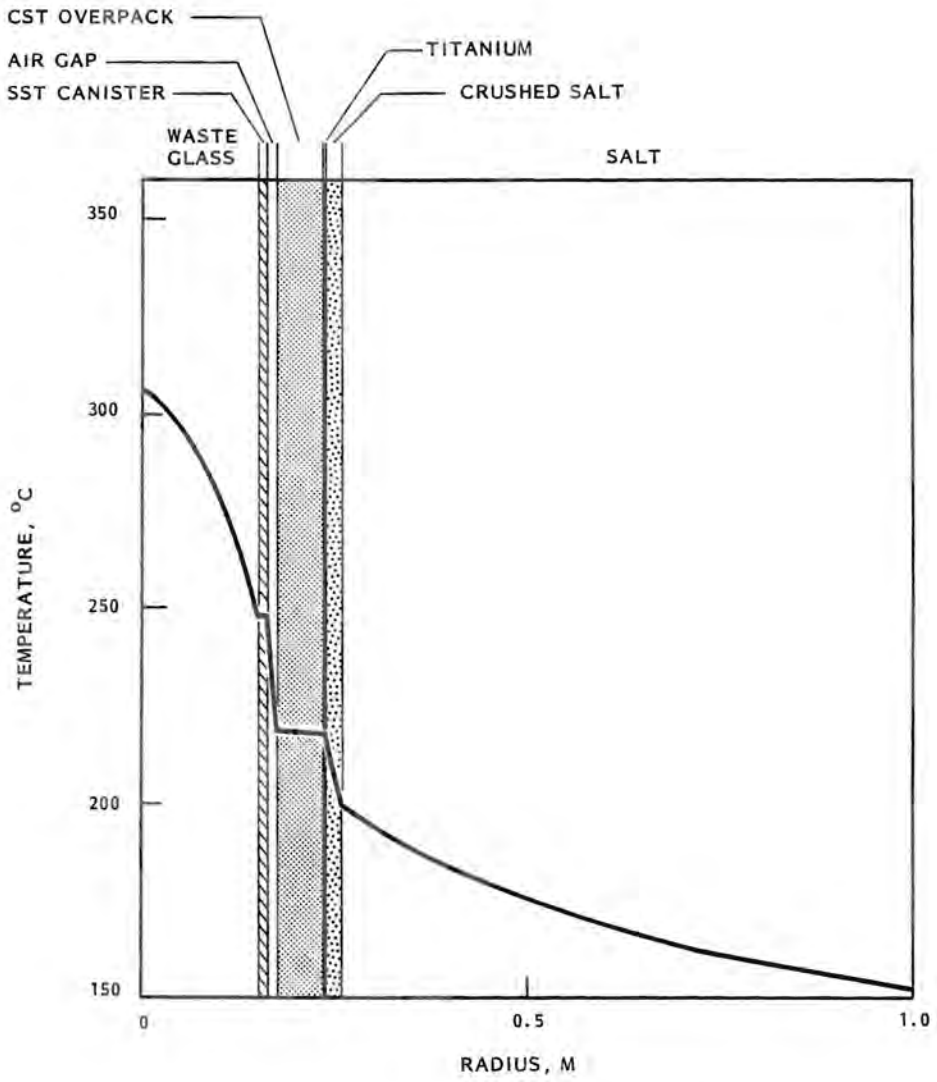

FIGURE A.37. Radial Temperature Profiles for Reference FHLW Cases in Salt

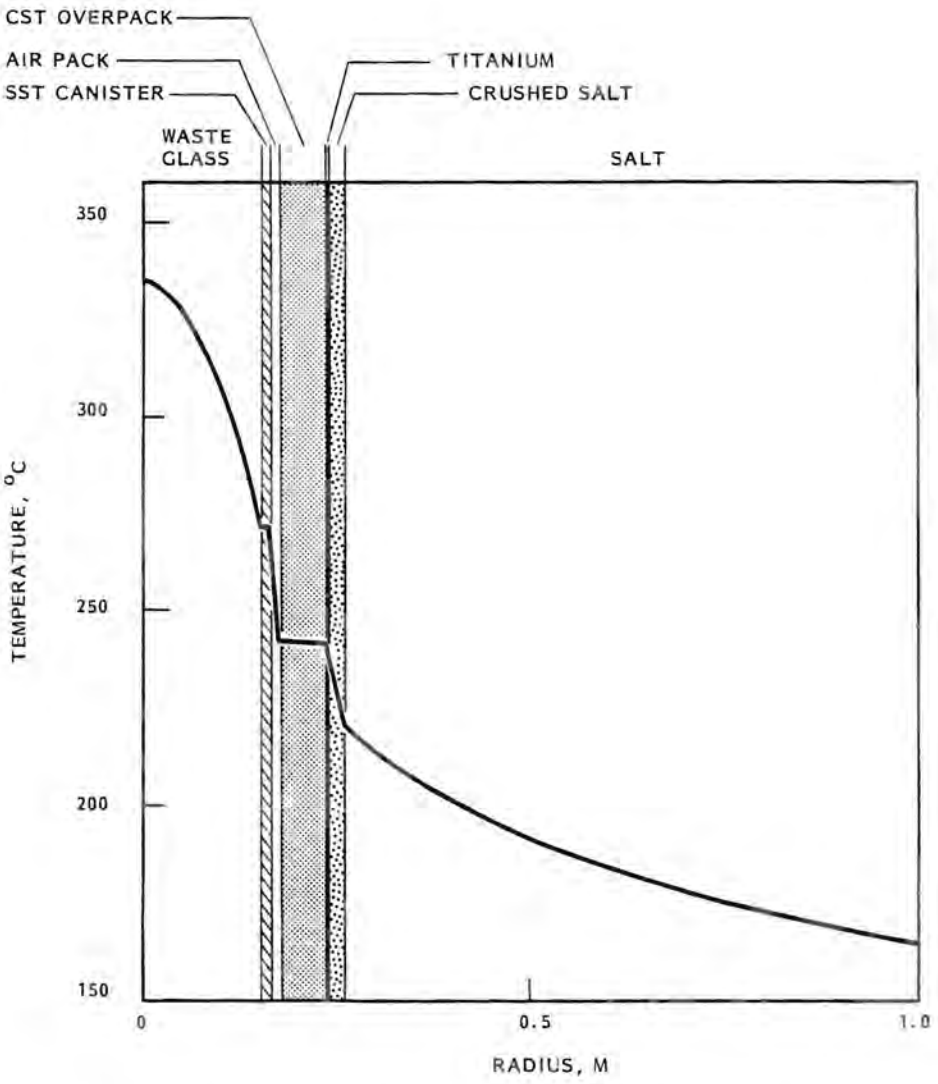

FIGURE A.38. Radial Temperature Profiles for Reference Cs/Sr Cases in Salt

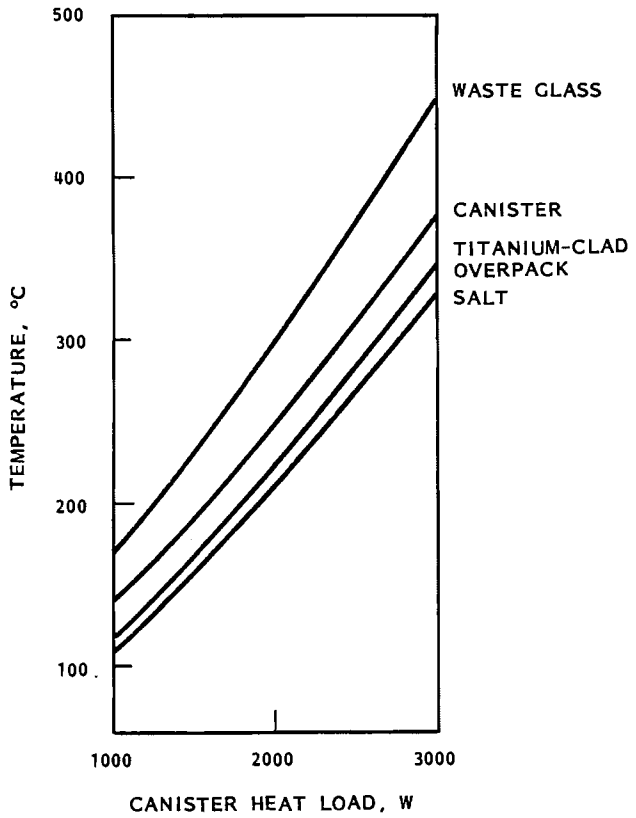

FIGURE A.39. Peak Component Temperatures Versus Initial Canister Heat Load for Reference HLW Cases in Salt

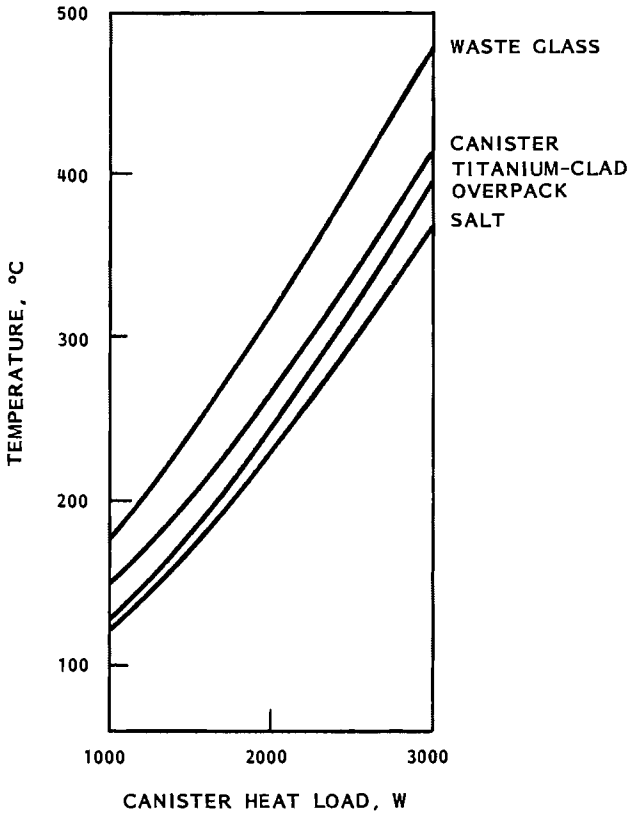

FIGURE A.40. Peak Component Temperatures Versus Initial Canister Heat Load for Reference Aged-HLW Cases in Salt

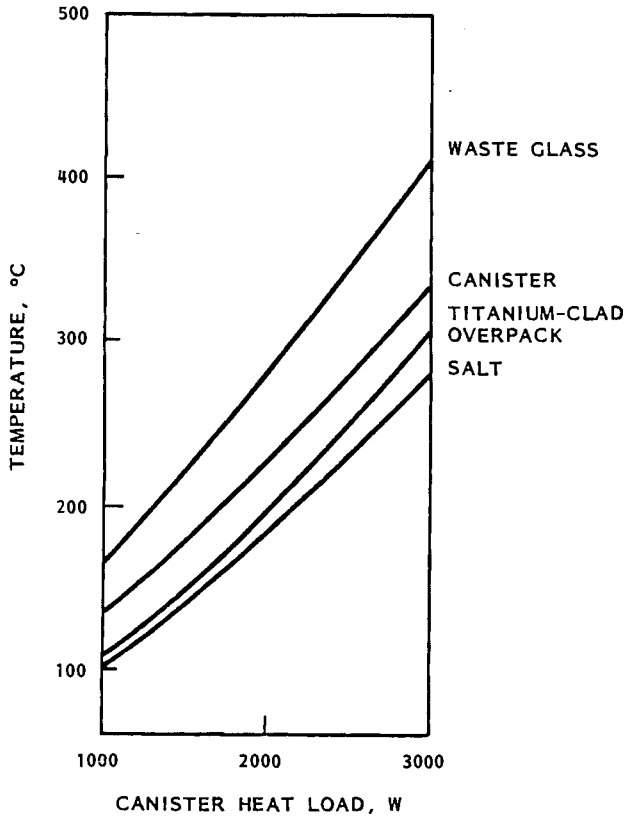

FIGURE A.41. Peak Component Temperatures Versus Initial Canister Heat Load for Reference FHLW Cases in Salt

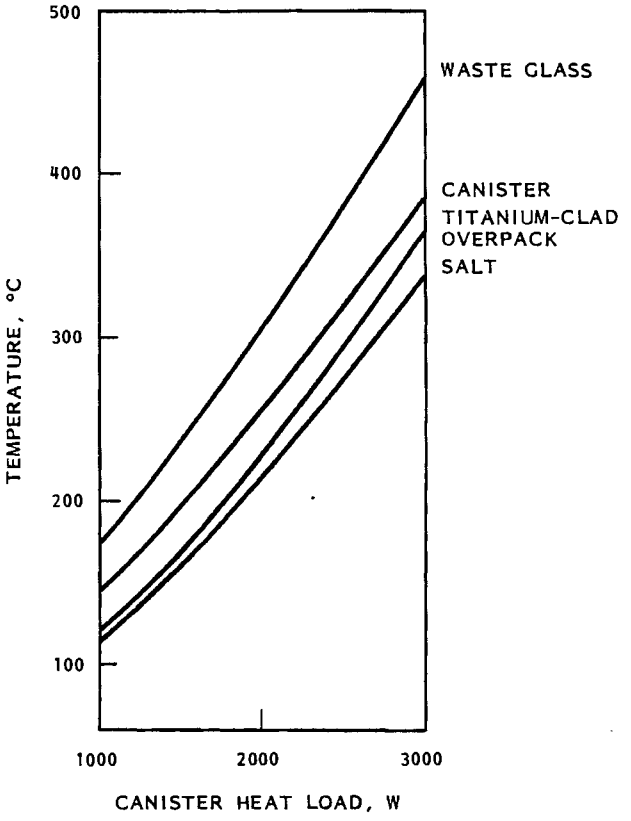

FIGURE A.42. Peak Component Temperatures Versus Initial Canister Heat Load for Reference Cs/Sr Cases in Salt

A.6 HORIZONTAL BOREHOLE CONCEPT

Details of the horizontal borehole case evaluated here are shown in Table A.10. The thermal analysis of the horizontal borehole design was patterned from the thermal analysis of the vertical borehole design. The finite-difference approximation and other imposed conditions and assumptions were similar for both analyses. With this approach the results were comparable.

TABLE A.10. Design Data for Horizontal Borehole Concept

Repository:		
Room Width	6.10 m	(20 ft)
Room Height	3.05 m	(10 ft)
Room Pitch	67.0 m	(220 ft)
Length of Borehole Between Rooms	61.0 m	(200 ft)
Canister Pitch	32.6 m	(107 ft)
Canisters Per Borehole	17	
Spacing Between Canister Ends	0.15 m	(6 in.)
Depth of Borehole to First Canister	2.06 m	(6.75 ft)
Areal Heat Load	69.50 kW/acre	
Borehole Diameter	0.69 m	(27 in.)
Waste Package:		
Canister ID	30.48 cm	(12 in.)
Canister Wall Thickness	0.95 cm	(0.375 in.)
Assembly Air Gap	0.32 cm	(0.125 in.)
Overpack ID	33.02 cm	(13.0 in.)
Overpack Wall Thickness	3.18 cm	(1.25 in.)
Overall Length of Package	3.20 m	(10.5 ft)
Active Length	2.44 m	(8.0 ft)
Initial Canister Heat Load	2.21 kW	

The most significant new problem with the horizontal borehole analysis was the necessity of providing an accurate convective heat transfer coefficient in the large annular gap. Several references were found which dealt with pertinent information. An equation for the average equivalent conductivity in the gap as a function of Rayleigh number was interpreted from data given in Projahn, Reiger and Beer (1981). This data fit the following equation, which was given in Kuehn and Goldstein (1976a):

$$\overline{k}_{eq} = 0.200\ Ra^{0.25}$$

The significant length in the Rayleigh number is the gap width. Other references included Eckert and Drake (1972), Kuehn and Goldstein (1973 and 1976b), and Kwon, Kuehn and Lee (1982). These references include thorough bibliographies.

In spite of the attention given to the convective heat transfer in the annulus between the waste package and borehole wall, the radiation heat transfer across this gap accounts for about 95% of the total heat transfer. The emissivities of both surfaces were defined to be 0.8.

The analysis was performed by considering a single canister in the borehole. Exact symmetry does not exist; therefore, the assumption of symmetry imposes a small discrepancy. End effects in the borehole were not modeled.

The peak temperatures in the various components of the waste package and host rock are presented in Table 3.10 in Chapter 3 of Volume 1. These results apply to a local heat load of 69.5 kW/acre and a canister head load of 2210 W. These results compare closely with those indicated by Figure 3.5 (Cs/Sr canister in a vertical borehole without bentonite backfill) for the same loadings.

The comparison of the thermal performance of the HLW canister in a horizontal borehole with a Cs/Sr canister in a vertical borehole suggests a strong heat transfer similarity for similar waste package configurations, i.e., no bentonite backfill.

APPENDIX B

FRACTIONATION PROCESS EXPERIMENTAL RESULTS SUPPLEMENT

This appendix contains a more detailed presentation of the experimental work described in Chapter 4, Volume 1 of this report. This work is divided into two sections: that in support of the fractionation process itself, which involves the sorption of Cs on titanium phosphate and the sorption of Sr on hydrated antimony pentoxide (discussed in Section B.1); and that to define glass compositions capable of containing the Cs- and Sr-loaded sorbers (discussed in Section B.2). Finally, a revised fractionation flowsheet is presented and discussed in Section B.3.

B.1 FRACTIONATION PROCESS

The experimental work performed here included preparation of a simulated HLLW solution, study of the sorption of Cs, Sr, and other fission products on the inorganic ion exchange materials, measurement of the extent of cosorption of Am, and preliminary determination of the extent of sorber dissolution.

B.1.1 Preparation of Simulated High-Level Liquid Waste

The reference composition of the high-level liquid waste (HLLW) for this study is the same as that in DOE (1979a) except for a lower uranium content and the absence of gadolinium added as a soluble neutron poison. This reference composition is given in Table B.1. The concentrated HLLW solution also contains 2 M HNO_3.

The simulated HLLW used in the experimental work contained the elements listed in Table B.1 except for P, Y, Tc, Rh, Pd, Sn, Sb, Te, La, Pr, Nd, Pm, Eu, Gd, and the actinides. Additional Sm was added to compensate for the La, Pr, Nd, Pm, Eu, and Gd. Except for Mo where MoO_3 was used, the feed was prepared by dissolution of nitrate salts of the elements. It was not possible to keep all of the materials in solution at the concentrations indicated in Table B.1, even when the solution was diluted two-fold with water. Slow precipitation of some (unknown) materials occurred as the mixture aged. Analysis of the aged and clarified solution showed good agreement between the quantities

TABLE B.1. Reference HLLW Composition

Before Treatment[a]		As Oxide[b]	
Constituent	Concentration, Moles/L @ 567 L/MTHM	Constituent	Oxides, kg/MTHM
Inerts (Reprocessing chemicals):		Inerts (Reprocessing chemicals):	
Na	0.007	Na_2O	0.12
Fe	0.036	Fe_2O_3	1.6
Cr	0.0064	Cr_2O_3	0.28
Ni	0.0023	NiO	0.10
P	0.028	P_2O_5	1.1
		Subtotal	3.2
Fission Products:		Fission Products:	
Rb	0.0056	Rb_2O	0.30
Sr	0.014	SrO	0.84
Y	0.0074	Y_2O_3	0.48
Zr	0.058	ZrO_2	4.2
Mo	0.055	MoO_3	4.6
Tc	0.013	Tc_2O_7	1.2
Ru	0.036	RuO_2	2.7
Rh	0.0065	Rh_2O_3	0.47
Pd	0.0023	PdO	1.6
Ag	0.0010	Ag_2O	0.069
Cd	0.0014	CdO	0.102
Sn	0.0007	SnO_2	0.061
Sb	0.0002	Sb_2O_3	0.015
Te	0.0071	TeO_2	0.65
Cs	0.031	Cs_2O	2.6
Ba	0.018	BaO	1.5
La	0.014	La_2O_3	1.3
Ce	0.028	CeO_2	2.7
Pr	0.012	Pr_6O_{11}	1.3
Nd	0.043	Nd_2O_3	4.1
Pm	0.0009	Pm_2O_3	0.087
Sm	0.0090	Sm_2O_3	0.89
Eu	0.0019	Eu_2O_3	0.19
Gd	0.0012	Gd_2O_3	0.12
		Subtotal	32.1
Actinides:		Actinides:	
U	0.007	U_3O_8	1.1
Np	0.004	NpO_2	0.64
Pu	0.0005	PuO_2	0.07
Am	0.003	Am_2O_3	0.50
Cm	0.0007	Cm_2O_3	0.11
		Subtotal	2.4
		Total	37.7

(a) As nitrate salts in approximately 2 M HNO_3.
(b) The waste constituents are converted to their oxide form in the treatment process.

added and those found except for Zr, Mo, and Sm (the discrepancy with Sm was due to analytical problems). The quantity of Zr found was 50% of that added while only 15% of the added Mo was found in the aged and clarified solution. Precipitation of zirconium molybdate from HLLW solutions has been observed previously by others.

The diluted, aged, and clarified solution (denoted HLLW/2 to reflect the dilution factor) was then used in the sorption experiments after the addition of radioactive tracers to follow the behavior of Cs, Sr, and Am.

B.1.2 Sorption of Cesium on Titanium Phosphate

The titanium phosphate ion exchanger was obtained several years ago from S.E.R.A.I., Brussels, Belgium, under the registered trademark name of ABEDEM TiA. It was used without treatment except for a brief wash to remove fines.

The sorber was contained in a glass column whose temperature was maintained at 50°C by the circulation of water through a surrounding jacket. The HLLW/2 solution was passed down through the bed of titanium phosphate. The flow rate was adjusted and controlled manually with a stopcock.

Two runs (5D and 6A) were made with ^{137}Cs-spiked HLLW/2. Run 6A was also spiked with ^{241}Am; the behavior of this radioisotope will be discussed in a subsequent section.

In Run 5D, HLLW/2 was passed through a 10-cm^3 column (0.92 cm dia. x 15 cm high) containing 7.3 g of the titanium phosphate sorber material. The results, which are plotted in Figure B.1 on log probability coordinates, show that not until the 16th column volume did the concentration of Cs in the effluent reach a value as high as 0.1% of that present in the feed (DF = 10^3). The Cs concentration in the effluent then increased rapidly with each succeeding column volume, reaching 1% of that present in the feed (DF =10^2) after 17.5 column volumes, 10% (DF = 10) after nearly 20 column volumes, and 50% (DF = 2) after 23 column volumes.

The data from this run are presented differently in Figure B.2. In this figure two parameters are presented as a function of effluent volume (on linear coordinates). The parameters are the fraction of the Cs in the feed that is present present in the composite effluent and the loading of Cs on the column

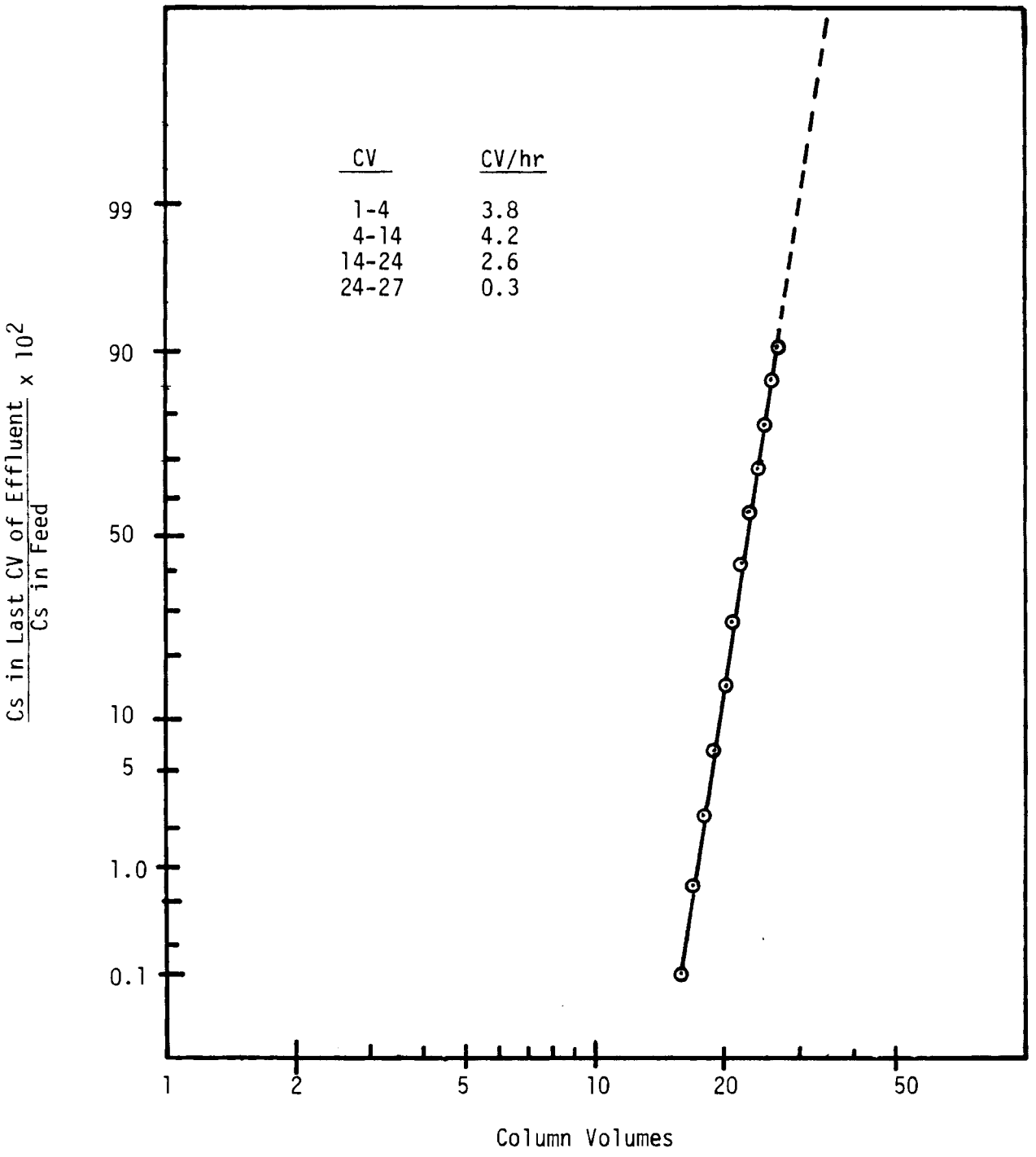

FIGURE B.1. Cs Sorption on Titanium Phosphate (Run 5D)

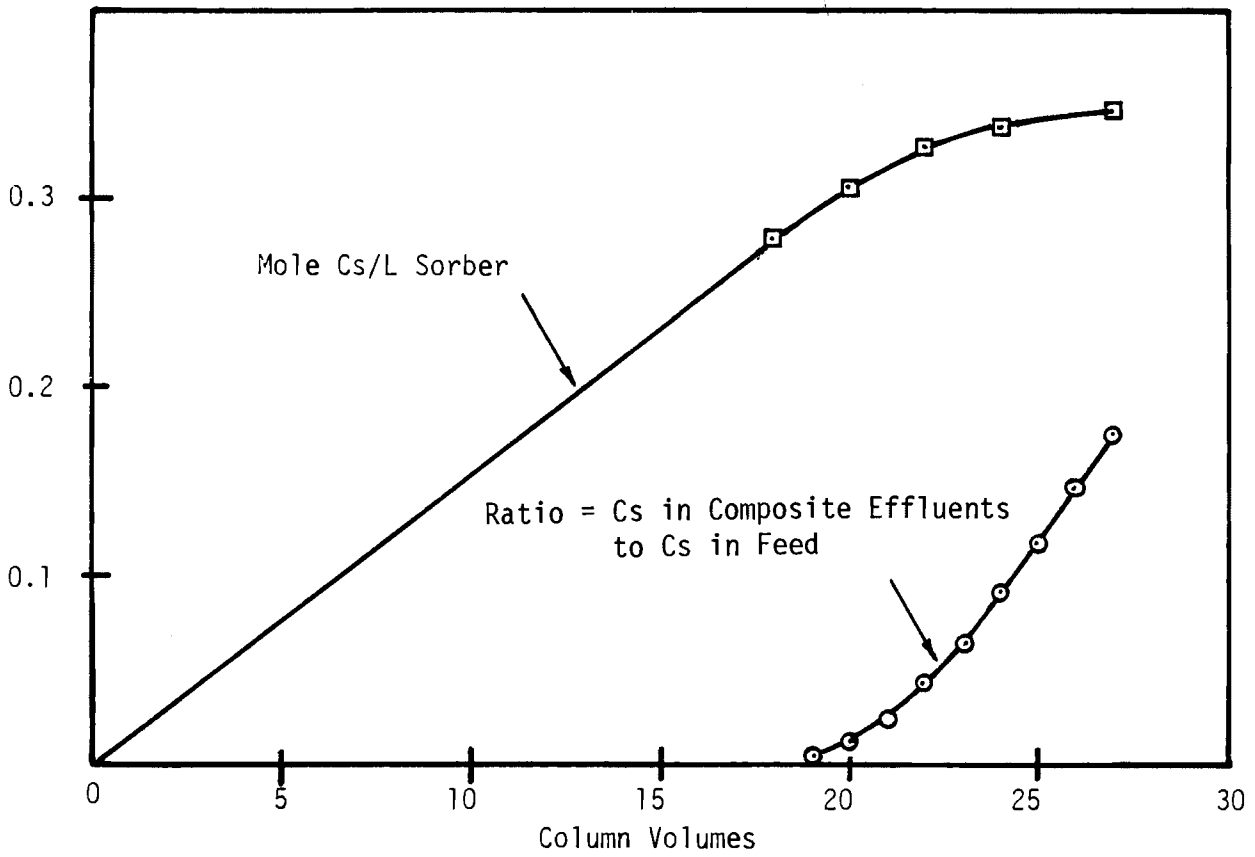

FIGURE B.2. Cs Loading on Sorber and Cs in Composite Effluent (Run 5D)

(mole Cs/L sorber). This figure shows, for example, that after 22 column volumes of feed have been passed through the column, the Cs content of the composite effluent was 4% of that present in the feed, and the quantity of Cs loaded on the sorber was 0.33 mole Cs/L sorber.

The quantity of Cs loaded on the sorber after 27 column volumes of feed was 0.346 mole Cs/L sorber (0.065 g Cs/g sorber). Because the concentration of Cs in the effluent at that time was nearly as high (90%) as that in the feed, very little additional Cs sorption would have occurred had the run been extended. This loading can thus be taken as the maximum possible from this solution.

Run 6A was done primarily to study ^{241}Am behavior in this system, but ^{137}Cs was also added to get additional data on Cs behavior. The Cs results,

shown in Figure B.3, are slightly different than those of Run 5D (Figure B.1) in that breakthrough occurred slightly earlier and a linear plot was not obtained. The reasons for these differences are not known.

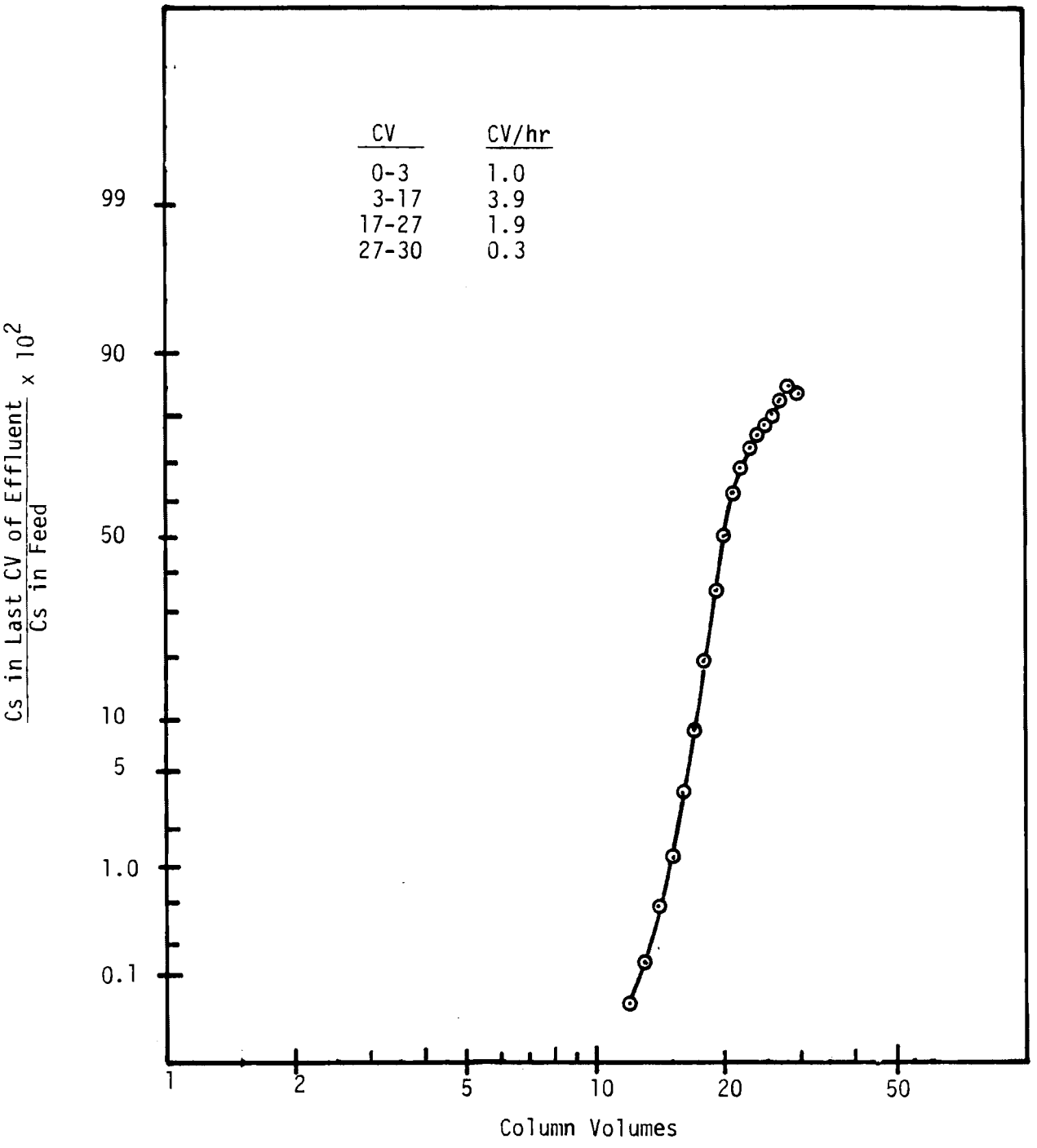

FIGURE B.3. Cs Sorption on Titanium Phosphate (Run 6A)

After the titanium phosphate sorber had been loaded to 85% Cs breakthrough in Run 6A, it was washed with 1 M HNO_3 to remove residual HLLW/2 solution (and possibly some weakly sorbed elements). The 1 M HNO_3 wash, which amounted to 6 CV, contained 10% of the Cs present in 30 CV of feed that had been fed to the column. This wash solution would have to be passed through a secondary column or be recycled to the feed to achieve a lower Cs loss.

B.1.3 Sorption of Strontium on Antimony Pentoxide

The hydrated antimony pentoxide ion exchanger, also known as polyantimonic acid (PAA), was obtained from Dr. L. H. Baetsle, Mol, Belgium, in 1968. It was precipitated by adding HCl to a solution of $K_2H_2Sb_2O_7$, and was recovered and dried. It was used without additional treatment except for acid washing to remove fines. The experimental procedures used with this sorber were the same as those used with titanium phosphate.

The first run with this sorber (Run 5E) used as feed the first portion of the effluent from C Run 5D, such that the Cs concentration was about 4% of that in the HLLW/2 solution. This solution was spiked with ^{85}Sr before being used in Run 5E so that the Sr behavior could be easily determined.

Run 5E employed a 10-cm^3 column of the hydrated antimony pentoxide sorber material, which weighed 9.23 g. The temperature was 50°C, and the flow rate was very low, an average of only 0.2 CV/hr. A low flow rate was desired because of the known slow kinetics of sorption of Sr on this sorber, but problems were encountered with column plugging that made the rate even lover than desired (and quite variable).

The Sr breakthrough data for Run 5E are plotted in Figure B.4. About 21 column volumes of solution passed through before the Sr content of the effluent reached 0.1% of that of the feed. After 23 column volumes, a 1% breakthrough was measured, a 10% breakthrough was achieved after 26 column volumes, and the breakthrough was about 50% after 30 column volumes.

The quantity of Sr loaded on the sorber at 50% breadthrough was 0.195 mole Sr/L sorber (0.0185 g Sr/g sorber). Extrapolation of the line in Figure B.4 to 90% breakthrough allows the Sr loading at that point to be estimated as 0.207 mole Sr/L sorber (0.0196 g Sr/g sorber).

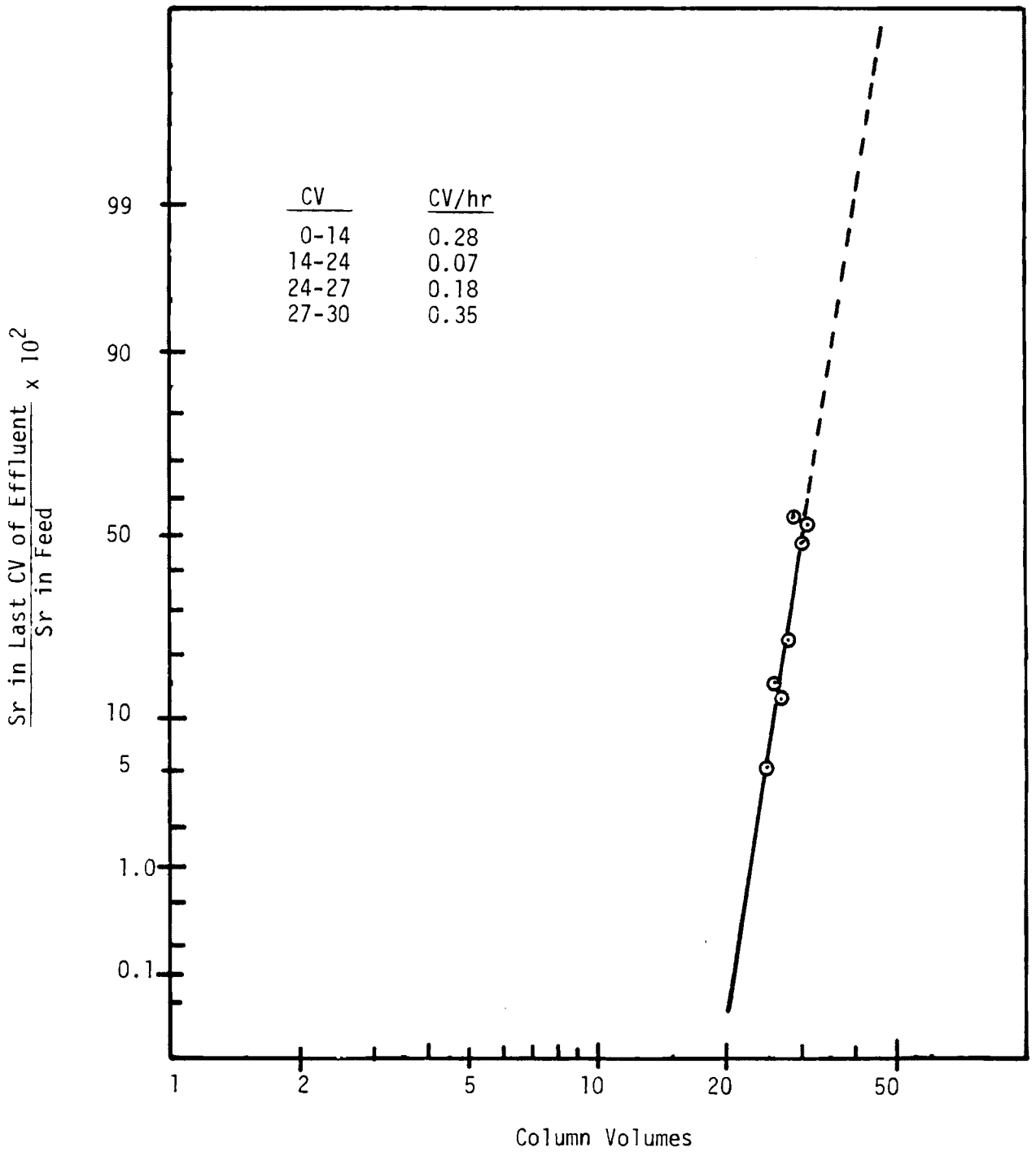

FIGURE B.4. Sr Sorption on Antimony Pentoxide (Run 5E)

The second run involving the sorption of Sr on hydrated antimony pentoxide (Run 9B) was done primarily to study ^{241}Am behavior with this sorber. The feed solution for this run was the first portion of the effluent from Run 6A (the Cs concentration was about 5% of that in the HLLW/2 solution), plus a spike of ^{85}Sr.

This run employed a 5-cm^3 column of the sorber material, which weighed 4.64 g. The temperature again was 50°C. The flow control was very poor during this run, which resulted in very erratic data but served to emphasize the importance of flow rate to Sr sorption.

Table B.2 contains a summary of the flow rate and Sr breakthrough data obtained in Run 6B. When the average flow rate during a 2 CV increment was near 1.0 CV/hr, the Sr breakthrough was very high (about 30%). However, much lower Sr breakthrough values (0.1%) were obtained at flow rates only 20-30%

TABLE B.2. Sr Breakthrough and Flow Rate Data (Run 6B)

Effluent Volume, CV	Flow Rate, CV/Hr	Sr Breakthrough, %[(a)]
2-4	0.87	2.9
4-6	0.95	30
6-8	0.95	16
8-10		0.7
10-12		0.1
12-14	0.77	0.2
14-16		0.5
16-18		1.8
18-20	1.00	8.3
20-22	0.80	31
22-24	1.00	30
24-26	0.67	4.6
26-28	0.80	0.9
28-30	0.54	0.3

(a) (Sr in Effluent) x 10^2/(Sr in Feed).

lower. This great a dependence of breakthrough on flow rate is surprising, but certainly emphasizes the point that flow rate is extremely important in this system.

B.1.4 Sorption of Americium

The Am (and other transuranic element) content of the separated Cs and Sr is desired to be low so that the containment requirements for the Cs/Sr waste can be less-stringent than for the fractionated high-level waste (FHLW). Americium is of primary concern here because the Pu is removed by other processes, and Np is not expected to be a problem.

Two sorption runs were made with feed spiked with ^{241}Am. One (Run 6A) tested the behavior of Am and Cs with titanium phosphate and the other (Run 6B) tested the behavior of Am and Sr with hydrated antimony pentoxide. The experimental conditions and the Cs and Sr results were discussed earlier. In neither of these runs was Am sorption detectable by comparison of the Am concentration in the effluent with that in the feed; the Am content of the effluent was approximately the same as that in the feed.

The loaded columns from these runs were washed with dilute HNO_3 to remove residual solution and then with 0.1 M EDTA (as a sodium salt) to complex and remove any Am that had been sorbed. The quantities of Am that were found in this manner were about 0.15% of that fed to the column in the titanium phosphate case and 0.35% in the hydrated antimony pentoxide case. These EDTA washes were continued well beyond the point at which the Am concentration in the wash solution reached a peak value in an effort to assure complete removal of Am from the sorbers.

The loadings of Cs and Sr on the sorbers in these experiments were only about 85% of the apparent maximum. It may be that a lower level of Am contamination could be achieved at higher loadings, but additional experimentation would be required to verify this.

B.1.5 Sorption of Fission Products Other Than Cesium and Strontium

The final sorption run of this project involved the use of HLLW/2 solution that did not contain any spikes of radionuclides. Instead the samples were analyzed by emission spectroscopy using an inductively coupled plasma (ICP)

spectrometer to see if any of the other fission product elements were sorbed by the exchangers used to remove the Cs and Sr.

This run (7A) used a single column made up of a mixture of the titanium phosphate and hydrated antimony pentoxide sorbers. Eleven grams of each sorber were used; the volume occupied by the mixture was 28.5 mL. Six 60 mL portions of the effluent were collected and analyzed, along with 120 mL of 1 M HNO_3 used to wash the column.

The only fission product element aside from Cs and Sr to be appreciably sorbed in this run was Zr. The data indicate that about 95% of the Zr fed to the column was sorbed by the exchangers. As was mentioned earlier, about half of the Zr added had been removed as a solid before the solution was used as feed. One of the exchangers evidently did sorb some colored material because some of the particles were blackened; it is likely that a small quantity of Ru accounted for this.

B.1.6 Dissolution of Sorbers

The ICP analyses of the effluent samples from Run 7A also provided some information on the dissolution of the titanium phosphate and hydrated antimony pentoxide sorbers. The apparent steady state concentrations of Ti and Sb in the effluent samples were about 0.6 g/L and 0.007 g/L, respectively. It is not known if these concentrations would vary with flow rate.

Phosphorus was also found in the effluent, but its pattern did not parallel that of Ti, indicating some unusual behavior. The P level in the first 60 mL was 1.1 g/L, but it rapidly decreased and leveled off at about 0.3 g/L. The 0.3 g/L value represents about 0.8 mole P/mole Ti, at the apparent steady state, whereas the P:Ti mole ratio over the total combined effluent and wash was about 1:4.

The total weights of Ti and P found in the effluent plus wash were equivalent to 0.0175 g Ti and 0.0161 g P per gram of titanium phosphate sorber. The Sb content of the effluent plus wash gave a value of 4.3×10^{-4} g Sb/g hydrated antimony pentoxide sorber. These values correspond to dissolution of about 7% of the titanium phosphate and 0.07% of the antimony pentoxide during this run.

B.2 VITRIFICATION OF CESIUM- AND STRONTIUM-LOADED SORBERS

Most of the details of this work were presented in Chapter 4 of Volume 1 and will not be repeated here. However, the composition of the frit used to prepare a glass containing the sorbers was not given previously. It is given in Table B.3.

TABLE B.3. Frit 131 Composition

Oxide	Wt%
SiO_2	57.9
B_2O_3	14.7
Na_2O	17.7
Li_2O	5.7
MgO	2.0
TiO_2	1.0
La_2O_3	0.5
ZrO_2	0.5

B.3 REVISED FRACTIONATION FLOWSHEET

The results of experimental work were generally in good agreement with the earlier estimates on which the preliminary reference flowsheet was based. However, some flowsheet revision was indicated by the experimental results. A revised flowsheet is shown schematically in Figure B.5, with flowsheet values presented in Table B.4. The flowsheet values that are based on the experimental work are identified with asterisks. A discussion of this flowsheet was presented in Chapter 4, but will be repeated here for completeness.

The first two process steps, HLW clarification and solvent extraction, serve to remove Pu so that the amount of this long-lived material associated with the Cs/Sr fraction will be minimized. The clarification step also reduces the likelihood of column plugging during the Cs/Sr sorption step.

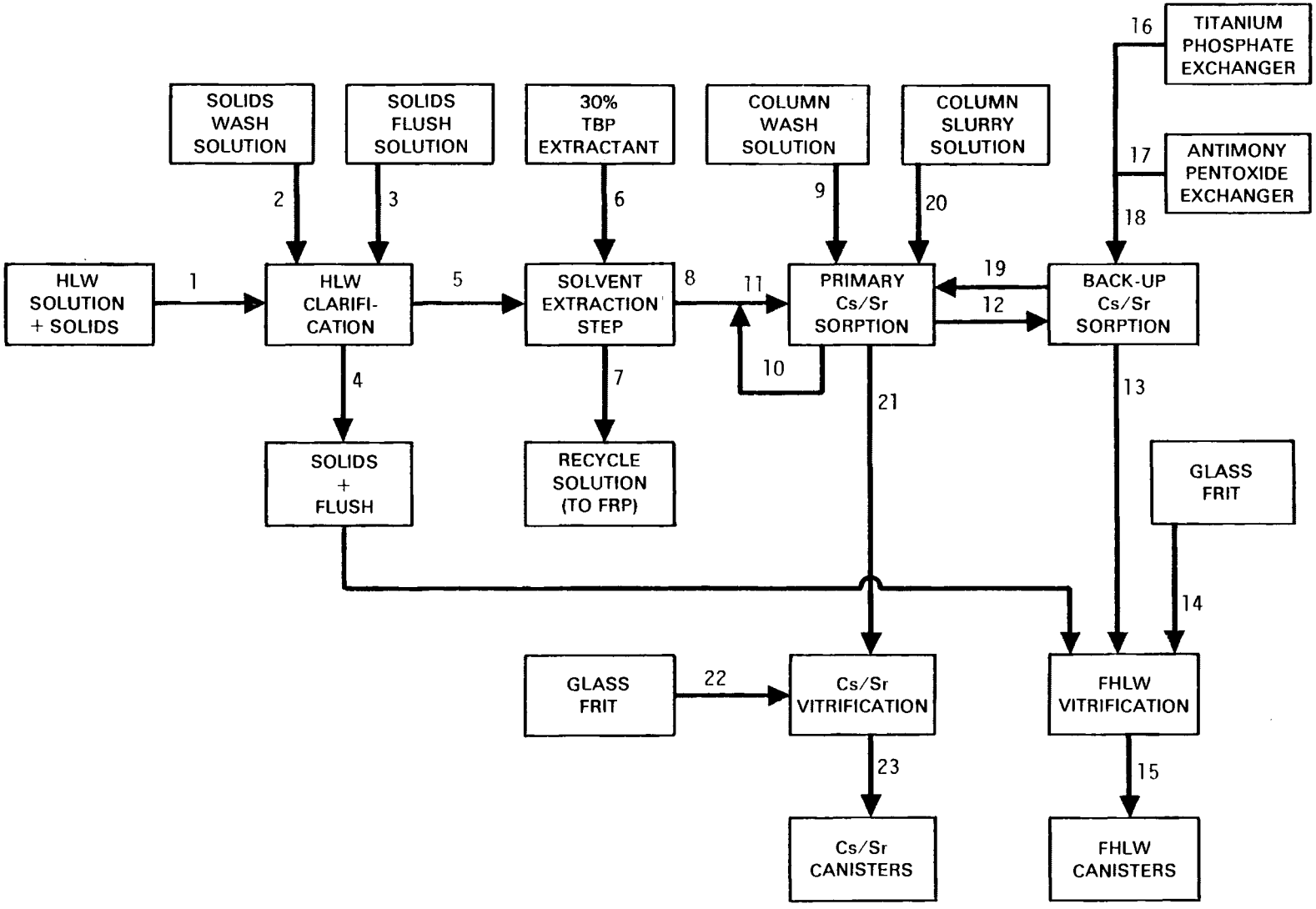

FIGURE B.5. Revised Cs/Sr Fractionation Flowsheet

TABLE B.4. Fractionation Flowsheet Values

	Stream Number																					
	1	2	3	4	5	6	7	8	9	10	11	12	13	14	15	16	17	18	19	20	21	22	23
M^3/MTHM (ft^3/MTHM)	0.57	0.10	0.22	0.22	0.67	0.67	0.67	0.67	0.46*	0.46*	1.14	1.14	1.14		0.036 (1.3)			0.093*					0.049* (1.73)
Column Volume/hr								2		0.7													
Kg/MTHM														79.6	114	36.0*	35.6*	71.6*				67.2*	132*
HNO_3,M	2.0	2.0	0.1	0.1	2.0		0.5	1.5	0.3	0.3	1.0	1.0	1.0										
Cs,M	0.031																						
Sr,M	0.014																						
Tl, kg/MTHM													0.63*										
P, kg/MTHM	0.49												1.07*										
Sb, kg/MTHM													0.015*										
Fission Product Fractions[a]																							
Cs	1.0			0.01	0.99			0.99		0.1	1.1	0.15	0.001		0.011				0.15		0 99*		
Sr	1.0			0.01	0.99			0.99		0.1	1.1	0.15	0.001		0.011				0.15		0.99*		
Ru	1.0			0.5	0.5			0.5				0.5	0.5		1.0						--		
Zr	1.0			0.2	0.8			0.8				--	--		0.2						0.8*		
Mo	1.0			0.5	0.5			0.5				0.5	0.5		1.0						--		
Rare Earths	1.0			0.01	0.99			0.99				0.99	0.99		1.0						--		
Actinide Fractions[a]																							
U	0.001			1×10^{-5}	0.001		0.001	5×10^{-5}					5×10^{-5}		6×10^{-5}						--		
Pu	0.005			0.004	0.001		0.001	5×10^{-5}					--		0.004						5×10^{-5}		
Np	1.0			0.01	0.99			0.99					0.99		1.0						0.005		
Am, Cm	1.0			1.01	0.99			0.99					0.99		1.0						0.005*		

(a) Radionuclide contents are given as fractions of the amount present in spent fuel.
* Values based on experimental results of this task.

The separated solids, estimated here to contain 80% of the Pu in the HLLW, are washed and then routed to fractionated high-level waste (FHLW) vitrification. These solids will also contain large fractions of the precious metals and Zr and Mo, and depending on the efficiency of washing, small fractions of all of the other materials present (1% of the Cs and Sr are assumed to accompany these solids).

The solvent extraction step is aimed solely at removing most of the Pu remaining in the HLLW (estimated as 0.1% of that in the fuel), to minimize the amount of Pu in the Cs/Sr fraction. Conservatively, only 95% extraction of this Pu is assumed, leaving 5×10^{-5} as much Pu in the HLLW as is present in the spent fuel being processed. The organic extract from this step is assumed to be recycled to the main fuel reprocessing plant (FRP) for recovery of the contained Pu and treatment of the solvent.

A possible alternative process for minimizing the Pu content of the Cs/Sr fraction, which could be used either instead of or in addition to the solvent extraction step, would be to treat the HLLW to reduce the Pu from the tetravalent state to the trivalent state or to oxidize it to the hexavalent state. Tetravalent Pu is sorbed along with the Cs and Sr, but trivalent Pu, by analogy with the behavior reported for U, would be sorbed very little. This process concept has not been evaluated, however.

The solvent extraction step also reduces the concentration of HNO_3 in the HLLW, which is desirable for more efficient Cs/Sr sorption. The acidity of this solution is further reduced (to 1 M) by blending in the sorption column wash solution before the solution is fed to the primary Cs/Sr sorption column.

The Cs/Sr sorption columns contain (for the reference feed) nearly equal weights of the two sorber materials, titanium phosphate and hydrated antimony pentoxide. They are mixed together in one column, rather than being contained in separate columns, because the combined vitrification process developed in the experimental work allows this simpler mode of operation. A secondary benefit of this mode of operation may be that the experiment with a mixed bed had no problems with column plugging and flow control, while those with hydrated antimony pentoxide alone did suffer from such problems.

The flow rate of the diluted HLLW through the combined Cs/Sr sorbent columns must be kept fairly low (0.7 CV/hr) even at a temperature of 50°C to allow good Sr recovery and loading. At this rate, about 17 hours would be required for a loading cycle on a column large enough to handle a 1-day output of HLLW from a 6.67 MTHM/day (2000 MTHM/yr) reprocessing plant.

Two Cs/Sr sorption columns in series are provided to allow maximum Cs/Sr loadings to be achieved, which may be required to minimize Am contamination of the Cs/Sr (although it has not been shown that high loadings are indeed necessary to accomplish this). The primary column is loaded to about 85% breakthrough, with the backup column serving to maintain very low Cs and Sr levels in the FHLW, before feed flow is diverted from it directly to the backup column. At this time, a third column is brought on line as a new backup column, with the initial backup column becoming the new primary column.

The primary column is washed with dilute HNO_3 to remove the residual feed solution and thus minimize the transuranic element contamination of the Cs/Sr. This wash solution also contains appreciable amounts of Cs and Sr, so it is recycled. This recycle stream also serves to dilute the incoming feed solution to 1 M HNO_3, for improved sorption efficiency.

The washed sorbers are then transferred to the Cs/Sr vitrification process. There they are mixed with the appropriate quantity of glass frit and melted to form a glass, encapsulated in steel canisters. This waste stream is estimated to contain about 99% of the Cs and Sr and about 80% of the Zr present in the processed fuel. The transuranic element content of this Cs/Sr fraction should be about 0.5% of the Am and Cm, <0.5% of the Np, and 0.005% of the Pu in the spent fuel. The Am and Cm contents are based on the experimental work. The Np content is based on the assumption that Np would be less-strongly sorbed than Am, and the Pu content is based on the estimated removal in the solvent extraction step.

The weight of the vitrified Cs/Sr was estimated from the input weights assuming that Cs, Sr, and Zr were converted to their most common oxides; that the titanium phosphate remained unchanged in the glass; and that the hydrated antimony pentoxide was converted to Sb_2O_3. The antimony content of the hydrated antimony pentoxide was assumed to be 58%.

After passing through the two Cs/Sr sorption columns in series, the HLLW solution contains only about 0.1% or less of the Cs and Sr present in the feed. It is mixed with the solids initially separated from the HLLW (estimated to contain 1% of the Cs and Sr) and with glass frit and is melted to form a glass, which also is encapsulated in steel canisters. This FHLW stream contains only about 1% of the Cs and Sr but essentially all of the Am, Cm, and Np present in the untreated HLLW. The volume of glass required to immobilize the FHLW is not increased due to the addition of chemicals during the processing; the required volume is actually decreased slightly because of the removal of the Cs, Sr, and Zr.

APPENDIX C

COST ANALYSIS SUPPLEMENT

This appendix provides some additional details relative to the procedures, assumptions and data used to develop the cost analysis described in Chapter 5, Volume 1 of this report. Section C.1 presents details of high-level waste transportation costs. Section C.2 describes the computer model developed to perform the cost-comparison analysis for the three alternative cases, and Section C.3 presents the system cost calculation results.

C.1 HIGH-LEVEL WASTE TRANSPORTATION COSTS

This section provides supplementary information on the derivation of the individual components of high-level waste (HLW) transportation costs. Table C.1 summarizes the important rail cost characteristics and shipping parameters as conceptually modified for this study.

TABLE C.1. Characteristics and Shipping Parameters for the Rail HLW Shipping Systems[a]

Canister Diameter[b] (ft)	Heat Generation Rates (kW/canister)	Cask Capacity (canisters)	Net Waste Capacity[c] (kg)	Thickness of Shielding (cm Pb/Du)[d]	Cask Empty Weight (mg)	Cask Loaded Weight (mg)
0.5	0.2	27	3780	16.4/11.5	92.5	97.9
	1	27	3780	19.2/12.5	98.9	104.3
	2	25	3500	20.0/12.7	101.4	106.4
1.0	0.2	9	4950	15.4/11.2	90.8	97.9
	1.5	9	4950	18.2/12.1	97.2	104.3
	3	9	4950	19.2/12.5	98.9	106.0
1.7	0.2	4	6400	14.2/10.7	88.1	96.8
	2	4	6400	17.7/11.9	96.0	104.7
	4	4	6400	18.2/12.1	97.2	105.9
2.5	0.2	2	6880	13.9/10.4	87.8	97.0
	2.5	2	6880	16.4/11.4	92.5	101.7
	5	2	6880	17.5/11.7	95.7	103.9

(a) Based on the conceptual rail cask described in Peterson and Rhoads (1978).
(b) All canisters are assumed to be 3.1 m (10 ft) in length.
(c) Given as kg of HLW glass per shipment.
(d) Given as cm of lead on cask body/cm of depleted uranium on cask ends.

C.1.1 Shipping Charges

Shipping charges are the fees assessed by railroad carriers to deliver the shipping containers to the terminal facilities.

Rail shipping charges are not uniform with the distance traveled and are specific for each origin-destination combination. Each origin and destination lies in a "rate-basing area," which is a major rail point where branch lines connect to local towns or communities. The shipping charges are assessed for transporting a commodity between specific rate-basing areas, regardless of the route or mileages traveled. Furthermore, the shipping charges can be affected by topography, competition, and state regulations. For this study, representative charges were obtained from the Traffic Division at Rockwell Hanford Operations (Daling 1983) for several origin-destination combinations that lie approximately 1500 miles apart. These data were normalized to a 1500-mile shipping distance and averaged. The average shipping charge obtained was $13.50 per 100 pounds and $12.75 per 100 pounds for loaded and empty shipments, respectively. These charges are for general freight service, i.e., it is assumed that special train shipments are not required. These freight charges are based on shipment of irradiated LWR fuel; however, HLW and spent fuel shipments are expected to be shipped under the same rail classification and thus the freight rates should be the same.

C.1.2 Shipping Container Leasing Fees

Shipping container leasing fees are the charges assessed by cask supplier companies for the use of their equipment. These charges are based on capital cost estimates that reflect manufacturers' profits, engineering and development costs, sales, overheads, and similar expenses in addition to material and fabrication costs. Cask use and service charges also include maintenance costs. Capital cost estimates for the reference conceptual rail cask have been calculated in DOE (1979a) in mid-1976 dollars and are escalated to mid-1982 dollars using an escalation factor of 1.71.

Leasing fees for each rail cask configuration are assumed to be proportional to the amount of shielding and therefore to the empty cask weight. A leasing fee was calculated in DOE (1979a) and was escalated to mid-1982 dollars

and used as a basis for calculating the leasing fees for other rail cask configurations. The base leasing fee is $3750/day (mid-1982 dollars), which converts to 0.037 dollars per day per kg of empty cask weight. This factor is applied to the other empty cask weights shown in Table 5.2 in Chapter 5 (Volume 1) and results in the leasing fees shown in Table C.2.

TABLE C.2. HLW Rail Shipping Cask Leasing Fees

Canister Diameter (ft)	Heat Generation Rate (kW/canister)	Cask Leasing Fee ($/day)
0.5	0.2	3400
	1	3650
	2	3750
1.0	0.2	3350
	1.5	3600
	3	3650
1.7	0.2	3250
	2	3550
	4	3600
2.5	0.2	3250
	2.5	3400
	5	3550

C.1.3 Special Equipment and Security Costs

Current NRC regulations (10 CFR 73) require specially trained personnel and specially equipped vehicles for shipments of spent nuclear fuel. It is not known at this time whether these precautions will be required for future shipments of HLW. For this study, it is assumed that these security precautions are required for rail shipments of HLW and an additional charge for these services is included in the total transportation costs.

Rail carriers have no provisions to supply an armed escort service. They have indicated, however, that they will supply a car or caboose for escorts to

ride in at the cost of a coach-class passenger ticket, or approximately $0.09 per mile per escort (Daling 1983). The wages and living expenses for the escorts must also be added to this charge. These charges were calculated for rail shipments, assuming two escorts per shipment for continuous surveillance, at $3.18 per mile. A special equipment charge of $0.92 per loaded mile was also applied to rail shipments.

C.1.4 Demurrage Fees

The final fee included in the transportation cost calculations is a charge for detention or demurrage of transportation equipment and drivers (or escorts) at the terminal facilities while the cargoes are being loaded or unloaded. This fee is assessed to compensate for idle equipment and for the drivers' wages and living expenses during this time. To calculate these charges, turnaround times must be defined for the shipping systems. Turnaround time is the length of time between arrival of an empty (or loaded) container at the facility and departure of the loaded (or empty) container from the facility. The average turnaround time for a rail cask is 48 hours.

Rail demurrage fees need not include the wages and living expenses of the escorts. Since the escorts are not required for empty shipments, they are assumed to return to their domicile locations or return to another shipment origin as soon as they arrive at the destination facility. Therefore, the demurrage fee for rail shipments is the cask rental fee per unit time multiplied by the average turnaround time for the rail cask. Demurrage fees are assessed both for the unloading and loading operations.

C.2 THE RECON MODEL

This section briefly describes the computer model developed to perform the cost-comparison analysis of the three basic alternative cases for the geologic repository design outlined in Section 5.1.5 of Chapter 5 (Volume 1). The model is designed to produce preliminary cost estimates and is particularly useful in parametric analyses such as this study.

The RECON model consists of a series of modules describing operations and costs for different repository segments. Figure C.1 is a simplified schematic

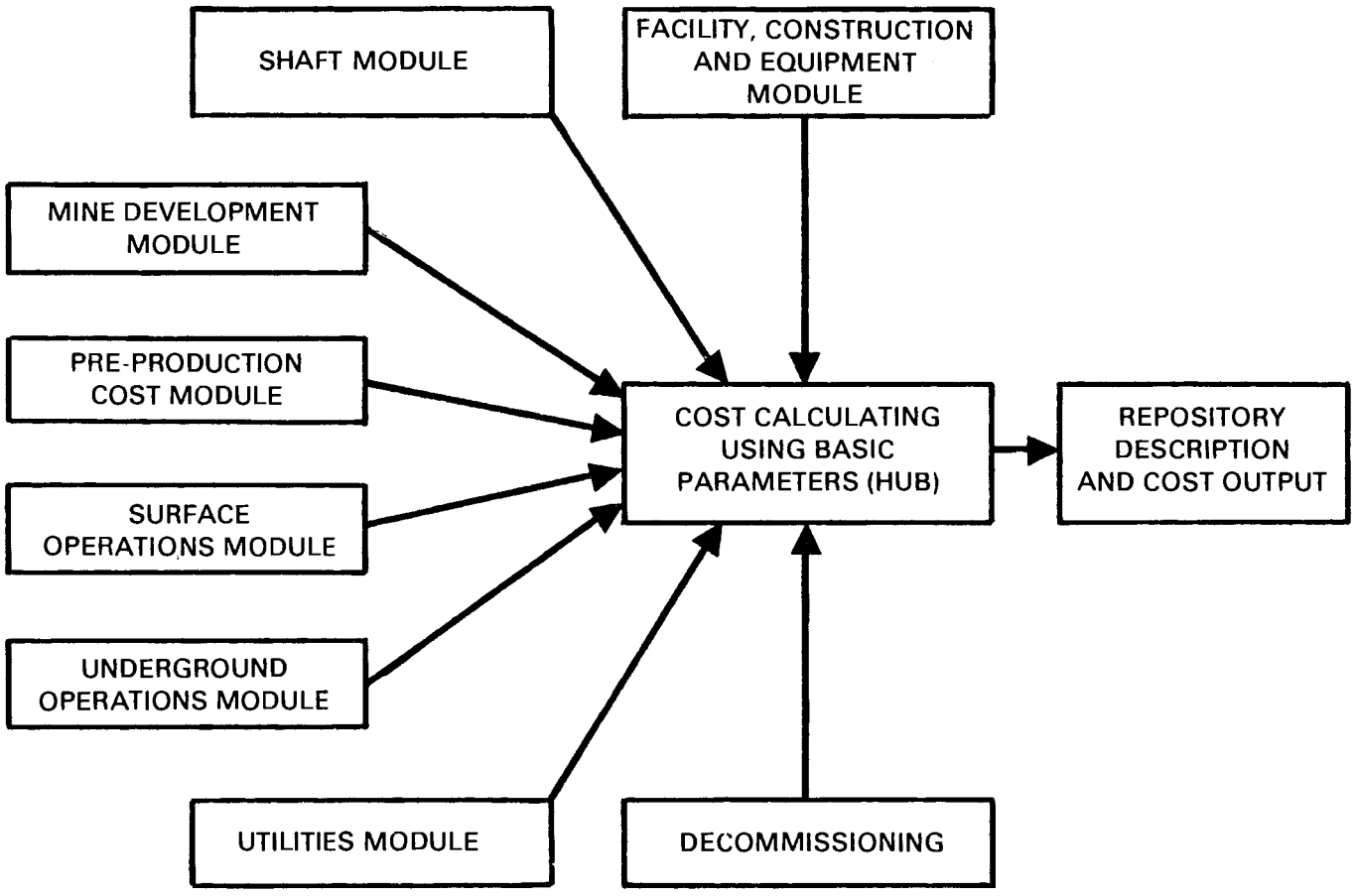

FIGURE C.1. RECON Cost Model Illustration

showing the different modules in the RECON model and the basic calculational flows. Calculations in one module affect and influence calculations in other modules, but these relationships are not shown. Each module is a cost center, meaning that cost calculations as a function of time and waste type are performed internally in each module and then are sent to the center module, which is called HUB. The HUB module takes each cost calculation and develops the total cost, the cash flow, and the levelized unit cost for each cost center. These costs are then combined into appropriate categories and summarized in the output tables. The modular construction of the cost model enhances the accuracy because it breaks the cost calculations down into more detailed cost components. The RECON model is able to handle long repository operating and decommissioning periods and multiple waste types and will calculate costs for multiple repositories. The basic logic and content of each of the modules in Figure C.1 are described in more detail in the following subsections.

C.2.1 Surface Operations

The surface operations module calculates three important repository parameters: the period of waste receipts, the labor requirements and costs, and the cost of materials used in waste operations.

An annual schedule of waste receipts is required as input. The RECON model attempts to process all of these wastes annually to the extent possible. Receipts are limited by a specified maximum number of shifts and the amount of wastes that can be processed per shift. Within these limits the model calculates the number of shifts that will be required to process the annual waste stream and the number of receiving modules required. The repository life is calculated by determining the annual repository area required for waste emplacement. The annual emplacement requirement is subtracted every year from a total available emplacement area within the repository. When the total available emplacement area reaches zero, the repository is filled.

Annual emplacement area requirements are determined by calculating canister emplacement densities by waste types and dividing these into the total number of canisters available for emplacement in that year. Canister emplacement densities for remote-handled wastes of each waste type are determined by the pitch (the spacing between canisters in a row), the number of rows per room

and the room spacing. Emplacement densities for contact-handled waste are based on room widths, room length, container dimensions, and room height.

Canister emplacement density is limited by three thermal criteria. The far-field thermal limit constrains heat loading in terms of heat per unit of repository area, based on the total area of the repository occupied by each waste type, including the shaft pillar and main corridors. The near-field thermal limit constrains heat loading in terms of heat per unit area for the repository's emplacement area. This area includes the room and the rock pillars supporting the room. The very-near-field thermal limit is defined by maximum allowable temperatures in both the media and the canister components. This latter criterion is handled in the model in terms of a limiting pitch (input) that is calculated externally as a function of the number of rows per room, room spacing, thermal output per canister, and package configuration.

Finally, this module calculates packaging and maintenance materials costs based on the number of canisters and the unit packaging materials costs. Maintenance materials are costs for miscellaneous materials in the repository and are assumed to be equal to 60% of direct labor costs for the reference case. The RECON model performs the above cost calculations for each waste type in the repository.

C.2.2 Mine Development

The mine development module calculates the mining and rock logistic parameters for the repository. The mining requirements are based on a mine configuration specified by the total available repository area, room sizes, panel sizes, extraction ratio, drift and main corridor dimensions, and exclusion areas. Exclusion areas include the main shaft pillar and other areas not available for mining rooms. The module logic is based on a rectangular layout for the rooms and corridors. Room heights are determined as a function of canister length or can be input-specified. Corridor heights are specified as input. A differentiation is made between main corridors and drift corridors serving the rooms. Mined-rock volume calculations assume a rectangular shape for the rooms and corridors.

Based on input-determined timing, mining of waste emplacement rooms begins before emplacement is required. After mining, the rock is transported either to the shaft for transportation to the surface or to backfilling operations if they have commenced. Calculations are made of rock quantities hoisted to the surface, stored on the surface, and transported offsite. Backfilling operations begin after a specified demonstration period. The module assumes that any rock needed for backfilling operations is supplied from rock mined for emplacement operations in that year. Rock volumes excavated in excess of that needed for backfilling are transported to the surface. Backfill volume calculations include the effect of rock expansion after it is mined, the addition of any supplemental backfill material, and the backfill density in the rooms. The module has the capability to examine different room sizes and extraction ratios for each waste type and assumes separate rooms for each waste type. After operations have ceased or the demonstration period has ended, rock is brought down from the surface to backfill remaining rooms, corridors, and shafts during the decommissioning period. Cost calculations in this module are based on unit costs times volume or mass for direct mining, hauling, storage, and backfilling. Fixed costs for mining equipment are also included.

C.2.3 Waste Receiving and Packaging

The waste receiving and packaging subroutine defines repository receiving and packaging capacity in terms of a unit module having specified capacity and cost. Different modules are specified for receiving remote-handled waste and contact-handled waste. The number of receiving and packaging modules required as a function of time is based on the number of waste units received and the capacities of each module. The RECON model also adds receiving modules if these are required during operations. The model distributes the capital costs for these receiving module additions over a specified time period before the module is needed to simulate a capital cost addition.

C.2.4 Shafts

This subroutine estimates cost functions for excavating, lining, and equipping the various shafts. The RECON model delineates seven different types of shafts:

- men and materials
- mining ventilation
- canistered waste
- low-level waste
- development exhaust
- storage exhaust
- mine production.

The user initially specifies the number and description of each type of shaft desired. Included in this description are the shaft diameter, the shaft depth, the lined depth, the hoisting and shaft equipment cost, and the underground shaft station cost of each shaft. Cost functions are defined for excavation and lining costs as functions of depth and diameter for each medium. Cost functions for water control determine these costs as a function of medium. The shaft module also defines the number of additional waste or mine production shafts needed, based on shaft capacity and annual rock and waste volumes handled.

C.2.5 Underground Operations

The underground operations module describes emplacement operations underground for the repository. Options are provided for hole drilling, trenching, or simple placement in rooms. For this study remote-handled waste packages were assumed to be placed in vertical holes in the floor. The package diameters for the various types of waste packages and the annular radii of hole barriers and backfill are required as input. Based on this data, the module determines the hole diameter for input to the hole drilling cost function.

Hole depth is also determined as a function of package length and cap length of input to the hole drilling cost function. Based on costs for a reference diameter and reference depth, unit barrier costs are determined as functions of their annular radii and the hole depth. Labor requirements for transporting and emplacing the wastes, hole barriers, and underground waste handling equipment costs are all included as separate items.

C.2.6 Utilities

This module estimates utilities' costs based on power, steam, water, and vehicle fuel requirements. Power costs are stated in terms of normal power operating levels in kilowatts for the different facilities in the repository. Time periods for power requirements are based on the average operating period for each type of facility each year. Utility requirements for mining operations are included as receipt rate functions.

C.2.7 Facility, Construction, and Equipment Costs

This module estimates construction costs for facilities and initial equipment and equipment replacement costs for capital equipment. Costs are estimated for each facility type. Equipment replacement costs are based on average equipment life for each type of facility. The timing of equipment replacement is also included to accurately model the cash flow requirements.

C.2.8 Preproduction

This module includes land acquisition, startup, and architect-engineering costs. Startup and architect-engineering costs are functions of equipment and total field costs, respectively. Field costs are defined as land, siting, construction, equipment, and preoperational mine excavation costs.

C.2.9 Decommissioning

This module includes final backfilling, shaft sealing, facility decommissioning, and surveillance costs. Final backfilling costs include backfilling of unfilled rooms, corridors, and the shaft pillar area. Shaft sealing costs are included as total costs per shaft as a function of shaft diameter. Facility decommissioning costs are estimated as a percentage of total facility construction costs. Surveillance costs are assumed to be a constant annual cost over a specified time period after decommissioning is completed.

C.2.10 HUB

This part of the program calls each of the above modules in the proper order so that calculational outputs from each module are available for input into succeeding modules. HUB also uses the results of the cost calculations in

each module to assemble costs, cash flows, and unit costs. After these calculations are made, HUB sends this data to the output table subroutines where they are printed. Output tables are printed for waste type for each repository as well as for repository totals.

C.3 SYSTEM COST CALCULATION RESULTS

Results of the waste management system cost calculations that led to determination of minimum (optimum) system cost configurations are presented in this section. The procedure for these calculations is discussed in Section 5.2 in Chaper 5 of Volume 1.

For the bentonite backfill cases, three system cost calculations at three different canister pitches were made at each bentonite temperature and each canister diameter for each waste type. The results of these calculations are presented in Tables C.3 through C.6 for the HLW, in Tables C.7 through C.10 for the FHLW recycle case, in Tables C.11 through C.14 for the FHLW W/O recycle case, and in Tables C.15 through C.17 for the aged-HLW case. Similar tables keyed to maximum basalt temperatures are shown in Tables C.18 through C.20 for the Cs/Sr case.

The minimum costs and the canister heat loadings that were obtained from plotting each of the above sets of three calculations are presented in Tables C.21 through C.32. These minimum costs were shown plotted against canister diameter in Figures 5.9 through 5.13 in Section 5.2.1 in Chapter 5. The canister heat loadings at these minimum costs were shown plotted against canister diameter in Figures 5.14 through 5.18, also in Section 5.2.1. It was from these latter plots that the optimum canister size and loading were obtained for specified minimum specific-waste-volume constraints.

Results of the system cost calculations for the modified procedure used for the comparison without the bentonite backfill are shown in Tables C.33 through C.37. Here calculations were made for each of the three pitch intersections at each centerline temperature in Figures 5.19 through 5.22. The optimum canister size and pitch (and indirectly the canister loading) were then obtained from a plot of the Table C.33 through C.37 results.

TABLE C.3. 50,000 MTE System Costs for HLW in 0.5-ft-Diameter Canisters

Maximum Bentonite Temperature, C°	100°			150°			200°			250°		
Pitch, m	2.0	3.0	6.0	2.0	3.0	6.0	2.0	3.0	6.0	2.0	3.0	6.0
KW/Canister	.15	.17	.20	.31	.38	.45	.50	.61	.73	.70	.85	1.03
MTE/Canisters	.139	.157	.185	.287	.352	.417	.463	.565	.676	.648	.787	.954
No. Canisters, 10^3	360.0	317.6	270.0	174.2	142.1	120.0	108.0	88.5	78.97	77.2	63.5	52.4
System Cost, $\$10^9$												
Fractionation												
Vitrification	4.86	4.37	3.92	2.70	2.34	2.04	1.89	1.64	1.44	1.49	1.30	1.13
Storage												
Transportation	2.23	1.97	1.67	1.10	.90	.76	.69	.57	.48	.50	.42	.35
Repository	11.7	11.5	15.1	7.2	7.1	8.3	5.4	5.2	5.8	4.55	4.40	4.80
Total	18.79	18.84	20.69	11.00	10.34	11.10	7.98	7.42	7.72	6.54	6.12	6.28
Repository Cost W/O Ti-clad Overpack	10.4	11.2	14.3	6.7	6.7	7.7	5.1	5.1	5.5	4.2	4.25	4.65
System Cost W/O Ti-clad Overpack	17.49	17.54	19.89	10.50	9.94	10.50	7.68	7.31	7.42	6.19	5.97	6.13

TABLE C.4. 50,000 MTE System Costs for HLW in 1.0-ft-Diameter Canisters

Maximum Bentonite Temperature, C°	100°			150°			200°			250°		
Pitch, m	2.4	4.0	7.2	2.4	4.0	7.2	2.4	4.0	7.2	2.4	4.0	7.2
KW/Canister	0.15	.19	.23	.37	.47	.54	.60	.76	.87	.87	1.09	1.23
MTE/Canisters	.130	.176	.213	.343	.435	.500	.556	.704	.806	.806	1.009	1.139
No. Canisters, 10^3	384.6	284.1	234.7	145.8	114.9	100.	89.93	71.02	62.09	62.04	49.55	43.90

System Cost, $\$10^9$												
Fractionation												
Vitrification	7.69	6.11	5.28	3.68	3.10	2.80	2.56	2.17	1.96	1.96	1.66	1.51
Storage												
Transportation	6.85	5.09	4.22	2.64	2.09	1.82	1.64	1.31	1.15	1.15	.92	.83
Repository	14.9	14.7	16.8	8.0	7.6	8.3	5.6	5.4	6.0	4.5	4.5	4.9
Total	29.44	25.90	26.30	14.32	12.79	12.92	9.80	8.88	9.11	7.61	7.08	7.24
Repository Cost W/O Ti-clad Overpack	12.9	13.1	15.0	7.1	6.9	7.7	5.1	5.1	5.7	4.20	4.25	4.70
TOTAL	27.44	24.30	24.50	13.42	12.09	12.32	9.30	8.58	8.81	7.31	6.83	7.04

TABLE C.5. 50,000 MTE System Costs for HLW in 1.7-ft-Diameter Canisters

Maximum Bentonite Temperature, C°	100°			150°			200°			250°		
Pitch, m	2.9	4.5	8.0	2.9	4.5	8.0	2.9	4.5	8.0	2.9	4.5	8.0
KW/Canister	.17	.23	.27	.43	.55	.64	.74	.91	1.04	1.08	1.29	1.46
MTE/Canisters	.157	.213	.250	.398	.509	.593	.685	.843	.963	1.00	1.194	1.352
No. Canisters, 10^3	318.5	234.7	200.0	125.6	98.2	84.3	73.0	59.3	51.9	50.0	41.88	36.98

System Cost, $\$10^9$												
Fractionation												
Vitrification	11.31	8.80	7.51	5.28	4.37	3.88	3.74	2.94	2.67	2.60	2.26	2.07
Storage												
Transportation	12.42	9.20	7.86	5.00	3.94	3.41	2.96	2.43	2.13	2.06	1.74	1.55
Repository	19.5	15.0	19.5	8.1	7.6	8.5	5.8	5.5	6.2	4.7	4.5	5.0
Total	43.23	33.00	34.87	18.38	15.91	15.79	12.50	10.87	11.00	9.36	8.50	8.62
Repository Cost W/O Ti-clad Overpack	16.5	12.8	15.8	7.2	7.0	7.8	5.2	5.1	5.7	4.2	4.3	4.6
TOTAL	40.23	30.80	31.17	17.48	15.31	15.09	11.90	10.47	10.50	8.86	8.30	8.22

TABLE C.6. 50,000 MTE System Costs for HLW in 2.5-ft-Diameter Canisters

Maximum Bentonite Temperature, C°	100°			150°			200°			250°		
Pitch, m	3.5	5.0	8.0	3.5	5.0	8.0	3.5	5.0	8.0	3.5	5.0	8.0
KW/Canister	.24	.33	.36	.58	.71	.80	.95	1.12	1.28	1.34	1.58	1.80
MTE/Canisters	.222	.306	.337	.537	.657	.741	.886	1.041	1.185	1.241	1.463	1.667
No. Canisters, 10^3	225.2	163.4	148.4	93.1	76.1	67.5	56.8	48.0	42.2	40.3	34.2	30.0

System Cost, $\$10^9$												
Fractionation												
Vitrification	12.27	9.56	8.83	6.14	5.29	4.79	4.23	3.67	3.38	3.26	2.89	2.63
Storage												
Transportation	17.68	12.84	11.68	7.35	6.03	5.36	4.52	3.84	3.38	3.23	2.76	2.43
Repository	14.0	12.9	14.1	8.1	7.7	8.0	5.7	5.6	5.6	4.7	4.35	4.45
Total	43.95	35.30	34.61	21.59	19.02	18.15	14.45	13.11	12.36	11.19	10.00	9.51
Repository Cost W/O Ti-clad Overpack	12.0	10.8	12.3	6.9	6.5	7.1	4.9	4.8	5.0	3.9	3.95	4.1
TOTAL	41.95	33.20	32.81	20.39	17.82	17.25	13.65	12.31	11.76	10.39	9.60	9.16

TABLE C.7. 50,000 MTE System Costs for FHLW (W/Recycle) in 0.5-ft-Diameter Canisters

Maximum Bentonite Temperature, C°	100°			150°			200°			250°		
Pitch, m	2.0	3.0	6.0	2.0	3.0	6.0	2.0	3.0	6.0	2.0	3.0	6.0
KW/Canister	.15	.17	.22	.31	.38	.45	.50	.61	.73	.70	.85	1.03
MTE/Canisters	.495	.561	.660	1.023	1.254	1.485	1.650	2.013	2.409	2.310	2.805	3.399
No. Canisters, 10^3	101.0	89.1	75.8	48.9	39.9	33.7	30.3	24.8	20.8	21.6	17.8	14.7
System Cost, $\$10^9$												
Fractionation	.88	.88	.88	.88	.88	.88	.88	.88	.88	.88	.88	.88
Vitrification	1.31	1.20	1.06	.76	.66	.59	.55	.46	.42	.43	.37	.32
Storage												
Transportation	.63	.55	.47	.31	.25	.22	.19	.16	.14	.14	.12	.10
Repository	5.20	5.40	6.10	3.93	3.95	4.07	3.32	3.40	3.52	3.05	3.15	3.32
Total	8.02	8.03	8.51	5.88	5.74	5.76	4.94	4.90	4.96	4.50	4.52	4.62

TABLE C.8. 50,000 MTE System Costs for FHLW (W/Recycle) in 1.0-ft-Diameter Canisters

Maximum Bentonite Temperature, C°	100°			150°			200°			250°		
Pitch, m	2.4	4.0	7.2	2.4	4.0	7.2	2.4	4.0	7.2	2.4	4.0	7.2
KW/Canister	.15	.195	.24	.37	.46	.54	.60	.77	.88	.84	1.10	1.23
MTE/Canisters	.495	.644	.792	1.221	1.518	1.782	1.980	2.541	2.904	2.772	3.630	4.059
No. Canisters, 10^3	101.0	77.6	63.1	41.0	32.9	28.0	25.2	19.7	17.2	18.0	13.8	12.3
System Cost, $\$10^9$												
Fractionation	.88	.88	.88	.88	.88	.88	.88	.88	.88	.88	.88	.88
Vitrification	2.02	1.69	1.42	1.03	.89	.78	.73	.61	.55	.57	.47	.43
Storage												
Transportation	1.80	1.39	1.14	.74	.60	.51	.46	.36	.32	.33	.26	.23
Repository	6.25	6.05	6.15	4.10	3.97	4.15	3.47	3.43	3.58	3.23	3.22	3.33
Total	10.95	10.01	9.59	6.75	6.34	6.32	5.54	5.28	5.33	5.01	4.83	4.87

TABLE C.9. 50,000 MTE System Costs for FHLW (W/Recycle) in 1.7-ft-Diameter Canisters

Maximum Bentonite Temperature, C°	100°			150°			200°			250°		
Pitch, m	2.9	4.5	8.0	2.9	4.5	8.0	2.9	4.5	8.0	2.9	4.5	8.0
KW/Canister	.17	.23	.27	.43	.55	.65	.74	.91	1.04	1.08	1.29	1.46
MTE/Canisters	.561	.759	.891	1.419	1.815	2.145	2.442	3.003	3.432	3.564	4.257	4.818
No. Canisters, 10^3	89.1	65.9	56.1	35.2	27.5	23.3	20.5	16.7	14.6	14.0	11.7	10.4
System Cost, $\$10^9$												
Fractionation	.88	.88	.88	.88	.88	.88	.88	.88	.88	.88	.88	.88
Vitrification	2.90	2.34	2.08	1.46	1.22	1.07	.97	.84	.76	.77	.65	.60
Storage												
Transportation	3.47	2.58	2.20	1.40	1.10	.94	.83	.68	.60	.58	.49	.44
Repository	6.70	5.50	7.00	4.20	4.10	4.20	3.40	3.50	3.65	3.20	3.20	3.45
Total	13.95	11.30	12.16	7.94	7.30	7.09	6.08	5.90	5.89	5.43	5.22	5.37

TABLE C.10. 50,000 MTE System Costs for FHLW (W/Recycle) in 2.5-ft-Diameter Canisters

Maximum Bentonite Temperature, C°	100°			150°			200°			250°		
Pitch, m	3.5	5.0	8.0	3.5	5.0	8.0	3.5	5.0	8.0	3.5	5.0	8.0
KW/Canister	.24	.33	.36	.58	.71	.80	.95	1.13	1.28	1.34	1.58	1.80
MTE/Canisters	.792	1.089	1.188	1.914	2.343	2.640	3.135	3.729	4.224	4.422	5.215	5.941
No. Canisters, 10^3	63.1	45.9	42.1	26.1	21.3	18.9	15.9	13.4	11.8	11.3	9.6	8.4
System Cost, $\$10^9$												
Fractionation	.88	.88	.88	.88	.88	.88	.88	.88	.88	.88	.88	.88
Vitrification	3.28	2.64	2.48	1.72	1.47	1.35	1.19	1.05	.96	.93	.83	.76
Storage												
Transportation	4.95	3.61	3.31	2.06	1.69	1.50	1.26	1.07	.94	.91	.77	.68
Repository	6.30	5.70	6.10	4.15	4.00	4.15	3.50	3.50	3.60	3.20	3.15	3.25
Total	15.41	12.83	12.77	8.81	8.04	7.88	6.83	6.50	6.38	5.92	5.63	5.57

TABLE C.11. 50,000 MTE System Costs for FHLW (W/O Recycle) in 0.5-ft-Diameter Canisters

Maximum Bentonite Temperature, C°	100°			150°			200°			250°		
Pitch, m	2.0	3.0	6.0	2.0	3.0	6.0	2.0	3.0	6.0	2.0	3.0	6.0
KW/Canister	0.15	0.17	0.22	0.31	0.38	0.45	.50	.61	.73	.70	.85	1.03
MTE/Canisters	.833	.944	1.222	1.722	2.111	2.500	2.778	3.389	4.056	3.889	4.722	5.722
No. Canisters, 10^3	60.0	53.0	40.9	29.0	23.7	20.0	18.0	14.8	12.3	12.9	10.6	8.7
System Cost, $\$10^9$												
Fractionation	.88	.88	.88	.88	.88	.88	.88	.88	.88	.88	.88	.88
Vitrification	0.90	0.81	0.68	.52	.46	.41	.39	.33	.29	.28	.26	.23
Storage												
Transportation	0.37	0.32	0.25	.18	.15	.13	.11	.09	.07	.08	.05	.05
Repository	3.86	4.05	4.45	3.28	3.25	3.46	2.98	3.00	3.10	2.88	2.92	2.97
Total	6.01	6.06	6.26	4.86	4.74	4.88	4.36	4.30	4.34	4.12	4.11	4.13

TABLE C.13. 50,000 MTE System Costs for FHLW (W/O Recycle) in 1.7-ft-Diameter Canisters

Maximum Bentonite Temperature, C°	100°			150°			200°			250°		
Pitch, m	2.9	4.5	8.0	2.9	4.5	8.0	2.9	4.5	8.0	2.9	4.5	8.0
KW/Canister	.17	.23	.27	.43	.55	.65	.74	.91	1.04	1.08	1.29	1.46
MTE/Canisters	.944	1.278	1.500	2.389	3.056	3.611	4.111	5.056	5.778	6.000	7.167	8.111
No. Canisters, 10^3	53.0	39.1	33.3	20.9	16.4	13.8	12.2	9.9	8.7	8.3	7.0	6.2
System Cost, $\$10^9$												
Fractionation	.88	.88	.88	.88	.88	.88	.88	.88	.88	.88	.88	.88
Vitrification	2.01	1.58	1.40	.98	.83	.73	.67	.57	.53	.51	.45	.42
Storage												
Transportation	2.07	1.53	1.30	.83	.66	.56	.49	.40	.36	.34	.29	.26
Repository	4.95	4.70	5.00	3.50	3.50	3.70	3.15	3.10	3.20	2.95	2.85	2.90
Total	9.91	8.69	8.58	6.19	5.87	5.87	5.19	4.95	4.97	4.68	4.47	4.46

TABLE C.12. 50,000 MTE System Costs for FHLW (W/O Recycle) in 1.0-ft-Diameter Canisters

Maximum Bentonite Temperature, C°	100°			150°			200°			250°		
Pitch, m	2.4	4.0	7.2	2.4	4.0	7.2	2.4	4.0	7.2	2.4	4.0	7.2
KW/Canister	.15	.195	.24	.37	.46	.54	.60	.77	.88	.87	1.10	1.23
MTE/Canisters	.833	1.083	1.333	2.056	2.556	3.000	3.333	4.278	4.889	4.883	6.111	6.833
No. Canisters, 10^3	60.0	46.2	37.5	24.3	19.6	16.7	15.0	11.7	10.2	10.3	8.2	7.3
System Cost, $\$10^9$												
Fractionation	.88	.88	.88	.88	.88	.88	.88	.88	.88	.88	.88	.88
Vitrification	1.38	1.13	.98	.70	.61	.54	.50	.42	.38	.39	.32	.30
Storage												
Transportation	1.07	.83	.68	.44	.35	.30	.27	.22	.19	.20	.15	.14
Repository	4.50	4.45	4.77	3.40	3.36	3.53	3.12	3.12	3.19	2.97	2.87	2.86
Total	7.83	7.29	7.31	5.42	5.20	5.25	4.77	4.64	4.64	4.44	4.22	4.18

TABLE C.14. 50,000 MTE System Costs for FHLW (W/O Recycle) in 2.5-ft-Diameter Canisters

Maximum Bentonite Temperature, C°	100°			150°			200°			250°		
Pitch, m	3.5	5.0	8.0	3.5	5.0	8.0	3.5	5.0	8.0	3.5	5.0	8.0
KW/Canister	.24	.33	.36	.58	.71	.80	.95	1.13	1.28	1.34	1.58	1.80
MTE/Canisters	1.333	1.833	2.000	3.222	3.944	4.444	5.278	6.278	7.111	7.444	8.778	10.000
No. Canisters, 10^3	37.5	27.3	25.0	15.5	12.7	11.3	9.5	8.0	7.0	6.7	5.7	5.0
System Cost, $\$10^9$												
Fractionation	.88	.88	.88	.88	.88	.88	.88	.88	.88	.88	.88	.88
Vitrification	2.27	1.79	1.68	1.17	1.02	.94	.83	.73	.66	.64	.57	.55
Storage												
Transportation	2.94	2.15	1.97	1.22	1.00	.90	.76	.64	.56	.54	.46	.41
Repository	4.95	4.55	4.70	3.50	3.55	3.55	3.20	3.20	3.20	3.00	2.95	2.90
Total	11.09	9.37	9.23	6.77	6.45	6.27	5.67	5.45	5.30	5.06	4.86	4.74

TABLE C.15. 50,000 MTE System Costs for Aged-HLW (to 0.3 kW/MTE) in 0.5-ft-Diameter Canisters

Maximum Bentonite Temperature, C°	100°			150°			200°			250°		
Pitch, m	2.0	3.0	6.0	2.0	3.0	6.0	2	3	6	2	3	6
KW/Canister	0.15	.017	0.22	0.31	0.38	0.47	0.50	0.61	0.74	0.70	0.86	1.03
MTE/Canisters	0.50	0.567	0.733	1.033	1.267	1.567	1.67	2.03	2.47	2.33	2.87	3.43
No. Canisters, 10^3	100	88.18	68.21	48.4	39.47	31.91	29.9	24.6	20.2	21.5	17.4	14.6
System Cost, $\$10^9$												
Fractionation												
Vitrification	1.80	1.65	1.36	1.06	0.93	0.81	0.77	0.67	0.59	0.61	0.53	0.47
Storage	3.00	2.65	2.05	1.45	1.18	0.96	0.90	0.74	0.60	0.65	0.56	0.51
Transportation	0.60	0.53	0.41	0.30	0.24	0.20	0.19	0.15	0.13	0.14	0.11	0.09
Repository	5.10	5.40	5.57	3.73	3.73	3.97	3.23	3.32	3.48	3.07	3.10	3.23
Total	10.50	10.23	9.39	6.54	6.08	5.94	5.09	4.88	4.81	4.47	4.30	4.30

TABLE C.16. 50,000 MTE System Costs for Aged-HLW (to 0.3 kW/MTE) in 1.0-ft-Diameter Canisters

Maximum Bentonite Temperature, C°	100°			150°			200°			250°		
Pitch, m	2.4	4.0	7.2	2.4	4.0	7.2	2.4	4.0	7.2	2.4	4.0	7.2
KW/Canister	0.15	0.20	0.23	0.37	0.46	0.54	0.60	0.77	0.88	0.87	1.10	1.23
MTE/Canisters	0.50	0.667	0.767	1.233	1.533	1.800	2.000	2.567	2.933	2.900	3.667	4.100
No. Canisters, 10^3	100.0	74.96	65.2	40.55	32.6	27.8	25.0	19.48	17.05	17.24	13.64	12.20
System Cost, $\$10^9$												
Fractionation												
Vitrification	2.78	2.26	2.04	1.44	1.23	1.10	1.02	0.86	0.78	0.79	0.67	0.63
Storage	6.80	5.10	4.43	2.76	2.22	1.89	1.70	1.32	1.16	1.17	0.93	0.83
Transportation	1.80	1.35	1.17	0.73	0.59	0.50	0.46	0.35	0.32	0.32	0.26	0.23
Repository	6.00	5.90	6.50	3.90	3.90	4.16	3.40	3.40	3.55	3.19	3.20	3.29
Total	17.3	14.61	14.14	8.83	7.94	7.65	6.58	5.93	5.81	5.47	5.06	4.98

TABLE C.17. 50,000 MTE System Costs for Aged-HLW (to 0.3 kW/MTE) in 1.7-ft-Diameter Canisters

Maximum Bentonite Temperature, C°	100°			150°			200°			250°		
Pitch, m	2.9	4.5	8.0	2.9	4.5	8.0	2.9	4.5	8.0	2.9	4.5	8.0
KW/Canister	0.17	0.23	0.27	0.43	0.55	0.64	0.74	0.91	1.04	1.08	1.29	1.46
MTE/Canisters	0.561	0.759	0.891	1.42	1.82	2.15	2.44	3.00	3.43	3.56	4.26	4.82
No. Canisters, 10^3	89.1	65.9	56.1	35.2	27.5	23.3	20.5	16.7	14.6	14.0	11.7	10.4
----- System Cost, $\$10^9$												
Fractionation												
Vitrification	4.10	3.23	2.83	2.00	1.68	1.49	1.36	1.19	1.08	1.05	0.92	0.85
Storage	11.49	8.50	7.24	4.54	3.55	3.01	2.64	2.18	1.88	1.81	1.51	1.34
Transportation	3.39	2.57	2.20	1.40	1.10	0.94	0.82	0.68	0.60	0.58	0.49	0.44
Repository	6.70	5.50	7.00	4.20	4.10	4.20	3.53	3.50	3.65	3.25	3.25	3.37
Total	25.68	19.80	19.27	12.14	10.43	9.64	8.36	7.55	7.21	6.69	6.17	6.00

TABLE C.18. 50,000 MTE System Costs for Cs/Sr Waste in 0.5-ft-Diameter Canisters

Maximum Basalt Temperature, C°	300°			350°			400°					
Pitch, m	2.4	4.0	7.2	2.4	4.0	7.2	2.4	4.0	7.2			
KW/Canister	1.38	1.89	2.26	1.80	2.44	2.90	2.20	2.98	3.56			
MTE/Canisters	1.78	2.43	2.91	2.32	3.14	3.73	2.83	3.84	4.58			
No. Canisters, 10^3	28.1	20.6	17.2	21.6	15.9	13.4	17.7	13.0	10.9			

System Cost, $\$10^9$												
Fractionation												
Vitrification	.79	.63	.55	.65	.52	.46	.56	.45	.40			
Storage												
Transportation	.53	.40	.33	.41	.31	.26	.34	.26	.21			
Repository	3.05	3.15	3.25	3.00	3.05	3.16	2.95	2.96	2.99			
Total	4.37	4.18	4.13	4.06	3.88	3.88	3.85	3.67	3.60			

TABLE C.19. 50,000 MTE System Costs for Cs/Sr Waste in 1.7-ft-Diameter Canisters

Maximum Basalt Temperature, C°	100°			150°			200°			250°		
Pitch, m	2.9	4.5	8.0	2.9	4.5	8.0	2.9	4.5	8.0			
KW/Canister	1.71	2.23	2.67	2.21	2.85	3.42	2.70	3.51	4.23			
MTE/Canisters	2.20	2.87	3.35	2.84	3.67	4.40	3.48	4.52	5.44			
No. Canisters, 10^3	22.7	17.4	14.9	17.6	13.6	11.4	14.4	11.1	9.2			
System Cost, $\$10^9$												
Fractionation												
Vitrification	1.05	.85	.77	.87	.72	.63	.75	.62	.55			
Storage												
Transportation	.95	.74	.64	.75	.59	.49	.62	.48	.40			
Repository	3.21	3.25	3.37	3.14	3.10	3.20	3.03	2.99	3.10			
Total	5.21	4.84	4.78	4.76	4.41	4.32	4.40	4.09	4.05			

TABLE C.20. 50,000 MTE System Costs for Cs/Sr Waste in 2.5-ft-Diameter Canisters

Maximum Basalt Temperature, C°	100°			150°			200°			250°		
Pitch, m	3.5	5.0	8.0	3.5	5.0	8.0	3.5	5.0	8.0			
KW/Canister	2.11	2.63	3.11	2.70	3.35	3.98	3.33	4.11	4.93			
MTE/Canisters	2.72	3.86	4.00	3.475	4.311	5.12	4.29	5.29	6.35			
No. Canisters, 10^3	18.4	13.0	12.5	14.4	11.6	9.8	11.7	9.5	7.9			

System Cost, $\$10^9$												
Fractionation												
Vitrification	1.32	1.03	1.00	1.11	.95	.84	.96	.82	.72			
Storage												
Transportation	1.50	1.07	1.04	1.19	.97	.82	.97	.80	.67			
Repository	3.23	3.25	3.40	3.17	3.17	3.22	3.10	3.08	3.10			
Total	6.05	5.35	5.44	5.47	5.09	4.88	5.03	4.70	4.49			

TABLE C.21. Minimum System Costs for HLW with Ti-Clad Overpack, 10^9

Canister Diameter, ft	Maximum Bentonite Temperatures, °C			
	100	150	200	250
0.5	18.8	10.2	7.3	6.0
1.0	25.4	12.5	8.8	7.0
1.7	32.0	15.3	10.7	8.4
2.5	34.0	18.2	12.4	9.5

TABLE C.22. Canister Heat Loading at Minimum System Cost for HLW with Ti-Clad Overpack, kW

Canister Diameter, ft	Maximum Bentonite Temperatures, °C			
	100	150	200	250
0.5	0.16	0.42	0.69	0.98
1.0	0.22	0.50	0.84	1.17
1.7	0.26	0.62	0.99	1.38
2.5	0.35	0.79	1.28	1.78

TABLE C.23. Minimum System Costs for HLW Without Ti-Clad Overpack, 10^9

Canister Diameter, ft	Maximum Bentonite Temperatures, °C			
	100	150	200	250
0.5	17.5	9.7	7.2	5.9
1.0	23.6	11.8	8.5	6.8
1.7	29.5	14.8	10.1	8.2
2.5	32.0	17.2	11.7	9.1

TABLE C.24. Canister Heat Loading at Minimum System Cost for HLW Without Ti-Clad Overpack, kW

Canister Diameter, ft	Maximum Bentonite Temperatures, °C			
	100	150	200	250
0.5	0.16	0.41	0.70	0.94
1.0	0.22	0.50	0.82	1.18
1.7	0.26	0.62	1.00	1.42
2.5	0.36	0.78	1.28	1.80

TABLE C.25. Minimum System Costs for FHLW Recyle Case, 10^9

Canister Diameter, ft	Maximum Bentonite Temperatures, °C			
	100	150	200	250
0.5	8.0	5.7	4.8	4.5
1.0	9.5	6.2	5.2	4.8
1.7	10.8	7.1	5.8	5.2
2.5	12.2	7.8	6.3	5.5

TABLE C.26. Canister Heat Loading at Minimum System Cost for FHLW Recycle Case, kW

Canister Diameter, ft	Maximum Bentonite Temperatures, °C			
	100	150	200	250
0.5	0.16	0.44	0.65	0.86
1.0	0.23	0.52	0.84	1.16
1.7	0.25	0.62	0.99	1.33
2.5	0.36	0.78	1.25	1.73

TABLE C.27. Minimum System Costs for FHLW No-Recycle Case, 10^9

Canister Diameter, ft	Maximum Bentonite Temperatures, °C			
	100	150	200	250
0.5	6.0	4.7	4.3	4.1
1.0	7.1	5.1	4.6	4.2
1.7	8.4	5.8	4.8	4.4
2.5	9.0	6.3	5.3	4.7

TABLE C.28. Canister Heat Loading at Minimum System Cost for FHLW No-Recycle Case, kW

Canister Diameter, ft	Maximum Bentonite Temperatures, °C			
	100	150	200	250
0.5	0.16	0.40	0.66	0.88
1.0	0.22	0.51	0.83	1.16
1.7	0.26	0.62	1.00	1.39
2.5	0.36	0.80	1.26	1.76

TABLE C.29. Minimum System Costs for Aged-HLW, 10^9

Canister Diameter, ft	Maximum Bentonite Temperatures, °C			
	100	150	200	250
0.5	9.4	5.9	4.8	4.2
1.0	13.9	7.5	5.7	5.0
1.7	18.6	9.6	7.1	5.9

TABLE C.30. Canister Heat Loading at Minimum System Cost for Aged-HLW, kW

Canister Diameter, ft	Maximum Bentonite Temperatures, °C			
	100	150	200	250
0.5	0.22	0.44	0.70	0.98
1.0	0.23	0.52	0.85	1.20
1.7	0.26	0.63	1.02	1.42

Canister Diameter, ft	Initial Loadings			
	100	150	200	250
0.5	0.79	1.58	2.52	3.53
1.0	0.83	1.87	3.06	4.32
1.7	0.94	2.27	3.67	5.11

TABLE C.31. Minimum System Costs for Cs/Sr Waste, $\$10^9$

Canister Diameter, ft	Maximum Basalt Temperatures, °C		
	300	350	400
1.0	4.15	3.85	3.60
1.7	4.75	4.30	4.00
2.5	5.25	4.90	4.50

TABLE C.32. Canister Heat Loading at Minimum System Cost for Cs/Sr Waste, kW

Canister Diameter, ft	Maximum Basalt Temperatures, °C		
	300	350	400
1.0	2.13	2.74	3.40
1.7	2.50	3.30	4.00
2.5	2.88	3.98	4.92

TABLE C.33. 50,000 MTE System Costs for HLW at 1.41 ft^3/MTE Without Bentonite Backfill in the Repository

Maximum Centerline Temperature, C°	100°			200°C			300°C			400°C		
Canister Diameter, ft	0.50	0.50	0.50	0.5	0.5	0.5	0.5	0.5	0.5	0.53	0.61	0.63
Pitch	2	4	7	2	4	7	2	4	7	2	4	7
kW/Canister	0.08	0.11	0.16	0.42	0.56	0.60	0.88	1.09	1.20	1.37	1.78	1.95
MTE/Canisters	0.074	0.10	0.15	0.39	0.52	0.56	0.81	1.01	1.11	1.27	1.65	1.81
No. Canisters, 10^3	676	500	333	128.2	96.2	89.3	61.7	49.5	45.0	39.4	30.3	27.6

System Cost, $\$10^9$												
Fractionation	-	-	-	-	-	-	-	-	-	-	-	-
Vitrification	8.11	6.25	4.50	2.18	1.73	1.65	1.28	1.09	1.04	0.95	0.85	0.83
Storage	-	-	-	-	-	-	-	-	-	-	-	-
Transportation	4.06	3.00	2.00	0.78	0.61	0.56	0.40	0.33	0.30	0.29	0.29	0.28
Repository	19.0	18.3	18.0	5.8	6.0	6.95	4.1	4.1	4.45	3.40	3.5	3.83
Total	31.2	27.6	24.5	8.76	8.34	9.16	5.78	5.52	5.79	4.64	4.64	4.94

TABLE C.34. 50,000 MTE System Costs for HLW at 3.14 ft^3/MTE Without Bentonite Backfill in the Repository

Maximum Centerline Temperature, C°	100°			200°C			300°C			400°C		
Canister Diameter, ft	0.5	0.5	0.5	0.5	0.51	0.53	0.64	0.73	0.77	0.81	0.94	1.00
Pitch	2	4	7	2	4	7	2	4	7	2	4	7
kW/Canister	0.08	0.11	0.16	0.42	0.56	0.61	0.90	1.15	1.30	1.43	1.92	2.16
MTE/Canisters	0.074	0.10	0.15	0.39	0.52	0.56	0.83	1.06	1.20	1.32	1.78	2.00
No. Canisters, 10^3	676	500	333	128.2	96.2	89.3	60.2	47.1	41.7	37.9	28.1	25.0
System Cost, $\$10^9$												
Fractionation	-	-	-	-	-	-	-	-	-	-	-	-
Vitrification	8.11	6.25	4.50	2.18	1.83	1.79	1.45	1.32	1.25	1.21	1.07	1.02
Storage	-	-	-	-	-	-	-	-	-	-	-	-
Transportation	4.06	3.00	2.00	0.78	0.67	0.67	0.57	0.59	0.56	0.59	0.49	0.48
Repository	19.0	18.3	18.0	5.8	6.0	6.95	4.2	4.0	4.35	3.40	3.48	3.75
Total	31.2	27.6	24.5	8.76	8.50	9.41	6.22	5.91	6.16	5.20	5.04	5.25

TABLE C.35. 50,000 MTE System Costs for FHLW (Recycle Case) at 1.2 ft^3/MTE Without Bentonite Backfill in the Repository

Maximum Centerline Temperature, C°	100°			200°C			300°C			400°C		
Canister Diameter, ft	0.50	0.50	0.50	0.52	0.60	0.625	0.755	0.865	0.925	0.96	1.125	1.205
Pitch	2	4	7	2	4	7	2	4	7	2	4	7
kW/Canister	0.08	0.11	0.16	0.425	0.58	0.625	0.91	1.195	1.35	1.46	2.00	2.27
MTE/Canisters	0.264	0.363	0.528	1.403	1.914	2.063	3.003	3.944	4.455	4.819	6.601	7.492
No. Canisters, 10^3	189.4	137.7	94.7	35.6	26.1	24.2	16.7	12.7	11.2	10.4	7.57	6.42
System Cost, $\$10^9$												
Fractionation	0.88	0.88	0.88	0.88	0.88	0.88	0.88	0.88	0.88	0.88	0.88	0.88
Vitrification	2.18	1.72	1.28	0.62	0.68	0.51	0.39	0.37	0.39	0.37	0.33	0.30
Storage	-	-	-	-	-	-	-	-	-	-	-	-
Transportation	1.14	0.83	0.57	0.23	0.22	0.22	0.21	0.20	0.20	0.18	0.17	0.16
Repository	6.9	7.2	7.2	3.34	3.40	3.70	3.10	3.04	3.15	2.96	2.86	2.92
Total	11.10	10.63	9.93	5.07	5.18	5.31	4.58	4.49	4.62	4.39	4.24	4.26

TABLE C.36. 50,000 MTE System Costs for FHLW (Recycle Case) at 2.7 ft^3/MTE Without Bentonite Backfill in the Repository

Maximum Centerline Temperature, C°	100°			200°C			300°C			400°C		
Canister Diameter, ft	0.5	0.5	0.5	0.81	0.94	1.00	1.16	1.36	1.46	1.48	1.80	2.0
Pitch	2	4	7	2	4	7	2	4	7	2	4	7
kW/Canister	0.08	0.11	0.16	0.47	0.63	0.71	0.95	1.34	1.54	1.58	2.26	2.69
MTE/Canisters	0.264	0.363	0.528	1.55	2.08	2.34	3.14	4.42	5.08	5.21	7.46	8.88
No. Canisters, 10^3	189.4	137.7	94.7	32.3	24.0	21.4	15.9	11.3	9.84	9.60	6.70	5.63
System Cost, $\$10^9$												
Fractionation	0.88	0.88	0.88	0.88	0.88	0.88	0.88	0.88	0.88	0.88	0.88	0.88
Vitrification	2.18	1.72	1.28	0.74	0.68	0.65	0.56	0.51	0.49	0.50	0.39	0.46
Storage	-	-	-	-	-	-	-	-	-	-	-	-
Transportation	1.14	0.83	0.57	0.44	0.37	0.39	0.35	0.29	0.28	0.28	0.31	0.31
Repository	6.9	7.2	7.2	3.31	3.38	3.67	3.12	3.04	3.10	2.97	2.87	2.89
Total	11.1	10.6	9.9	5.37	5.31	5.59	4.91	4.72	4.75	4.63	4.45	4.54

TABLE C.37. 50,000 MTE System Costs for FHLW (No-Recycle Case) at 1.2 ft^3/MTE Without Bentonite Backfill in the Repository

Maximum Centerline Temperature, C°	100°			200°C			300°C			400°C		
Canister Diameter, ft	0.5	0.5	0.5	0.67	0.80	0.84	0.99	1.16	1.24	1.27	1.50	1.62
Pitch	2	4	7	2	4	7	2	4	7	2	4	7
kW/Canister	0.08	0.11	0.16	0.44	0.61	0.67	0.94	1.28	1.47	1.53	2.14	2.50
MTE/Canisters	0.44	0.61	0.89	2.44	3.39	3.72	5.22	7.11	8.17	8.50	11.89	13.89
No. Canisters, 10^3	113.6	82.0	56.2	20.5	14.7	13.4	9.58	7.03	6.12	5.88	4.21	3.60
System Cost, $\$10^9$												
Fractionation	0.88	0.88	0.88	0.88	0.88	0.88	0.88	0.88	0.88	0.88	0.88	0.88
Vitrification	1.36	1.15	0.87	0.48	0.42	0.41	0.35	0.32	0.31	0.30	0.27	0.24
Storage	-	-	-	-	-	-	-	-	-	-	-	-
Transportation	0.68	0.49	0.34	0.18	0.16	0.16	0.17	0.16	0.15	0.18	0.14	0.13
Repository	5.50	5.50	5.15	3.15	3.10	3.24	2.94	2.74	2.90	2.81	2.77	2.80
Total	8.42	8.02	7.24	4.69	4.56	4.69	4.34	4.10	4.24	4.17	4.06	4.05

APPENDIX D

RADIOLOGICAL RISK ANALYSIS SUPPLEMENT

This appendix contains supplementary information related to details of the radiological risk comparisons presented in Chapter 6, Volume 1 of this report. Section D.1 concerns near-term radiological risk calculations, Section D.2 concerns interim storage radiological risk calculations, and Section D.3 concerns long-term radiological risk calculations.

D.1 NEAR-TERM RADIOLOGICAL RISK CALCULATIONS

This section contains details used in the calculations for the near-term radiological risk analysis presented in Section 6.1 in Chapter 6. The process by which accidents are selected for radiological impact analysis is outlined in Subsection D.1.1, and details on the methods and assumptions used to calculate the maximum-exposed individual and regional population doses are presented in Subsection D.1.2.

D.1.1 Radiological Impact in the Event of Accidents

Accidents which could result in the release of radioactivity during the processing, transportation, and disposal of HLW have been analyzed to determine if there are any significant differences between the alternative study cases for the reference HLW, fractionated waste and aged-HLW. The process by which accidents are first postulated to occur and then selected for analysis is described in DOE (1980) as an umbrella source-term approach. This approach, used to evaluate near-term risks at waste management facilities, is discussed below.

The first step in the umbrella source-term approach is to define a set of accidents which could occur at various waste management facilities and during various waste management operations. This was accomplished in DOE (1980) through the use of several technology task groups and with the assistance of safety specialists. Step two involves development of source-terms. These terms are obtained by using successive release fractions (the portion of a radionuclide inventory escaping to the next containment barrier or to the

biosphere). The last step requires estimating accident frequencies based on previous experience with similar or related equipment and on engineering judgment.

Following these three steps, the individual accidents are combined into 41 release groups. These 41 groups can be defined by such parameters as:

- release pathways
- chemical form
- isotope types released.

In each release group, that accident having the largest release to the environment is denoted the "umbrella-source term" since it produces the largest environmental impact for that group of accidents, and by analyzing its effect, the other accidents are covered by the "umbrella" or magnitude of the analyzed accident.

Once the release groups are developed and the umbrella accidents identified, these groups and their associated umbrella accidents are further classified into three accident severity categories: minor, moderate, and severe.

Minor. Relatively frequent occurrences involving interruptions without potential for the significant release of radioactive or other materials.

Moderate. Infrequent events with the potential for small material release, major equipment damage, or the creation of radiation fields in occupied zones, which could result in occupational exposures exceeding 10 CFR 20 units (5 rem/yr).

Severe. Unlikely events with the potential for significant radiation hazard. These events are postulated to establish performance requirements for plant safety systems. Accidental releases of sufficient radionuclides to cause occupational exposures which could result in detectable clinical effects are included in this category.

These three groups cover the spectrum of what are termed design basis accidents. Facility safety systems are generally constructed to confine and mitigate design basis accidents. Non-design basis accidents were not

considered for waste treatment and storage facilities nor during the construction and operation phases of a geologic repository.

Accidents analyzed in detail were chosen on the basis of the greatest probability of occurrence and the greatest radiological consequences. It is assumed that if these accidents were to occur, clean-up measures would be taken to restore the facility to a safe condition.

Several minor and moderate accidents or other events associated with waste solidification by vitrification that would be expected to lead to releases of radioactive material have been identified in DOE (1979b). Table D.1 shows postulated minor and moderate accidents for the waste vitrification facility. 70-year dose commitments were calculated for the maximum-exposed individual. For minor accidents, in no case was the dose to the maximum-exposed individual greater than 1×10^{-6} rem/yr and was generally several orders of magnitude less.

TABLE D.1. Postulated Accidents for Vitrification Facility

Accident Number	Description
Minor	
1	Hydrogen explosion in feed tank
2	HLLW feed system leakage
3	Calcine spill from calcine handling equipment due to process irregularity
4	Sintered metal filter failure
5	Calcine overheating in canister
Moderate	
6	Feed solution backup in air line or contamination spread to occupied zone
7	Calciner pressurization due to malfunction of fuel ignition system
8(a)	Failure of off-gas filter or scrubber
9	Loss of off-gas system flow
10	Failure of cell exhaust filters

(a) Umbrella source-term accident.

Of the moderate accidents, number 8 (process off-gas clean-up system failure) was judged to be the most severe and was taken as the umbrella source-term accident. The doses to the maximum-exposed individual from this accident are shown in Table D.2.

TABLE D.2. 70-Year Whole-Body Maximum-Exposed Individual Dose from Vitrification Plant Accident (rem)

Case	Maximum Bentonite Temperature, °C	Dose from Waste Type
FHLW Case (1)		
FHLW	100	1.9×10^{-5}
Cs/Sr[(a)]	-	2.2×10^{-4}
FHLW Case (2)		
FHLW	250	1.9×10^{-5}
Cs/Sr	-	2.2×10^{-5}
HLW Case (1)	100	2.4×10^{-4}
HLW Case (2)	250	2.4×10^{-4}
Aged-HLW	100	1.8×10^{-5}

(a) For Cs/Sr there is no bentonite. Canister sizes and loading optimized for 300°C maximum basalt temperatures.

Several minor accidents associated with rail transport of HLW were identified that could be expected to lead to release of radioactive materials. Scenarios for these accidents are provided in DOE (1979a). The accidents are listed in Table D.3. Accidents postulated to release radioactive material in amounts larger than those released by minor accidents are classified as moderate and severe accidents. For Moderate Accident 4 (loss of neutron shielding in a solidified high-level waste [SHLW] cask) it is assumed that 10-year wastes from 27.4 MTHM will produce neutron streaming for 5 hours. No other materials are released and only recovery workers in close proximity are expected to receive any dose. Severe Accident 5 (HLW cask subjected to severe impact and fire) results in a ground-level release that lasts for 15 minutes. The

TABLE D.3. Postulated Accidents for Transportation

Accident Number	Description
	Minor
1	Train derailment involves HLW cask
2	Train derailment and fire of 30 min. (or less) in HLW cask
3	Unusual transport conditions erode cask surface
	Moderate
4	Loss of neutron shielding in a SHLW cask
	Severe
5	HLW cask is subjected to severe impact and fire

postulated frequency of this accident is 3×10^{-6} per year. Doses to the maximum-exposed individual for the 70-year dose commitment are given in Table D.4.

TABLE D.4. 70-Year Whole-Body Dose Commitment to Maximum-Exposed Individual During Rail Transport

Case	Maximum Bentonite Temperature, °C	Dose (rem) Minor Accident	Dose (rem) Severe Accident
FHLW Case (1)	100	3.0×10^{-7}	0.4
FHLW Case (2)	250	4.4×10^{-7}	0.6
HLW Case (1)	100	7.5×10^{-7}	1.1
HLW Case (2)	250	4.1×10^{-6}	5.2
Cs/Sr Fraction[a]	-	3.7×10^{-6}	4.7
Aged-HLW	100	2.8×10^{-7}	0.3

(a) For Cs/Sr there is no bentonite. Canister sizes and loadings optimized for 300°C maximum basalt temperature.

Table D.5 presents postulated minor and moderate accidents for a repository. No severe accidents were postulated for a repository. Accident 6 (canister drop down mine shaft) was chosen as the umbrella source-term accident based on information from DOE (1979b). Accident 6 is postulated to result in the release of a portion of four canisters to the mine atmosphere. The release occurs over a period of 1 hour.

TABLE D.5. Postulated Accidents for Geologic Repository (DOE 1979b)

Accident Number	Accident
Minor	
1	CH-TRU waste drum rupture caused by handling error
2	Minor canister failure due to rough handling
3	Externally contaminated canister
4	Receipt of dropped shipping cask
Moderate	
5	Canister drop in surface facility
6(a)	Canister drop down mine shaft
7	Tornado strikes salt storage piles
8	CH-TRU waste drum rupture caused by mechanical damage and fire
9	CH-TRU waste drum rupture caused by internal explosion

(a) Umbrella source-term accident.

Canistered waste is assumed to be in one of the following forms:

- Solidified HLW--13 kg of particles less than 10 μm in diameter released to the mine filters.
- Remotely handled (RH) TRU wastes--1.3 kg of zircaloy fines less than 10 μm released to the mine filters.

Isotopes released to the external environment from Accident 6 are assumed to pass through one-roughing and two-HEPA filters (decontamination factor = 10^7) and escape via a 110-m (360-ft) stack. The dose to the maximum-exposed individual from a canister drop under the study cases is shown in Table D.6.

TABLE D.6. 70-Year Whole-Body Dose Commitments to Maximum-Exposed Individual from Canister Drop into Geologic Repository (rem)

Case	Maximum Bentonite Temperature, °C	Dose from Waste Type
FHLW Case (1)		7.2×10^{-7}
FHLW	100	7.2×10^{-7}
Cs/Sr[(a)]	-	8.7×10^{-6}
FHLW Case (2)		1.0×10^{-6}
FHLW	250	1.0×10^{-6}
Cs/Sr	-	8.7×10^{-6}
HLW Case (1)	100	1.8×10^{-6}
HLW Case (2)	250	9.8×10^{-6}
Aged-HLW	100	6.8×10^{-7}

(a) For Cs/Sr there is no bentonite. Canister sizes and loadings optimized for 300°C maximum basalt temperatures.

D.1.2 Methods and Assumptions Used to Calculate Radiological Effects

Radiological risks of radioactive waste management for this study are described principally in terms of dose to the public (regional population) for routine operations and dose to the individual receiving the maximum dose in the case of accidents, based on results described in DOE (1979b). Dose conversion factors calculated using the assumptions outlined below were used in the DOE (1979b) analysis and were adjusted for this analysis by ratioing the isotopic content and quantity of the releases in curies for the cases selected.

To provide a description of radiological effects over the reference scenarios, doses are presented from releases of radioactive material associated

with routine operation and accidents for individual facilities and transportation systems. Amounts of radionuclides released are based on information presented in DOE (1979b). These source-terms were derived from Waste Treatment Data Sheets that appear in DOE (1979a).

Doses to the public from waste management operations arise mainly from inhalation of radionuclides and by direct radiation, but also from ingestion of food products (e.g., vegetables, meat, and dairy products) grown on land contaminated by radionuclides either deposited on the ground or deposited directly on the food products themselves. No releases of radionuclides to any body of water or to ground have been identified from routine operations.

Dose from radiation exposure resulting from releases is addressed for two main categories of the public: the maximum-exposed individual and the population within an 80-km radius of the plant (~2 million).

Maximum-Exposed Individual Dose Assumptions

The maximum-exposed individual is a hypothetical area resident whose habits would tend to maximize his dose. The following assumptions (from DOE 1979b) governed the calculations of dose to this category:

- The individual resides at the point of the maximum offsite dispersion factor ($\overline{\chi}/Q'$).
- The individual continuously occupies this location (no allowance for possible shielding effects).
- Food is consumed and food products are produced at the point of residency.
- The maximum likely intake of foods is assumed.
- The individual is submersed in a semi-infinite cloud of gaseous effluents.
- The exposure pathways of interest are air submersion, inhalation, ingestion, and in some cases direct radiation.
- Environmental pathway parameters used are defined in the reference environment description.

- Points and manner of release of gaseous effluents are defined in the reference plant description.
- Organs of principal interest are the whole body, lung, thyroid, and bone.

Annual doses are given for the whole body for the maximum-exposed individual. These doses are presented for each facility (process or function) described and are summed for several facilities that may make up the waste management facilities at a given reference plant. In addition, a 70-year integrated dose for the maximum-exposed individual is calculated for each process. The 70-year dose is based on the assumption that the maximum-exposed individual resides near the plant during its 30-year operating life and for 40 years thereafter. In essence, the 70-year integrated dose is a lifetime dose commitment.

Regional Population Dose Assumption

Dose to the regional population is calculated using factors that can be described as average or typical rather than maximum. The following assumptions (from DOE 1979b) are used to calculate the regional population dose:

- Annual average dispersion factors ($\overline{\chi}/Q'$) are developed for annular sectors of residence in the reference environment (22.5° by 1.6-km increments from 1.6 to 8 km and 22.5° by 16-km increments from 8 to 80 km from the plant).
- Average food consumption rate and recreational use rates are assumed for the region.
- Consumption of food products in the region is linked to actual production specified for the reference environment.
- Pathways of interest are inhalation, air submersion, and ingestion. (Direct radiation is included in the case of transport of radioactive materials.)
- The organs of principal interest are whole body, lung, thyroid, and bone.

Annual dose to the regional population is calculated for both the facilities (processes) and plants. A 70-year integrated dose is calculated for the regional population to include the period of reference plant operation and 40 years thereafter. The 70-year integrated dose is considered to be that for one generation. Although a generation in the usual sense is taken to be 30 years, this analysis uses the simplifying assumption that the regional population consists of adults who reside in the region for 70 years, die and are instantly replaced by other adults for the next 70 years (aged-related parameters are not used).

D.2 SUPPLEMENTARY INFORMATION ON INTERIM STORAGE RADIOLOGICAL RISK CALCULATIONS

The purpose of this section is to present supporting information to that provided in Section 6.2 in Chapter 6. Additional detail on a cell handling failure and assumptions used to develop dose estimates associated with this accident are provided in Subsection D.2.1. Additional detail on process effluents and assumptions used to develop dose estimates resulting from such effluents are provided in Subsection D.2.2.

D.2.1 Cell Handling Failure

The analysis in DOE (1979b) indicates that only one accident, a canister failure in the receiving cell, would result in release of radioactive material from a sealed cask storage facility. In DOE (1979a) it was assumed that 10 m would be the maximum drop height possible in a receiving cell and that all canisters dropped from this height would be breached. If breached, approximately 0.1% of the canister contents would be broken and released to the cell filters (DF = 10^{10}). The frequency of such a failure occurring is assumed to be 2.0×10^{-6} per handling operation.

Characteristics of the canisters in Alternatives A and B are shown in Table D.7. Two subcases are presented for Alternative A, the difference being the canister loading (i.e., MTE/canister) assumed.

TABLE D.7. Input Data for Canister Drop in Receiving Cell Accident

	Alternative A-1	Alternative A-2	Alternative B
MTHM/Canister	0.627	3.66	2.64
No. of Canisters	7.97×10^4	1.37×10^4	1.89×10^4

The radionuclide spectrum of the Alternative A canisters and those under Alternative B also differ because of additional processing associated with Alternative A. The relative fraction of selected radionuclides in stored waste under Alternatives A and B versus that contained in spent fuel is outlined in Table D.8.

TABLE D.8. Relative Fraction of Selected Radionuclides in Stored Waste Versus Spent Fuel

Radionuclide	Alternative A	Alternative B
Sr	9.5×10^{-1}	1.0
Tc	-	2.0
Ru	-	1.0
Cs	9.5×10^{-1}	1.0
U	-	5.0×10^{-5}
Pu	4.0×10^{-5}	4.05×10^{-3}
Np	-	1.0
Am	1.0×10^{-2}	1.0
Cm	1.0×10^{-2}	1.0

Using information from Tables D.7 and D.8, as well as Ci/MTE values from Tables 3.3.9 and 3.3.15 in DOE (1979b) as input data, 70-year doses to a maximum-exposed individual were calculated and are presented in Table D.9. The formulation of these doses incorporates the frequency of a cell handling

TABLE D.9. Impacts from Cell Handling Failure (rem)

Alternative	70-Year Dose Commitment		
	Whole-Body	Bone	Lung
A-1	8.2×10^{-11}	1.5×10^{-9}	1.6×10^{-9}
A-2	8.2×10^{-11}	1.5×10^{-9}	1.6×10^{-9}
B	3.5×10^{-11}	3.9×10^{-10}	4.5×10^{-11}

failure mentioned previously. Therefore, values in Table D.9 can be considered as the expected impacts[a] associated with cell handling failure.

As shown in Table D.9, the expected impact values for Alternatives A and B are extremely small and are believed to be insignificant. The difference in doses is attributable to the presence of more ^{244}Cm and plutonium isotopes in aged-HLW than in Cs/Sr waste.

D.2.2 Process Effluents

It is expected that small amounts of radionuclides will be released to the biosphere during normal operation of a storage facility. These releases will result from decontaminating any surface-contaminated casks and from processing wastes which are generated during receipt and handling of canisters. It is assumed in DOE (1979a) that the controlling release of radioactivity occurs during secondary wet waste concentration. An overall release factor of 10^{-16} is assumed in DOE (1979a), which is the product of a waste processing factor of 10^{-6} (provided by two sequential evaporation processes) and a filter reduction factor of 10^{-10} (equivalent to a DF of 10^{10}).

The storage facility in DOE (1979a) is assumed to have a capacity of 2.0×10^{-4} canisters. Consequently, the number of facilities required under each of the alternatives will vary as shown in Table D.10. Additionally, it is assumed that canisters will be received at a rate of 2.0×10^{3} per year for a 10-year period at each facility. This results in a receiving scheme for each alternative as shown in Table D.11.

(a) The term "expected impact" is used here in the same manner "expected value" is used in statistics. Expected impact is the mathematical product of the likelihood of an event occurring multiplied by the consequences of occurrence.

TABLE D.10. Storage Facility Requirements for Alternatives A and B

Alternative	No. of Canisters	No. of Storage Facilities[a]
A-1	7.97×10^4	~4
A-2	1.37×10^4	<1
B	1.89×10^4	~1

(a) Based on 2.0×10^4 canisters per storage facility.

TABLE D.11. Waste Receiving Scheme for Alternatives (canisters per year)

Year	Alternative		
	A-1[a]	A-2	B
1	2000	2000	2000
2	2000	2000	2000
3	2000	2000	2000
4	2000	2000	2000
5	2000	2000	2000
6	2000	2000	2000
7	2000	~1700	2000
8	2000	--	2000
9	2000	--	2000
10	~1900	--	~900

(a) The total canisters received under this alternative would be equal to four times the values shown in this column as four, 2000-canister facilities would be necessary to accommodate the total number of canisters for this alternative.

Using information from Tables D.7, D.8, and D.11, as well as Ci/MTHM values from Tables 3.3.9 and 3.3.15 in DOE (1979b) as input data, 70-year lifetime doses to a regional population were calculated and presented in Table D.12. As shown in Table D.12, the doses are extremely small and are believed to be insignificant. The difference in doses is attributable to the presence of more ^{244}Cm and plutonium isotopes in aged-HLW than in Cs/Sr waste.

TABLE D.12. 70-Year Lifetime Doses to Regional Population from Process Effluents (man-rem)

Alternative	Whole-Body	Bone	Lung
A-1	1.7×10^{-5}	6.0×10^{-5}	1.8×10^{-7}
A-2	2.4×10^{-5}	8.8×10^{-5}	2.2×10^{-6}
B	1.7×10^{-5}	5.8×10^{-5}	1.4×10^{-6}

D.3 SUPPLEMENTARY INFORMATION ON LONG-TERM RADIOLOGICAL RISK CALCULATIONS

The purpose of this section is to present supporting information to the discussion in Section 6.3 in Chapter 6. In Subsection D.3.1, a generalized equation for estimating radionuclide release to ground water from a faulting event is developed. Impacts of a faulting event are presented in some detail in Subsections D.3.1.1, D.3.1.2 and D.3.1.3 for the Reference Case, Alternative A, and Alternative B, respectively. Subsection D.3.2 is structured similarly to Subsection D.3.1; however, its emphasis is on human intrusion into a repository via drilling.

D.3.1 Faulting Event

The purpose of this discussion is: 1) to develop generalized equations for determining radionuclide releases to and radionuclide concentrations in ground water from a faulting event; 2) to identify which parameters in the equations are constants (and, therefore, do not affect the impacts associated with one alternative in comparison to another); 3) to identify which parameters in the equation are variables (and, therefore, do influence the impacts of the Reference Case with respect to Alternative Cases A and B); and 4) to present the impacts of a faulting event(s) for each alternative and for the range of values assumed for the impact parameters.

For purposes of analysis, the natural release mechanism involves a seismic event that creates a fault and allows ground water to enter and exit a repository. The release of nuclides from the waste form into the ground water is described in a generic sense as the product of the following terms:

$$\text{Nuclide release} = (\text{rate of faulting}) \times \left(\frac{\text{canisters exposed}}{\text{event}}\right) \left(\frac{\text{kg of waste}}{\text{canister}}\right) \times \left(\frac{\text{isotopic inventory}}{\text{kg of waste}}\right) \quad \text{(D.1)}$$

The rate of faulting, R, is obtained by multiplying the frequency of occurrence, f (in units of events per unit time per unit area), by repository area, A_R (in units of km^2). This analysis assumes that a fault intersects an 8-km^2 repository once over a 1.0×10^4-yr period. This results in the following for the rate of events term:

$$R = (f) \times (A_R) \quad \text{(D.2)}$$

The number of canisters exposed per event, C_E, is obtained by first determining the proportion of the repository area exposed by the fault, A_E, and multiplying by the total number of canisters in the repository,

$$\text{(i.e., } C_E \left(\frac{A_E}{A_R}\right) \times (N)\text{)}$$

It is assumed that canisters are evenly distributed throughout the repository area and, therefore, the same fraction of canisters is exposed as the fraction of repository area intersected by the fault. Assuming that the fault zone extends beyond the repository horizon, increasing (or decreasing) repository size will tend to increase (or decrease) the fault area within a repository. The exposed repository area is defined as the length of the fault (i.e., the length of the repository, or $(A_R)^{1/2}$, if the repository is a square) multiplied by the distance across the repository that the fault covers [i.e., repository thickness x contangent of the fault angle, or $(T_R) \times (\cot \theta)$]. These relationships are depicted in Figure 6.1 in Chapter 6 of Volume 1.

The term for number of canisters, N, can be described as:

$$N = \frac{(I_R) \times (G)}{\pi(Rc)^2 \times (H) \times (D)} \qquad (D.3)$$

Where I_R is the repository inventory of metric ton equivalent (MTE), G the glass loading in kg glass/MTE, $\pi(Rc)^2$ the area of a canister in cm^2, H the canister height in cm, and D the glass density in kg/cm^3.

Inserting this expression and the relationship for exposed repository area into Equation D.2 yields the term for canisters exposed per event:

$$C_E = \frac{(A_R)^{1/2} \times (T_R) \times (\cot \theta) \times (I_R) \times (G)}{(A_R) \times \pi(Rc)^2 \times (H) \times (D)} \qquad (D.4)$$

The kg of waste leached per canister, W_L, is obtained by multiplying the leach rate (L_R, in units of g/cm-day) by the exposed surface area of each canister (A_S, in units of cm^2) by the period of time (T, in days) over which leaching occurs. This is equal to:

$$W_L = (L_R) \times (A_S) \times (T) \qquad (D.5)$$

It is assumed that the canisters are bisected into two remnants by a fault. As a result, the surface area exposed per canister is equal to $2\pi(Rc)^2/\cos \theta$, where θ is the fault angle with respect to the horizontal plane. Inserting the surface area parameter into the overall term yields:

$$W_L = (L_R) \times \frac{2\pi(Rc)^2}{\cos \theta} \times (T) \qquad (D.6)$$

As the waste form is predominantly SiO_2, it is assumed that radionuclides are released as the SiO_2 matrix dissolves (i.e., congruent leaching). As a result, each radionuclide is released in proportion to its concentration in the waste glass with the glass dissolving at a rate of 1.0×10^{-5} $g/cm^2/day$ (Mendel et al. 1981). This is believed to be a conservative assumption because if silicon solubility in water were exceeded, silicon (and, hence, the waste) would be released at a slower rate.

The isotopic inventory per kg of waste term identifies how the inventory for a particular isotope (within leached waste) changes over time. This term is equal to:

$$(I_G) \times \int_{T_1}^{T_2} e^{-\lambda T}\, dt \quad \text{(a)} \tag{D.7}$$

where I_G is the initial inventory of an isotope in glass in Ci/kg glass, λ is the ln 2 divided by the half-life of the isotope, T_1 is the year the fault is assumed to occur, and T_2 is the year of termination of the calculation. This expression can be expanded to:

$$\frac{(I_o) \times \left(\frac{e^{-\lambda T_1} - e^{-\lambda T_2}}{\lambda} \right)}{(G)} \tag{D.8}$$

where I_o is the initial isotopic inventory in HLW.

By combining all previous terms, the amount of each nuclide released into the ground water is described with the equation below:

$$\text{Nuclide Release} = [(f) \times (A_R)] \tag{D.9}$$

$$\times \left[\frac{(A_R)^{1/2} \times (T_R) \times (\cot\ \theta) \times (I_R) \times (G)}{(A_R) \times \pi (R_c)^2 \times (H) \times (D)} \right]$$

$$\times\ (L_R) \times \left[\frac{2\pi (R_c)^2}{(\cos\ \theta)} \times (T) \right]$$

$$\times \left[\frac{(I_o) \times \left(\frac{e^{-\lambda T_1} - e^{-\lambda T_2}}{\lambda} \right)}{(G)} \right]$$

(a) It is recognized that some radionuclides exhibit more complex decay chains. For these radionuclides, the appropriate decay chains were used.

Cancellation of common terms yields the following simplified equation:

$$\text{Nuclide Release} = (f) \times (A_R)^{1/2} \times (T_R) \times (I_R) \times \left(\frac{(L_R) \times (2)\ (T) \times I_o \times \left(\frac{e^{-\lambda T_1} - e^{\lambda T_2}}{\lambda} \right)}{(H) \times (D) \times (\sin \theta)} \right) \quad \text{(D.10)}$$

Upon examination of Equation D.10, it is observed that the only variable present is A_R [e.g., $(A_R)^{1/2}$]. Other variables (e.g., G, Rc) were eliminated in the transformation from the generalized to the simplified equation. Because the fault zone is assumed to extend beyond the repository horizon, increasing repository area will tend to increase the size of the zone of intersection (e.g., exposed repository area). As a result, varying repository size will influence cumulative curies released to ground water from a hypothetical faulting event. If fault area were not defined as a function of repository area [e.g., $(A_R)^{1/2} \times (T_R) \times (\cot \theta)$], increasing repository area would tend to increase the theoretical frequency of a fault occurring, but would tend to decrease proportionally the number of canisters contacted for a given fault.

The kg glass loading term does not influence cumulative release (assuming a constant repository area) because while varying this parameter will tend to vary number of canisters (and, thereby, canisters exposed from a faulting event), any change will be counterbalanced by an offsetting change in waste inventory per canister. Canister radius also does not influence cumulative release. Varying canister radius (assuming a constant repository area) will be accompanied by either a change in glass loading or a change in number of canisters. If either of these parameters changes, then the waste per canister will vary as a function of the change in the square of canister radius. The available leaching area will also change as a function of the square of canister radius, but in a compensating manner. Canister loading, canister radius, and canister spacing can be considered as variables but only to the extent that they increase or decrease repository area.

The maximum concentration in ground water can be considered a function of surface area exposed, leach rate, and volume of water contacting the exposed surface area per unit time (i.e., flow rate). If the amount of material dissolved exceeds the solubility limit of the material, the dissolution rate is said to be solubility limited. However, if the solubility limit of the material is not exceeded, the dissolution rate is said to be leach rate limited. The assumption used for this study was that the dissolution rate was leach rate limited. This is believed to be a conservative assumption because if silicon solubility in water were exceeded, silicon and waste radionuclides immobilized with silicon in the glass waste form would be released at a slower rate.

By using previous assumptions regarding radionuclide inventory, the maximum concentration of each radionuclide in ground water is described with the following equation:

$$\text{Concentration} = \frac{(L_R) \times (2) \times (\pi) \times (Rc)^2 \times (I_0)\ (e^{-\lambda T_1})}{(G) \times (F_R) \times (\cos\ \theta)} \qquad \text{D.11}$$

where: L_R = leach rate in g/cm^2-day
R_c = canister radius in cm
I_0 = initial isotopic inventory in Ci/MTE
λ = ln 2 divided by half-life of isotope
T_1 = year which fault occurs
G = glass loading in kg glass/MTE
F_R = flow rate in mL/day
θ = fault angle with respect to the horizontal plane.

D.3.1.1 Reference Case

Under the Reference Case it is assumed that the entire waste inventory (i.e., 50,000 MTE) is in a geologic repository. Ten-year-old HLW is assumed solidified (e.g., as borosilicate glass) prior to emplacement.

The hypothetical faulting event used in this analysis is assumed to occur at either 100 or 1,000 years after closure. The fault intersects the repository and allows hydraulic interconnection of the upper and lower aquifer systems. The angle of the fault with respect to the horizontal plane is 30° (Dove

et al. 1982). Shear at the fault plane is assumed to cut the waste canisters in two, leaving two remnants, each open on one end, over which water can flow. The flow rate through each remnant is from 0.24 to 2.4 m^3/yr (Dove et al. 1982). The maximum rate of 2.4 m^3/yr is assumed for the present study. The effective width of the fault zone is 2.0 m and the hydraulic head in the lower aquifer system ranges from 2.0 to 10.0 m higher than in the upper system.

As mentioned previously, because the calculation of radionuclides released to groundwater is performed deterministically (i.e., the event occurs at a specified point(s) in time), the "rate of faulting" term is a constant. Additional assumptions made in order to determine cumulative release to ground water follow:

1. T_1 in the isotopic inventory term is either 100 or 1,000.
2. T_2 in the isotopic inventory term is 10,000.
3. The time frame, T, (over which the calculation was made) is either 9,900 years for a fault at year 100 or 9,000 years for a fault at year 1,000.

Other input parameters used in the calculations are presented in Table D.13.

Inserting these values into Equation D.10 yields cumulative curies of ^{241}Am released to the ground water as shown in Table D.14. In Table D.14 the ^{241}Am release is highest for the subcase where the largest repository area is assumed (Subcase a) and lowest for the subcase where the smallest repository area is assumed (Subcase d). The ratio of the cumulative release for one subcase versus another is approximately equal to the ratio of the square root of the repository areas for the respective subcases. This is in agreement with Equation D.10.

Cumulative releases of selected radionuclides to the fault zone over a 10,000-year period are presented in Tables D.15 and D.16. These releases are the result of ground-water leaching action caused by a fault occurring 100 or 1,000 years after repository closure. These isotopes exhibit the same behavior as ^{241}Am (i.e., ratio of releases being equal to ratio of the square root of the respective repository areas).

TABLE D.13. Input Parameters to Faulting-Event Calculation--Reference Case

Subcase[a]	MTE / Canister	kg Glass / MTE	cm^3 Glass / kg Glass	Number of Canisters	Canister Radius (m)	Canister Spacing (m)	Repository Area (km^2)	Repository Thickness (cm)	Leach Rate (g/cm^2-day)
a (100°C)	0.167	833	319	2.99×10^5	0.0762	3.5	31.6	305	1.0×10^{-5}
b (150°C)	0.389	358	319	1.29×10^5	0.0762	4.0	19.4	305	1.0×10^{-5}
c (200°C)	0.639	218	319	7.82×10^4	0.0762	4.2	13.4	305	1.0×10^{-5}
d (250°C)	0.907	153	319	5.51×10^4	0.0762	4.5	10.5	305	1.0×10^{-5}

(a) Repository thermal design limits.

TABLE D.14. Cumulative Release of ^{241}Am to Ground Water, Over 10,000 Years, from Faults Occurring at 100 and 1,000 Years After Repository Closure--Reference Case

Subcase	Canister Radius (m)	Canister Spacing (m)	Repository Area (km^2)	Release (Ci) Fault at Year 100	Release (Ci) Fault at Year 1,000
a	0.076	3.5	29.5	730	160
b	0.076	4.0	17.28	560	120
c	0.076	4.2	11.28	450	97
d	0.076	4.5	8.38	390	83

TABLE D.15. Cumulative Release of Radionuclides to Ground Water Over 10,000 Years from a Faulting Event Occurring 100 Years After Repository Closure (Ci)--Reference Case

Radionuclide	Subcase a	Subcase b	Subcase c	Subcase d
^{241}Am	7.3×10^{2}	5.6×10^{2}	4.5×10^{2}	3.9×10^{2}
^{243}Am	5.9×10^{2}	4.5×10^{2}	3.7×10^{2}	3.1×10^{2}
^{14}C	6.2	4.8	3.8	3.3
^{135}Cs	6.0	4.6	3.7	3.2
^{137}Cs	6.3×10^{2}	4.8×10^{2}	3.9×10^{2}	3.4×10^{2}
^{237}Np	6.0×10^{1}	4.6×10^{1}	3.7×10^{1}	3.2×10^{1}
^{238}Pu	8.4	6.4	5.2	4.5
^{239}Pu	3.0×10^{1}	2.3×10^{1}	1.9×10^{1}	1.6×10^{1}
^{240}Pu	1.1×10^{2}	8.8×10^{1}	7.1×10^{1}	6.1×10^{1}
^{242}Pu	3.8×10^{-1}	2.9×10^{-1}	2.3×10^{-1}	2.0×10^{-2}
^{226}Ra	9.4×10^{-2}	7.2×10^{-2}	5.8×10^{-2}	5.0×10^{-2}
^{90}Sr	3.7×10^{2}	2.8×10^{2}	2.3×10^{2}	2.0×10^{2}
^{126}Sn	1.0×10^{1}	7.9	6.4	5.5
^{99}Tc	2.5×10^{2}	1.9×10^{2}	1.5×10^{2}	1.3×10^{2}
^{129}I	6.8×10^{-1}	5.2×10^{-1}	4.2×10^{-1}	3.6×10^{-1}

TABLE D.16. Cumulative Release of Radionuclides to Ground Water Over 10,000 Years from a Faulting Event Occurring 1,000 Years After Repository Closure (Ci)--Reference Case

Radionuclide	Subcase a	Subcase b	Subcase c	Subcase d
^{241}Am	1.6×10^{2}	1.2×10^{2}	9.7×10^{1}	8.3×10^{1}
^{243}Am	4.7×10^{2}	3.6×10^{2}	2.9×10^{2}	2.5×10^{2}
^{14}C	4.8	3.7	3.0	2.6
^{135}Cs	4.9	3.8	3.1	2.6
^{137}Cs	5.3×10^{-7}	4.1×10^{-7}	3.3×10^{-7}	2.8×10^{-7}
^{237}Np	5.0×10^{1}	3.8×10^{1}	3.1×10^{1}	2.7×10^{1}
^{238}Pu	6.4×10^{-3}	4.9×10^{-3}	3.9×10^{-3}	3.4×10^{-3}
^{239}Pu	2.5×10^{1}	1.9×10^{1}	1.5×10^{1}	1.3×10^{1}
^{240}Pu	9.0×10^{1}	6.9×10^{1}	5.6×10^{1}	4.8×10^{1}
^{242}Pu	3.1×10^{-1}	2.4×10^{-1}	1.9×10^{-1}	1.7×10^{-1}
^{226}Ra	5.7×10^{-2}	4.4×10^{-2}	3.5×10^{-2}	3.1×10^{-2}
^{90}Sr	1.5×10^{-7}	1.2×10^{-7}	9.4×10^{-8}	8.1×10^{-8}
^{126}Sn	8.5	6.5	5.2	4.5
^{99}Tc	2.0×10^{2}	1.6×10^{2}	1.3×10^{2}	1.1×10^{2}
^{129}I	5.6×10^{-1}	4.3×10^{-1}	3.5×10^{-1}	3.0×10^{-1}

The transport time of each radionuclide away from the repository is a function of ground-water velocity and the Kd of each element. Estimated transport times and distances for elements released in the basalt repository used for this study are contained in Table D.17. At velocities shown, no elements reach the accessible environment [as defined by the Environmental Protection Agency (EPA) as 10 km from the repository boundary].

Estimates of the concentration of selected radionuclides in ground water following leaching of the waste form caused by a faulting event occurring 100 or 1,000 years after repository closure are presented in Tables D.18 and D.19. For perspective, these concentrations are compared to NRC's Radionuclide Concentration Guide (RCG) values (NRC 1981a). Only the isotope ^{90}Sr at year 100 exceeds the RCG value for general populations. However, assuming a 550 m^3/day well as a practical minimum for a well drilled to a depth of 600 m or greater below ground surface, the dilution factor of 4,700 (Dove et al. 1982) would reduce withdrawn waters to below RCG levels.

TABLE D.17. Estimated Transport Times for Radionuclides in a Basalt Repository

Element	Kd	Retardation Factor	Estimated Migration Distance (km)[a]		
			1,000 Yr	10,000 Yr	1.0×10^5 Yr
Am	50	580	3.8×10^{-4}	3.8×10^{-3}	0.038
C	0	1.0	0.22	2.2	22
Cs	300	3500	6.4×10^{-5}	6.4×10^{-4}	6.4×10^{-3}
I	0	1.0	0.22	2.2	22
Np	150	1700	1.3×10^{-4}	1.3×10^{-3}	0.013
Pu	500	5800	3.6×10^{-5}	3.6×10^{-4}	3.6×10^{-3}
Ra	50	580	3.8×10^{-4}	3.8×10^{-3}	0.038
Sn	50	580	3.8×10^{-4}	3.8×10^{-3}	0.038
Sr	100	120	1.9×10^{-4}	1.9×10^{-3}	0.019
Tc	20	230	9.4×10^{-4}	9.4×10^{-3}	0.094

(a) Migration distance based on water velocity of 0.22 m/yr.

TABLE D.18. Estimated Maximum Concentration of Selected Radionuclides in Fracture for Event Occurring 100 Years After Repository Closure (μCi/mL)--Reference Case

Radionuclide	Subcase a	Subcase b	Subcase c	Subcase d	RCG[a]
^{241}Am	1.4×10^{-7}	1.7×10^{-7}	2.1×10^{-7}	2.4×10^{-7}	4.0×10^{-6}
^{243}Am	1.0×10^{-8}	1.3×10^{-8}	1.6×10^{-8}	1.8×10^{-8}	4.0×10^{-6}
^{14}C	1.2×10^{-10}	1.5×10^{-10}	1.9×10^{-10}	2.1×10^{-10}	8.0×10^{-4}
^{135}Cs	6.7×10^{-11}	8.5×10^{-11}	1.0×10^{-10}	1.2×10^{-10}	1.0×10^{-4}
^{137}Cs	2.0×10^{-6}	2.6×10^{-6}	3.1×10^{-6}	3.5×10^{-6}	2.0×10^{-5}
^{237}Np	1.2×10^{-10}	1.5×10^{-10}	1.9×10^{-10}	2.1×10^{-10}	3.0×10^{-6}
^{238}Pu	1.1×10^{-8}	1.4×10^{-8}	1.7×10^{-8}	2.0×10^{-8}	5.0×10^{-6}
^{239}Pu	4.1×10^{-10}	5.3×10^{-10}	6.4×10^{-10}	7.3×10^{-10}	5.0×10^{-6}
^{240}Pu	4.8×10^{-9}	6.1×10^{-9}	7.4×10^{-9}	8.3×10^{-9}	5.0×10^{-6}
^{242}Pu	4.5×10^{-12}	5.8×10^{-12}	6.9×10^{-12}	7.9×10^{-12}	5.0×10^{-6}
^{226}Ra	1.5×10^{-16}	1.9×10^{-16}	2.3×10^{-16}	2.6×10^{-16}	3.0×10^{-8}
^{90}Sr	1.2×10^{-6}	1.5×10^{-6}	1.8×10^{-6}	2.0×10^{-6}	3.0×10^{-7}
^{126}Sn	1.2×10^{-10}	1.5×10^{-10}	1.8×10^{-10}	2.1×10^{-10}	Not determined
^{99}Tc	2.2×10^{-9}	3.6×10^{-9}	4.3×10^{-9}	4.9×10^{-9}	3.0×10^{-4}
^{129}I	7.6×10^{-12}	9.7×10^{-12}	1.2×10^{-11}	1.3×10^{-11}	6.0×10^{-8}

(a) Values for Radionuclide Concentration Guide (RCG) were taken from 10 CFR 20, Appendix B, Table 2 (NRC 1981a).

TABLE D.19. Estimated Maximum Concentration of Selected Radionuclides in Fracture for Event Occurring 1,000 Years After Repository Closure (μCi/mL)--Reference Case

Radionuclide	Subcase a	Subcase b	Subcase c	Subcase d	RCG[a]
^{241}Am	3.3×10^{-8}	4.2×10^{-8}	5.0×10^{-8}	5.7×10^{-8}	4.0×10^{-6}
^{243}Am	9.3×10^{-9}	1.2×10^{-8}	1.4×10^{-8}	1.6×10^{-8}	4.0×10^{-6}
^{14}C	1.1×10^{-10}	1.4×10^{-10}	1.7×10^{-10}	1.8×10^{-10}	8.0×10^{-4}
^{135}Cs	6.7×10^{-11}	8.5×10^{-11}	1.0×10^{-10}	1.2×10^{-10}	1.0×10^{-4}
^{137}Cs	1.9×10^{-15}	2.4×10^{-15}	2.9×10^{-15}	3.3×10^{-15}	2.0×10^{-5}
^{237}Np	3.2×10^{-10}	4.1×10^{-10}	5.0×10^{-10}	5.6×10^{-10}	3.0×10^{-6}
^{238}Pu	2.2×10^{-10}	2.8×10^{-10}	3.3×10^{-10}	3.8×10^{-10}	5.0×10^{-6}
^{239}Pu	6.5×10^{-10}	8.3×10^{-10}	1.0×10^{-9}	1.1×10^{-9}	5.0×10^{-6}
^{240}Pu	4.5×10^{-9}	5.7×10^{-9}	6.8×10^{-9}	7.7×10^{-9}	5.0×10^{-6}
^{242}Pu	5.5×10^{-12}	6.5×10^{-12}	7.8×10^{-12}	8.8×10^{-12}	5.0×10^{-6}
^{226}Ra	1.4×10^{-14}	1.7×10^{-14}	2.1×10^{-14}	2.4×10^{-14}	3.0×10^{-8}
^{90}Sr	2.6×10^{-16}	3.3×10^{-16}	4.0×10^{-16}	4.5×10^{-16}	3.0×10^{-7}
^{126}Sn	1.2×10^{-10}	1.5×10^{-10}	1.8×10^{-10}	2.1×10^{-10}	Not determined
^{99}Tc	2.8×10^{-9}	3.6×10^{-9}	4.3×10^{-9}	4.9×10^{-9}	3.0×10^{-4}
^{129}I	7.6×10^{-12}	9.6×10^{-12}	1.2×10^{-11}	1.3×10^{-11}	6.0×10^{-8}

(a) Values for Radionuclide Concentration Guide (RCG) were taken from 10 CFR 20, Appendix B, Table 2 (NRC 1981a).

Variation in the estimated concentration of selected radionuclides present in the fracture is a function of the concentration of radionuclides per unit volume of waste (i.e., waste loading). Increasing the radionuclide content per unit volume of solidified waste increases radionuclide concentration per unit volume of waste leached.

D.3.1.2 Alternative A

Under Alternative A, it is assumed that the entire waste inventory is placed in a geologic repository following separation of Cs and Sr. Ten-year-old HLW is fractionated into a Cs/Sr component and a "fractionated HLW" (FHLW) component. The Cs/Sr and FHLW components are solidified and disposed of directly in a repository but in separate regions.

The faulting event is assumed to occur at either 100 or 1,000 years after repository closure and has the same characteristics as described under the Reference Case. Other input parameters for Alternative A are presented in Table D.20. Inserting these values into Equation D.10, yields cumulative curies of ^{241}Am released to ground water (as shown in Table D.21).

As expected, ^{241}Am is released into ground water principally from the FHLW portion of the overall repository. The ^{241}Am release is highest for the subcase where the largest FHLW repository section is assumed (Subcase a) and lowest for the subcase where the smallest FHLW repository section is assumed (Subcase d). The ratio of the cumulative release for one subcase versus another is approximately equal to the ratio of the square root of the repository areas for the respective subcases. This is in agreement with Equation D.10.

Cumulative releases of selected radionuclides to the fault zone over a 10,000-year period are presented in Tables D.22 and D.23. These releases are the result of ground water leaching action caused by a fault zone occurring 100 or 1,000 years after repository closure. These isotopes exhibit the same behavior as ^{241}Am in Table D.20 (i.e., the ratio of releases being approximately equal to the ratio of the square root of repository areas for the respective subcases). The ^{241}Am relationship also exists when cumulative releases of isotopes from subcases within Alternative A are compared to their corresponding values in subcases of the Reference Case.

In general, cumulative releases for Alternative A are less than cumulative releases under the Reference Case. This difference is due primarily to the fractionation step associated with Alternative A. Fractionation enables concentration of the non-heat-generating isotopes, allows a more efficient emplacement of these waste canisters, and results in a smaller repository area for a given canister sizing and spacing because of higher canister loadings (e.g., MTE/canister).

As shown previously in Table D.17, no elements would reach the accessible environment in 10,000 years. Estimates of maximum concentrations of radionulides in ground water following the leaching action of the waste form caused by a faulting event occurring 100 or 1,000 years after repository closure are contained in Tables D.24 and D.25. The results are similar to the Reference Case,

TABLE D.20. Input Parameters to Faulting-Event Calculation--Alternative A

Inventory	Subcase	MTE / Canister	kg Glass / MTE	cm^3 Glass / kg Glass	Number of Canisters	Canister Radius (m)	Canister Spacing (m)	Repository Area (km^2)(b)	Repository Thickness (cm)	Leach Rate (g/cm^2-day)
Fractionated High-Level Waste	a	0.627	222	319	7.97×10^4	0.0762	3.8	12	305	1.0×10^{-5}
	b	1.45	958	319	3.44×10^4	0.0762	4.6	7.49	305	1.0×10^{-5}
	c	2.48	110	319	2.02×10^4	0.107	5.0	5.55	305	1.0×10^{-5}
	d	3.63	111	319	1.38×10^4	0.130	4.5	4.25	305	1.0×10^{-5}
Cs/Sr		2.64	171	319	1.89×10^4	0.137	4.7	3.00	305	1.0×10^{-5}

(a) Subcase a defined as Row 1 of FHLW + Cs/Sr row; Subcase b defined as Row 2 from FHLW + Cs/Sr row; Subcase c defined as Row 3 from FHLW + Cs/Sr row; Subcase d defined as Row 4 from FHLW + Cs/Sr row.
(b) Areas for FHLW include shafts and other common areas in addition to waste emplacement area. Area for Cs/Sr only includes waste emplacement requirements.

TABLE D.21. Cumulative Release of ^{241}Am to Ground Water, Over 10,000 Years, from Faults Occurring at 100 and 1,000 Years After Repository Closure--Alternative A[a]

Inventory	Subcase	Canister Radius (m)	Canister Spacing (m)	Repository Area (km^2)[b]	Release (Ci) Fault at Year 100	Release (Ci) Fault at Year 1000
Fractionated High-Level Waste (FHLW)	a	0.076	3.8	12	420	90
	b	0.076	4.6	7.49	310	67
	c	0.11	5.0	5.55	250	53
	d	0.13	4.5	4.25	200	42
Cs/Sr		0.14	4.7	3.00	2.79	0.67×10^{-1}

(a) Subcase a defined as Row 1 from FHLW + Cs/Sr row; Subcase b defined as Row 2 from HLW + Cs/Sr row; Subcase c defined as Row 3 from FHLW + Cs/Sr row; Subcase d defined as Row 4 from FHLW + Cs/Sr row.

(b) Areas for FHLW include shafts and other common areas in addition to waste emplacement area. Area for Cs/Sr only includes waste emplacement requirements

TABLE D.22. Cumulative Release of Radionuclides to Ground Water Over 10,000 Years from a Faulting Event Occurring 100 Years After Repository Closure (Ci)--Alternative A

Radionuclide	Subcase a	Subcase b	Subcase c	Subcase d
^{241}Am	4.2×10^{2}	3.1×10^{2}	2.5×10^{2}	2.0×10^{2}
^{243}Am	3.4×10^{2}	2.5×10^{2}	2.0×10^{2}	1.6×10^{2}
^{14}C	3.6	2.7	2.1	1.7
^{135}Cs	1.9	2.0	1.9	1.9
^{137}Cs	2.0×10^{2}	2.0×10^{2}	2.0×10^{2}	2.0×10^{2}
^{237}Np	3.5×10^{1}	2.6×10^{1}	2.1×10^{1}	1.6×10^{1}
^{238}Pu	4.8	3.6	2.9	2.3
^{239}Pu	1.7×10^{1}	1.3×10^{1}	1.0×10^{1}	8.2
^{240}Pu	6.6×10^{1}	4.9×10^{1}	3.9×10^{1}	3.1×10^{1}
^{242}Pu	2.2×10^{-1}	1.6×10^{-1}	1.3×10^{-1}	1.0×10^{-1}
^{226}Ra	5.4×10^{-2}	4.0×10^{-2}	3.2×10^{-2}	2.5×10^{-2}
^{90}Sr	1.1×10^{2}	1.2×10^{2}	1.1×10^{2}	1.2×10^{1}
^{126}Sn	5.9	4.4	3.5	2.8
^{99}Tc	1.4×10^{2}	1.1×10^{2}	8.4×10^{1}	6.6×10^{1}
^{129}I	3.9×10^{-1}	2.9×10^{-1}	2.3×10^{-1}	1.8×10^{-1}

TABLE D.23. Cumulative Release of Radionuclides to Ground Water Over 10,000 Years from a Faulting Event Occurring 1,000 Years After Repository Closure (Ci)--Alternative A

Radionuclide	Subcase a	Subcase b	Subcase c	Subcase d
^{241}Am	9.0×10^{1}	6.7×10^{1}	5.3×10^{1}	4.2×10^{1}
^{243}Am	2.7×10^{2}	2.0×10^{2}	1.6×10^{2}	1.2×10^{2}
^{14}C	2.8	2.1	1.6	1.3
^{135}Cs	1.6	1.6	1.6	1.6
^{137}Cs	1.7×10^{-7}	1.7×10^{-7}	1.7×10^{-7}	1.7×10^{-7}
^{237}Np	2.9×10^{1}	2.1×10^{1}	1.7×10^{1}	1.3×10^{1}
^{238}Pu	3.7×10^{-3}	$2.7 \times 1-^{-3}$	2.2×10^{-3}	1.7×10^{-3}
^{239}Pu	1.4×10^{1}	1.1×10^{1}	8.4	6.7
^{240}Pu	5.2×10^{1}	3.8×10^{1}	3.1×10^{1}	2.4
^{242}Pu	1.8×10^{-1}	1.3×10^{-1}	1.1×10^{-1}	8.4×10^{-2}
^{226}Ra	3.3×10^{-2}	2.4×10^{-2}	2.0×10^{-2}	1.5×10^{-2}
^{90}Sr	4.8×10^{-8}	4.8×10^{-8}	4.9×10^{-8}	4.8×10^{-8}
^{126}Sn	4.8	3.6	2.9	2.3
^{99}Tc	1.1×10^{2}	8.7×10^{1}	7.0×10^{1}	5.5×10^{1}
^{129}I	3.2×10^{-1}	2.4×10^{-1}	1.9×10^{-1}	1.5×10^{-1}

TABLE D.24. Estimated Maximum Concentration of Selected Radionuclides in Fracture for Event Occurring 100 Years After Repository Closure (μCi/mL)--Alternative A

Radionuclide	Subcase a	Subcase b	Subcase c	Subcase d	RCG[a]
^{241}Am	2.3×10^{-7}	3.0×10^{-7}	3.7×10^{-7}	4.6×10^{-8}	4.0×10^{-6}
^{243}Am	1.7×10^{-8}	2.3×10^{-8}	2.8×10^{-8}	3.4×10^{-8}	4.0×10^{-6}
^{14}C	2.0×10^{-10}	2.7×10^{-10}	3.3×10^{-10}	4.1×10^{-10}	8.0×10^{-4}
^{135}Cs	2.0×10^{-10}	2.0×10^{-10}	1.9×10^{-10}	1.9×10^{-10}	1.0×10^{-4}
^{137}Cs	6.0×10^{-6}	5.9×10^{-6}	5.9×10^{-6}	5.9×10^{-6}	2.0×10^{-5}
^{237}Np	2.0×10^{-10}	2.7×10^{-10}	3.3×10^{-10}	4.1×10^{-10}	3.0×10^{-6}
^{238}Pu	1.9×10^{-8}	2.5×10^{-8}	3.1×10^{-8}	3.8×10^{-8}	5.0×10^{-6}
^{239}Pu	6.9×10^{-10}	9.3×10^{-10}	1.1×10^{-9}	1.4×10^{-9}	5.0×10^{-6}
^{240}Pu	8.0×10^{-9}	1.1×10^{-8}	1.3×10^{-8}	1.6×10^{-8}	5.0×10^{-6}
^{242}Pu	7.5×10^{-12}	1.0×10^{-11}	1.2×10^{-11}	1.5×10^{-11}	5.0×10^{-6}
^{226}Ra	2.5×10^{-16}	3.3×10^{-16}	4.0×10^{-16}	5.1×10^{-16}	3.0×10^{-8}
^{90}Sr	3.4×10^{-6}	3.4×10^{-6}	3.3×10^{-6}	3.3×10^{-6}	3.0×10^{-7}
^{126}Sn(b)	2.0×10^{-10}	2.6×10^{-10}	3.2×10^{-10}	4.1×10^{-10}	Not determined
^{99}Tc	4.6×10^{-9}	6.2×10^{-9}	7.7×10^{-9}	9.6×10^{-9}	3.0×10^{-4}
^{129}I	1.3×10^{-11}	1.7×10^{-12}	2.1×10^{-11}	2.6×10^{-11}	6.0×10^{-8}

(a) Values for Radionuclide Concentration Guide (RCG) were taken from 10 CFR 20, Appendix B, Table 2 (NRC 1981a).

(b) Did not specifically address separations efficiency relative to ^{126}Sn as part of study. It was assumed all ^{126}Sn would remain in FHLW.

TABLE D.25. Estimated Maximum Concentration of Selected Radionuclides in Fracture for Event Occurring 1,000 Years After Repository Closure (μCi/mL)--Alternative A

Radionuclide	Subcase a	Subcase b	Subcase c	Subcase d	RCG[a]
^{241}Am	5.4×10^{-8}	7.2×10^{-8}	8.9×10^{-8}	1.1×10^{-7}	4.0×10^{-6}
^{243}Am	1.6×10^{-8}	2.0×10^{-8}	2.5×10^{-8}	3.2×10^{-8}	4.0×10^{-6}
^{14}C	1.8×10^{-10}	2.4×10^{-10}	3.0×10^{-10}	3.7×10^{-10}	8.0×10^{-4}
^{135}Cs	2.0×10^{-10}	2.0×10^{-10}	1.9×10^{-10}	1.9×10^{-10}	1.0×10^{-4}
^{137}Cs	5.6×10^{-15}	5.6×10^{-15}	5.5×10^{-15}	5.5×10^{-15}	2.0×10^{-5}
^{237}Np	5.4×10^{-10}	7.2×10^{-10}	8.8×10^{-10}	1.1×10^{-9}	3.0×10^{-6}
^{238}Pu	3.6×10^{-10}	4.8×10^{-10}	5.6×10^{-10}	7.3×10^{-10}	5.0×10^{-6}
^{239}Pu	1.1×10^{-9}	1.5×10^{-9}	1.8×10^{-9}	2.2×10^{-9}	5.0×10^{-6}
^{240}Pu	7.4×10^{-9}	9.9×10^{-9}	1.2×10^{-8}	1.5×10^{-8}	5.0×10^{-6}
^{242}Pu	8.4×10^{-12}	1.1×10^{-11}	1.4×10^{-11}	1.7×10^{-11}	5.0×10^{-6}
^{226}Ra	2.3×10^{-14}	3.0×10^{-14}	3.7×10^{-14}	4.6×10^{-14}	3.0×10^{-8}
^{90}Sr	7.7×10^{-16}	7.6×10^{-16}	7.5×10^{-16}	7.5×10^{-16}	3.0×10^{-7}
^{126}Sn[b]	1.9×10^{-10}	2.6×10^{-10}	3.2×10^{-10}	4.0×10^{-10}	Not determined
^{99}Tc	4.6×10^{-9}	6.2×10^{-9}	7.7×10^{-9}	9.6×10^{-9}	3.0×10^{-4}
^{129}I	1.3×10^{-11}	1.7×10^{-11}	2.1×10^{-11}	2.0×10^{-11}	2.9×10^{-8}

(a) Values for Radionuclide Concentration Guide (RCG) were taken from 10 CFR 20, Appendix B, Table 2 (NRC 1981a).

(b) Did not specifically address separations efficiency relative to ^{126}Sn as part of study. It was assumed all ^{126}Sn would remain in FHLW.

with only ^{90}Sr at year 100 exceeding RCG values. However, the dilution factor of 4,700 previously discussed for the Reference Case would reduce withdrawn waters to below RCG values.

The concentration of radionuclides in ground water following the leaching action of the waste form is a function of the concentration of radionuclides per unit volume of waste (i.e., waste loading). Increasing the radionuclide content per unit volume of solidified waste increases radionuclide concentration per unit volume of waste leached.

D.3.1.3 Alternative B

Under Alternative B, it is assumed that the entire waste inventory is placed in a geologic repository following extended storage. Ten-year-old HLW is assumed solidified and stored on the surface for an additional 50 years prior to disposal.

The faulting event is assumed to occur at either 100 or 1,000 years after repository closure and has the same characteristics as described in the Reference Case. Other input parameters for Alternative B are presented in Table D.26. Inserting these values into Equation D.10 yields cumulative curies of ^{241}Am released to ground water as shown in Table D.27. In Table D.27, the ^{241}Am release is highest for the subcase where the largest repository area is assumed (Subcase a) and lowest for the subcase where the smallest repository area is assumed (Subcase d). The ratio of the cumulative release for one case versus another is approximately equal to the ratio of the square root of the repository areas for the respective cases. This is in agreement with Equation D.10.

Cumulative releases of selected radionuclides to the fault zone over a 10,000-year period are presented in Tables D.28 and D.29. These releases are the result of ground-water leaching action caused by a fault occurring 100 or 1,000 years after repository closure. These isotopes exhibit the same behavior as ^{241}Am in Table D.27 (i.e., ratio of releases being equal to ratio of the square root of repository areas for the respective cases). This relationship exists when cumulative releases of isotopes from cases within Alternative B are compared to their corresponding values in subcases of either the Reference Case or Alternative A.

TABLE D.26. Input Parameters to Faulting-Event Calculation--Alternative B

Subcase[a]	MTE / Canister	kg Glass / MTE	cm^3 Glass / kg Glass	Number of Canisters	Canister Radius (m)	Canister Spacing (m)	Repository Area (km^2)	Repository Thickness (cm)	Leach Rate (g/cm^2-day)
a (100°C)	0.627	222	319	7.97×10^4	0.0762	3.8	12	305	1.0×10^{-5}
b (150°C)	1.45	95.8	319	3.44×10^4	0.0762	4.6	7.49	305	1.0×10^{-5}
c (200°C)	2.48	110	319	2.02×10^4	0.107	5.0	5.55	305	1.0×10^{-5}
d (250°C)	3.63	111	319	1.38×10^4	0.130	4.5	4.25	305	1.0×10^{-5}

(a) Repository thermal design limits.

TABLE D.27. Cumulative Release of ^{241}Am to Ground Water Over 10,000 Years from Faults Occurring at 100 and 1,000 Years After Repository Closure--Alternative B

Subcase	Canister Radius (m)	Canister Spacing (m)	Repository Area (km^2)	Release (Ci) Fault at Year 100	Release (Ci) Fault at Year 1000
a	0.076	3.8	12	420	90
b	0.076	4.6	7.49	310	67
c	0.11	5.0	5.55	250	53
d	0.13	4.5	4.25	200	42

TABLE D.28. Cumulative Release of Radionuclides to Ground Water Over 10,000 Years from a Faulting Event Occurring 100 Years After Repository Closure (Ci)--Alternative B

Radionuclide	Subcase a	Subcase b	Subcase c	Subcase d
^{241}Am	4.2×10^{2}	3.1×10^{2}	2.5×10^{2}	2.0×10^{2}
^{243}Am	3.4×10^{2}	2.5×10^{2}	2.0×10^{2}	1.6×10^{2}
^{14}C	3.6	2.7	2.1	1.7
^{135}Cs	3.4	2.6	2.0	1.6
^{137}Cs	3.6×10^{2}	2.7×10^{2}	2.1×10^{2}	1.7×10^{2}
^{237}Np	3.5×10^{1}	2.6×10^{1}	2.1×10^{1}	1.6×10^{1}
^{238}Pu	4.8	3.6	2.9	2.3
^{239}Pu	1.7×10^{1}	1.3×10^{1}	1.0×10^{1}	8.2
^{240}Pu	6.6×10^{1}	4.9×10^{1}	3.9×10^{1}	3.1×10^{1}
^{242}Pu	2.2×10^{-1}	1.6×10^{-1}	1.3×10^{-1}	1.0×10^{-1}
^{226}Ra	5.4×10^{-2}	4.0×10^{-2}	3.2×10^{-2}	2.5×10^{-2}
^{90}Sr	2.1×10^{2}	1.6×10^{2}	1.2×10^{2}	9.9×10^{1}
^{126}Sn	5.9	4.4	3.5	2.8
^{99}Tc	1.4×10^{2}	1.1×10^{2}	8.4×10^{1}	6.6×10^{1}
^{129}I	3.9×10^{-1}	2.9×10^{-1}	2.3×10^{-1}	1.8×10^{-1}

TABLE D.29. Cumulative Release of Radionuclides to Ground Water Over 10,000 Years from a Faulting Event Occurring 1,000 Years After Repository Closure (Ci)--Alternative B

Radionuclide	Subcase a	Subcase b	Subcase c	Subcase d
^{241}Am	9.0×10^{1}	6.7×10^{1}	5.3×10^{1}	4.2×10^{1}
^{243}Am	2.7×10^{2}	2.0×10^{2}	1.6×10^{2}	1.2×10^{2}
^{14}C	2.8	2.1	1.6	1.3
^{135}Cs	2.9	2.1	1.7	1.3
^{137}Cs	3.0×10^{-7}	2.3×10^{-7}	1.8×10^{-7}	1.4×10^{-7}
^{237}Np	2.9×10^{1}	2.1×10^{1}	1.7×10^{1}	1.3×10^{1}
^{238}Pu	3.7×10^{-3}	2.7×10^{-3}	2.2×10^{-3}	1.7×10^{-3}
^{239}Pu	1.4×10^{1}	1.1×10^{1}	8.4	6.7
^{240}Pu	5.2×10^{1}	3.8×10^{1}	3.1×10^{1}	2.4
^{242}Pu	1.8×10^{-1}	1.3×10^{-1}	1.1×10^{-1}	8.4×10^{-2}
^{226}Ra	3.3×10^{-2}	2.4×10^{-2}	2.0×10^{-2}	1.5×10^{-2}
^{90}Sr	8.7×10^{-8}	6.5×10^{-8}	5.2×10^{-8}	4.1×10^{-8}
^{126}Sn	4.8	3.6	2.9	2.3
^{99}Tc	1.1×10^{2}	8.7×10^{1}	7.0×10^{1}	5.5×10^{1}
^{129}I	3.2×10^{-1}	2.4×10^{-1}	1.9×10^{-1}	1.5×10^{-1}

In general, cumulative releases for Alternative B are less than cumulative releases under the Reference Case. This difference is due primarily to the extended surface storage period associated with Alternative B. Extended storage enables high heat-generating isotopes to decay, allows a more efficient emplacement of waste canisters, and results in a smaller repository area for a given canister sizing and spacing because of higher canister loadings (e.g., MTE/canister).

Cumulative releases for Alternative B are generally the same as Alternative A, because of the similar emplacement areas. Releases of Cs and Sr tend to be less for Alternative A than B, as the Cs/Sr subregion is usually smaller than the aged-HLW emplacement area(s).

In general, cumulative releases under Alternative B are slightly greater than releases under Alternative A. This is principally due to the fact that the repository in Alternative A is assumed to be comprised of two

sub-repositories (one for Cs/Sr waste, one for FHLW). The area of each of the individual sub-repositories for the four cases in Alternative A is always less than the overall repository area for the corresponding cases under Alternative B. This subdivision causes the total fault plane area, and ultimately the cumulative releases, in Alternative A to be lower than the corresponding values in Alternative B.

As for the Reference Case and Alternative A, no elements reach the accessible environment in 10,000 years (Table D.17). Estimates of maximum concentrations in ground water following leaching of the waste form caused by a faulting event occurring 100 or 1,000 years after repository closure are presented in Tables D.30 and D.31. The results are similar to the Reference

TABLE D.30. Estimated Maximum Concentration of Selected Radionuclides in Fracture for Event Occurring 100 Years After Repository Closure (μCi/mL)--Alternative B

Radionuclide	Subcase a	Subcase b	Subcase c	Subcase d	RCG[a]
^{241}Am	2.2×10^{-7}	2.8×10^{-7}	3.3×10^{-7}	3.7×10^{-7}	4.0×10^{-6}
^{243}Am	1.6×10^{-8}	2.1×10^{-8}	2.4×10^{-8}	2.8×10^{-8}	4.0×10^{-6}
^{14}C	1.9×10^{-10}	2.5×10^{-10}	2.9×10^{-10}	3.3×10^{-10}	8.0×10^{-4}
^{135}Cs	1.1×10^{-10}	1.4×10^{-10}	1.6×10^{-10}	1.8×10^{-10}	1.0×10^{-4}
^{137}Cs	3.3×10^{-6}	4.2×10^{-6}	4.9×10^{-6}	5.5×10^{-6}	2.0×10^{-5}
^{237}Np	1.9×10^{-10}	2.5×10^{-10}	2.9×10^{-10}	3.3×10^{-10}	3.0×10^{-6}
^{238}Pu	1.8×10^{-8}	2.3×10^{-8}	2.7×10^{-8}	3.1×10^{-8}	5.0×10^{-6}
^{239}Pu	6.7×10^{-10}	8.6×10^{-10}	1.0×10^{-9}	1.1×10^{-9}	5.0×10^{-6}
^{240}Pu	7.7×10^{-9}	9.9×10^{-9}	1.2×10^{-8}	1.3×10^{-8}	5.0×10^{-6}
^{242}Pu	7.2×10^{-12}	9.3×10^{-12}	1.1×10^{-11}	1.2×10^{-11}	5.0×10^{-6}
^{226}Ra	2.4×10^{-16}	3.1×10^{-16}	3.6×10^{-16}	4.1×10^{-16}	3.0×10^{-8}
^{90}Sr	1.8×10^{-6}	2.4×10^{-6}	2.7×10^{-6}	3.1×10^{-6}	3.0×10^{-7}
^{126}Sn	1.9×10^{-10}	2.4×10^{-10}	2.8×10^{-10}	3.2×10^{-10}	Not determined
^{99}Tc	4.5×10^{-9}	5.8×10^{-9}	6.7×10^{-9}	7.7×10^{-9}	3.0×10^{-4}
^{129}I	1.2×10^{-11}	1.6×10^{-11}	1.8×10^{-11}	2.7×10^{-11}	6.0×10^{-8}

(a) Values for Radionuclide Concentration Guide (RCG) were taken from 10 CFR 20, Appendix B, Table 2 (NRC 1981a).

TABLE D.31. Estimated Maximum Concentration of Selected Radionuclides in Fracture for Event Occurring 1,000 Years After Repository Closure (μCi/mL)--Alternative B

Radionuclide	Subcase a	Subcase b	Subcase c	Subcase d	RCG[a]
^{241}Am	5.2×10^{-8}	6.7×10^{-8}	7.8×10^{-8}	8.9×10^{-8}	4.0×10^{-6}
^{243}Am	1.5×10^{-8}	1.9×10^{-8}	2.2×10^{-8}	2.6×10^{-8}	4.0×10^{-6}
^{14}C	1.7×10^{-10}	2.2×10^{-10}	2.6×10^{-10}	3.0×10^{-10}	8.0×10^{-4}
^{135}Cs	1.1×10^{-10}	1.4×10^{-10}	1.6×10^{-10}	1.8×10^{-10}	1.0×10^{-4}
^{137}Cs	3.0×10^{-15}	3.9×10^{-15}	4.5×10^{-15}	5.2×10^{-15}	2.0×10^{-5}
^{237}Np	5.2×10^{-10}	6.7×10^{-10}	7.7×10^{-10}	8.9×10^{-10}	3.0×10^{-6}
^{238}Pu	3.5×10^{-10}	4.4×10^{-10}	5.2×10^{-10}	5.9×10^{-10}	5.0×10^{-6}
^{239}Pu	1.0×10^{-9}	1.3×10^{-9}	1.6×10^{-9}	1.8×10^{-9}	5.0×10^{-6}
^{240}Pu	7.1×10^{-9}	9.2×10^{-9}	1.1×10^{-8}	1.2×10^{-8}	5.0×10^{-6}
^{242}Pu	8.1×10^{-12}	1.0×10^{-11}	1.2×10^{-11}	1.4×10^{-11}	5.0×10^{-6}
^{226}Ra	2.2×10^{-14}	2.8×10^{-14}	3.3×10^{-14}	3.7×10^{-14}	3.0×10^{-8}
^{90}Sr	4.2×10^{-16}	5.3×10^{-16}	6.2×10^{-16}	7.1×10^{-16}	3.0×10^{-7}
^{126}Sn	1.9×10^{-10}	2.4×10^{-10}	2.8×10^{-10}	3.2×10^{-10}	Not determined
^{99}Tc	4.5×10^{-7}	5.8×10^{-9}	6.7×10^{-9}	7.7×10^{-9}	3.0×10^{-4}
^{129}I	1.2×10^{-11}	1.6×10^{-11}	1.8×10^{-11}	2.1×10^{-11}	6.0×10^{-8}

(a) Values for Radionuclide Concentration Guide (RCG) were taken from 10 CFR 20, Appendix B, Table 2 (NRC 1981a).

Case and Alternative A, with only ^{90}Sr at year 100 exceeding RCG values. However, the dilution factor of 4,700 previously discussed for the Reference Case would reduce withdrawn waters to below RCG values.

Variations in the estimated concentration of selected radionuclides present in the fracture is a function of the concentration of radionuclides per unit volume of waste (i.e., waste loading). Increasing the radionuclide content per unit volume of solidified waste increases radionuclide concentration per unit volume of waste leached.

D.3.2 Direct Drilling

The purpose of this discussion is: 1) to develop a generalized equation for determining the expected impact of drilling events occurring over 10,000 years; 2) to identify which parameters in the equation are constants (and, therefore, do not affect the impacts associated with one alternative in comparison to the others); 3) to identify which parameters in the equation are variables (and, therefore, do influence the impacts of the Reference Case with respect to Alternatives A and B); and 4) to compare the impacts of the drilling events for each alternative and for the range of input parameters assumed.

Direct drilling into a geologic repository, an inadvertent action, could result either from exploration for resources or from geologic study. In a generic sense, the expected impact[(a)] from direct drilling is considered the product of the following terms:

Expected impact = (Rate of drilling)
x (Likelihood of contacting canister if drilling occurs)
x (Fraction of canister removed if contacted)
x (Canister Inventory) (D.12)

Rate of drilling, R, is determined by multiplying the frequency of drilling, f (in units of events per unit time per unit area), by the repository area, A_R (in units of km^2). The result is:

$$R = (f) \times (A_R) \quad (D.13)$$

Likelihood of contacting a canister, L, is defined as the ratio of the canister target area to the repository area. Since, in theory, a drill bit intersects a canister when the two objects are tangential (or when the point of the drill bit lies within the drill radius of the canister), the target area for one canister is considered equal to: $\pi(Rc + Rd)^2$, where Rc and Rd are the canister and drill radii, respectively (in units of cm^2). The likelihood of any canister contact if drilling occurs is:

(a) Expected impact is used here in the same manner the term "expected value" is used in statistics. Expected impact is the mathematical product of the likelihood of an event occurring multiplied by the consequences of occurrence.

$$L = \frac{\pi(Rc + Rd)^2 \times (N)}{A_R} \qquad (D.14)$$

where N is the number of canisters.

The number of canisters is defined as total waste quantity divided by the quantity of waste per canister, which is equal to:

$$N = \frac{(I_R) \times (G)}{\pi(Rc)^2 \times (H) \times (D)} \qquad (D.15)$$

where I_R is the inventory of the repository in MTE, G the glass loading in kg glass/MTE, H the canister height in cm, and D the glass density in kg/cm^3. Substituting this into the term above yields the following for the likelihood of contacting a canister in a repository if drilling occurs:

$$L = \frac{\pi(Rc + Rd)^2 \times (I_R) \times (G)}{(A_R) \times (H) \times (D)} \qquad (D.16)$$

The fraction of canister removed if contacted is a term which identifies what portion of a waste canister on average (i.e., weighted fraction) is brought to the surface should a drill bit intersect a canister. Intersection is defined as the two objects being at least tangential to each other (Figure D.1).

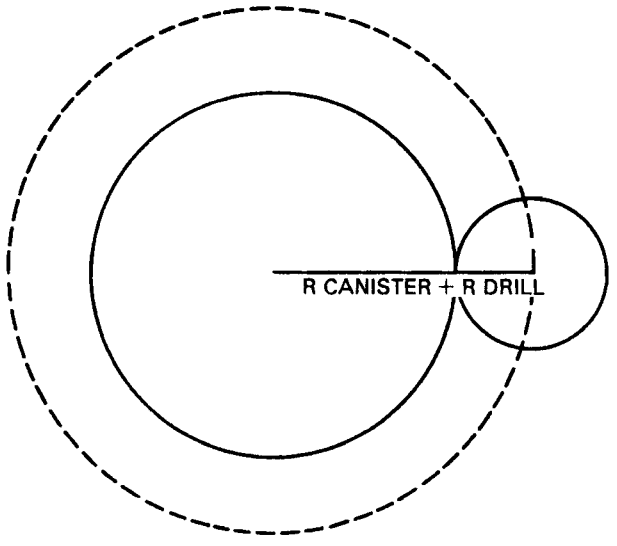

FIGURE D.1. Intersection of Two Objects

A lengthy geometric analysis yields the following equation for the weighted fraction removed (f(x)):

$$f(\overline{x}) = \left(\frac{2}{(Rc + RD)^2}\right)\left[\int_0^R \left(\frac{Rd}{Rd}\right)^2 (X)\, dX + \int_R^R \left(\left(\frac{Rd}{2(Rc)^2}\right) x\ (Rc + Rd) - \left(\frac{(Rd)\ x\ (X)}{2(Rc)^2}\right)\right)(X)\, dX\right] \quad (D.17)$$

After integrating and simplifying, the weighted fraction removed is described as:

$$f(\overline{x}) = \frac{(Rd)^2\ x\ \left((Rc)^2 + \frac{1}{3}(Rd)^2\right)}{(Rc)^2\ x\ (Rc + Rd)^2} \quad (D.18)$$

The canister inventory term, c, identifies how the inventory for a particular isotope (within a canister) changes over time. For a single drilling event this term would be equal to:

$$C = (W)\ x\ (I_0)\ x\ (e^{-\lambda T}) \quad (D.19)$$

where W is the canister loading in MTE/canister, I_0 is the initial isotopic inventory in Ci/MTE, λ is the ln 2 divided by the isotope's half-life, and T is the time in years when the event is assumed to occur after repository closure.

For a limited number of drilling events, Equation D.18 would be transformed to:

$$C = (W)\ x\ (I_0)\ x \sum_{i=1}^{n} e^{-\lambda T_i} \quad (D.20)$$

For multiple drilling events (which is the case in this analysis), Equation D.19 would converge to the following:

$$C = (W)\ x\ (I_0)\ x \int_{T_1}^{T_2} e^{-\lambda T}\, dT$$

where T_1 is the year when the calculation is initiated, or when the first drilling event occurs, and T_2 is the year when the calculation is terminated, or when the last drilling event occurs. After integration, this expression is simplified to:

$$C = (W) \times (I_o) \times \left(\frac{e^{-\lambda T_1} - e^{-\lambda T_2}}{\lambda} \right)^{(a)} \qquad (D.21)$$

Assuming multiple events, the expected impact of drilling into a geologic repository can, therefore, generically be described with the following equation:

$$\text{Expected impact} = \left[(f) \times (A_R) \right] \left[\left(\frac{\pi (Rc + Rd)^2}{A_R} \right) \times \frac{(I_R) \times (G) \times (\text{kg glass})}{\pi (RC)^2 \times (H) \times (D)} \right]$$

$$\times \left[\frac{(Rd)^2 \times (Rc)^2 + \frac{1}{3} (Rd)^2}{(Rc)^2 \times (Rc + Rd)^2} \right]$$

$$\times \left[(W) \times (I_o) \times \left(\frac{e^{-\lambda T_1} - e^{-\lambda T_2}}{\lambda} \right) \right] \qquad (D.22)$$

After cancellation, the above equation is simplified to:

$$\text{Expected impact} = (f) \times \frac{(I_R) \times (G)}{(H) \times (D)} \times \left[\left(\frac{Rd}{Rc} \right)^2 + \frac{1}{3} \left(\frac{Rd}{Rc} \right)^4 \right] \times (W) \times (I_o)$$

$$\times \left(\frac{e^{-\lambda T_1} - e^{-\lambda T_2}}{\lambda} \right) \qquad (D.23)$$

The A_R term, which appears in Equation D.22, is cancelled out of Equation D.23.[(b)] While increasing repository area tends to increase the rate of

---

(a) It is recognized that some radionuclides exhibit more complex decay chains. For these radionuclides, the appropriate decay chains were used.

(b) This discussion and the paragraph that follows assumes that the repository inventory (i.e., I_R) is constant.

drilling term, it decreases by a proportional amount the likelihood of contact term. For a given canister radius, repository area is a function of canister spacing. Therefore, spacing does not influence the expected impact, other parameters being constant. In addition, physically changing the location of canisters should not alter the likelihood of contacting any one canister given a random drilling event. Canister loading also does not influence expected impact, other parameters being equal. While increasing canister loading (e.g., MTE/canister) tends to increase the release from each drill-canister intersection, it decreases by a proportional amount the number of canisters in a repository, and, hence reduces the likelihood of intersection. Cumulative releases, however, would vary to some degree as a function of canister radius. This is confirmed by again examining Equation D.23 where a:

$$\left(\frac{Rd}{Rc}\right)^2 + \frac{1}{3}\left(\frac{Rd}{Rc}\right)^4 \text{ term is present.}$$

As canister radius increases (drill bit size remaining constant), the above term would tend to decrease and become asymptotic. While increasing canister radius would tend to slightly increase the likelihood of contact term (e.g., $(Rc + Rd)^2 > (Rc)^2$), this increase would diminish at larger radii and would be more than compensated for by a decrease in the weighted fraction removed term. Specifically, when drill bit size exceeds canister size, a direct hit is not required to bring up the maximum fraction (i.e., 100%) from the canister. When drill bit and canister size are equal, only for a hit where the centers are concentric would the maximum fraction be brought to the surface. When canister size exceeds drill bit size, the maximum fraction brought to the surface will be limited by drill size and will be a successively smaller fraction of the canister contents as canister size increases.

D.3.2.1 Reference Case

Under the Reference Case it is assumed that the entire waste inventory (e.g., 50,000 MTE) is placed in a geologic repository. Ten-year-old HLW is assumed solidified prior to emplacement.

The drilling rate estimates used are those in EPA (1980). These values are defined as the rate of drilling over the repository area in terms of holes

per first century after loss of institutional control, and holes per subsequent centuries (see Table D.32). This distinction in drilling rates is based on several factors:

- Since the site is controlled for a century or more, it is more attractive for exploration as less is known about it.
- The availability of the site provides an opportunity for new recovery operations, recognizing that commercial viability of mineral and energy resources changes over 100 years.
- The thermal anomaly encourages drilling.

TABLE D.32. Future Drilling Rate Estimates for Various Media (events/100 year/8 km^2)

Future Periods	Bedded Salt	Granite	Basalt	Shale	Domed Salt
First Century	5[(a)] to 50[(b)]	1 to 10	3 to 20	5 to 50	5 to 30
Subsequent Centuries	2 to 5	0.25 to 2	1 to 5	2 to 5	2 to 5

(a) The Environmental Protection Agency's (EPA) so-called "first-estimate" is defined as an assumption that the site exhibits favorable characteristics with respect to the particular conditions.
(b) The EPA's so-called "second estimate" is defined as an assumption that the site exhibits somewhat less favorable characteristics with respect to the particular breach conditions.

The EPA notes that the future drilling rates shown (Table D.32) are not strict extrapolations based on scientific, or statistical observation, but are rough estimates by A. D. Little, Inc., staff employing resource exploration and recovery experience. The EPA (1980) notes that these estimates do attempt to account for the time interval over which factors change significantly enough to justify another hole. Recognizing the inherent uncertainty in predicting future human behavior, the same uncertainty is attached to the EPA drilling-rate estimates.

Other input parameters used in the calculation of expected impact from a drilling event are presented in Table D.33. The time frame over which the

TABLE D.33. Input Parameters to Drilling Event Calculation--Reference Case

Subcase	MTE/Canister	kg Glass/MTE	cm^3 Glass/kg glass	Number of Canisters	Canister Radius (m)	Canister Spacing (m)	Repository Area (km^2)
a	0.167	833	319	3.0×10^5	0.076	3.5	31.6
b	0.389	358	319	1.3×10^5	0.076	4.0	19.4
c	0.639	218	319	7.8×10^4	0.076	4.2	13.4
d	0.907	153	319	5.5×10^4	0.076	4.5	10.5

calculation is made is 10,000 years. This is consistent with current EPA release limits for disposal of high-level and transuranic (TRU) waste and enables comparisons to be made to these limits.

Inserting the values in Tables D.32 and D.33 into Equation D.23 yields cumulative releases (of ^{241}Am) from drilling events occurring over 10,000 years (see Table D.34). In Table D.34 the cumulative release of ^{241}Am over a 10,000-year period remains constant for the canister loadings (i.e., MTE/canister), repository areas, and the canister spacings examined.

TABLE D.34. Cumulative Release of ^{241}Am from Drilling Events Occurring Over 10,000 Years at a Basalt Repository--Reference Case

Subcase	Canister Radius (m)	Canister Spacing (m)	Release (Ci)
a	0.076	3.5	13
b	0.076	4.0	13
c	0.076	4.2	13
d	0.076	4.5	13

Cumulative releases for all isotopes are presented in Table D.35. For perspective, these releases are compared to EPA release limits. All individual isotopes in Table D.35 are within their corresponding release limits. In addition, the sum of the ratios of releases for each isotope divided by its cumulative release limit is less than one.

TABLE D.35. Cumulative Releases from Drilling Events Occurring Over 10,000 Years at a Basalt Repository[a] (Ci)--Reference Case

Radionuclide	Cumulative Release	EPA[b]
^{241}Am	1.3×10^{1}	5.1×10^{2}
^{243}Am	7.7	2.1×10^{2}
^{14}C	8.2×10^{-2}	1.0×10^{4}
^{135}Cs	7.7×10^{-2}	1.0×10^{5}
^{137}Cs	2.8×10^{1}	2.5×10^{4}
^{237}Np	2.6×10^{-2}	1.0×10^{3}
^{238}Pu	3.4×10^{-1}	2.0×10^{4}
^{239}Pu	4.2×10^{-1}	5.0×10^{3}
^{240}Pu	3.5	5.0×10^{3}
^{242}Pu	5.2×10^{-3}	5.0×10^{3}
^{266}Ra	7.1×10^{-4}	1.6×10^{2}
^{90}Sr	1.5×10^{1}	4.0×10^{3}
^{99}Tc	3.2	1.0×10^{5}
^{126}Sn	1.3×10^{-1}	4.0×10^{3}
^{129}I	8.7×10^{-3}	5.1×10^{2}

(a) Assume Environmental Protection Agency's (EPA) first estimates of drilling rates and 0.076 m radius HLW canisters.

(b) Based on information provided by EPA (1982) and assuming the 50,000 metric ton equivalent (MTE) repository contains roughly 8.7×10^{5} Ci of alpha-emitting transuranic (TRU) waste.

D.3.2.2 Alternative A

Under Alternative A, it is assumed that the entire waste inventory is placed in a geologic repository following separation of Cs and Sr. Ten-year-old HLW is fractionated into a Cs/Sr component and a FHLW component. The FHLW and Cs/Sr components are solidified and disposed of directly in different regions of the same repository.

Drilling rates used in Alternative A are those previously presented in Table D.32. Other input parameters used in the calculation of expected impact from a drilling event are shown in Table D.36. The time frame over which the calculation is made is 10,000 years.

Inserting the values in Tables D.32 and D.36 into Equation D.23 yields cumulative releases (of ^{241}Am) from drilling events occurring over 10,000 years (see Table D.37). As stated previously, the cumulative release from a drilling event is independent of canister loading (i.e., MTE/canister, for a given canister radius), repository area, and canister spacing. Varying canister radius, however, does influence cumulative release. This is a result of the relationship between the fraction of the canister removed when contacted and the canister radius (e.g., as canister radius increases the average fraction removed tends to decrease).

Cumulative releases for all isotopes under Alternative A are presented in Table D.38. For perspective, the releases are compared to EPA release limits. All individual isotopes in Table D.38 are within their corresponding release limits. In addition, the sum of the ratios of releases for each isotope divided by its cumulative release limit is less than one.

Releases for Subcases a and b (under Alternative A) are similar to releases under the Reference Case, with the exception of Cs and Sr values. The Cs and Sr values in Alternative A (Subcases a and b) are lower than those for the Reference Case. This is due to the following: 1) approximately 99% of the prefractionated Cs and Sr is assumed to be present in the Cs/Sr waste component following separation; 2) the Cs/Sr canister is larger (e.g., 0.14-m radius) than the FHLW canister (e.g., 0.076-m radius); and 3) examination of Equation D.22 indicates that as canister radius increases cumulative release tends

TABLE D.36. Input Parameters to Drilling Event Calculations--Alternative A[a]

Waste Inventory	Subcase	MTE / Canister	kg Glass / MTE	cm^3 Glass / kg Glass	Number of Canisters	Canister Radius (m)	Canister Spacing (m)	Repository Area (km^2)[b]
Fractionated High-Level Waste (FHLW)	a	0.627	222	319	8.0×10^3	0.076	3.8	12
	b	1.45	95.8	319	3.4×10^4	0.076	4.6	7.5
	c	2.48	117	319	2.0×10^4	0.11	5.0	5.6
	d	3.63	117	319	1.4×10^4	0.13	4.5	4.3
Cs/Sr		2.64	117	319	1.7×10^4	0.14	4.7	3.0

(a) Subcase a for Alternative A defined as row 1 from FHLW + Cs/Sr row; Subcase b defined as row 2 from FHLW + Cs/Sr row; Subcase c defined as row 3 from FHLW + Cs/Sr row; Subcase d defined as row 4 from FHLW + Cs/Sr row.
(b) Areas for FHLW include shafts and other common areas in addition to waste emplacement area. Area for Cs/Sr only includes waste emplacement requirements.

TABLE D.37. Cumulative Release of ^{241}Am from Drilling Events Occurring Over 10,000 Years at a Basalt Repository--Alternative A

Inventory	Sub-Case	Canister Radius (m)	Canister Spacing (m)	Release (Ci)
Fractionated High-Level Waste (FHLW)	a	0.076	3.8	13
	b	0.076	4.6	13
	c	0.11	5.0	11
	d	0.13	4.5	10
Cs/Sr		0.14	4.7	0.01

(a) Subcase a defined as row 1 from FHLW + Cs/Sr row; Subcase b defined as row 2 from FHLW + Cs/Sr row; Subcase c defined as row 3 from FHLW +Cs/Sr row; Subcase d defined as row 4 from FHLW + Cs/Sr row.

TABLE D.38. Cumulative Releases from Drilling Events Occurring Over 10,000 Years at a Basalt Repository(a) (Ci)--Alternative A

Radionuclide	Subcases a, b	Subcase c	Subcase d	EPA(b)
^{241}Am	1.3×10^{1}	1.1×10^{1}	1.0×10^{1}	5.1×10^{2}
^{243}Am	7.7	6.3	5.9	2.1×10^{2}
^{14}C	8.2×10^{-2}	6.8×10^{-2}	6.3×10^{-2}	1.0×10^{4}
^{135}Cs	5.9×10^{-2}	5.8×10^{-2}	5.8×10^{-2}	1.0×10^{5}
^{137}Cs	2.2×10^{1}	2.1×10^{1}	2.1×10^{1}	2.5×10^{4}
^{237}Np	2.6×10^{-2}	2.2×10^{-2}	2.0×10^{-2}	1.0×10^{3}
^{238}Pu	3.4×10^{-1}	2.7×10^{-1}	2.6×10^{-1}	2.0×10^{4}
^{239}Pu	4.2×10^{-1}	3.5×10^{-1}	3.2×10^{-1}	5.0×10^{3}
^{240}Pu	3.5	2.9	2.7	5.0×10^{3}
^{242}Pu	5.1×10^{-3}	4.2×10^{-3}	3.9×10^{-3}	5.0×10^{3}
^{226}Ra	7.1×10^{-4}	5.8×10^{-4}	5.4×10^{-4}	1.6×10^{2}
^{90}Sr	1.1×10^{1}	1.1×10^{1}	1.1×10^{1}	4.0×10^{3}
^{99}Tc	3.2	2.6	2.4	1.0×10^{5}
^{126}Sn(c)	1.3×10^{-1}	1.1×10^{-1}	1.0×10^{-1}	4.0×10^{3}
^{129}I	8.7×10^{-3}	7.2×10^{-3}	6.6×10^{-3}	5.1×10^{2}

(a) Assumed Environmental Protection Agency's (EPA) first estimates of drilling rates.
(b) Based on information in EPA (1982) and assuming the 50,000 metric tons equivalent (MTE) repository contains 8.7×10^{5} Ci of alpha-emitting transuranic (TRU) waste.
(c) Did not specifically address separation efficiency relative to ^{126}Sn as part of study. Assumed all ^{126}Sn would remain in FHLW.

to decrease. Conversely, releases for the remaining isotopes under Subcases a and b, of Alternative A, are similar to Reference Case releases because these isotopes are predominately in the FHLW which has a canister radius of 0.076 m, identical to that of the Reference Case.

D.3.2.3 Alternative B

Under Alternative B, it is assumed that the entire waste inventory is placed in a geologic repository following extended storage. Ten-year-old HLW is assumed solidified, and stored on the surface for an additional 50 years prior to disposal.

Drilling rates used in Alternative B are those previously presented in Table D.32. Other input parameters used in the calculation of expected impact from a drilling event are shown in Table D.39. The time frame over which the calculation is made is 10,000 years.

TABLE D.39. Input Parameters to Drilling Event Calculation--Alternative B

Subcase	MTE / Canister	kg glass / MTE	cm^3 glass / kg glass	Number of Canisters	Canister Radius (m)	Canister Spacing (m)	Repository Area (km^2)
a	0.627	222	319	8.0×10^4	0.076	3.8	12
b	1.45	95.8	319	3.4×10^4	0.076	4.6	7.5
c	2.48	119	319	2.0×10^4	0.076	5.0	5.6
d	3.63	112	319	1.4×10^4	0.076	4.5	4.3

Inserting the values in Tables D.32 and D.39 into Equation D.23 yields cumulative releases of ^{241}Am from drilling events, occurring over 10,000 years (see Table D.40). As stated previously, the cumulative release from a drilling event (given as a fixed repository loading) is independent of canister loading (i.e., MTE/canister, for a given canister radius), repository area, and canister spacing. Varying canister radius, however, does influence cumulative release slightly, a result of the relationship between the fraction of the canister removed when contacted and the canister radius (e.g., as canister radius increases, the average fraction of the canister removed tends to decrease). The relationship between canister radius and the cumulative release is shown in Figure D.2.

TABLE D.40. Cumulative Release of ^{241}Am from Drilling Events Occurring Over 10,000 Years at a Basalt Repository--Alternative B

Subcase	Canister Radius (cm)	Canister Spacing (m)	Release (Ci)
a	7.6	3.8	13
b	7.6	4.6	13
c	11	5.0	11
d	13	4.5	10

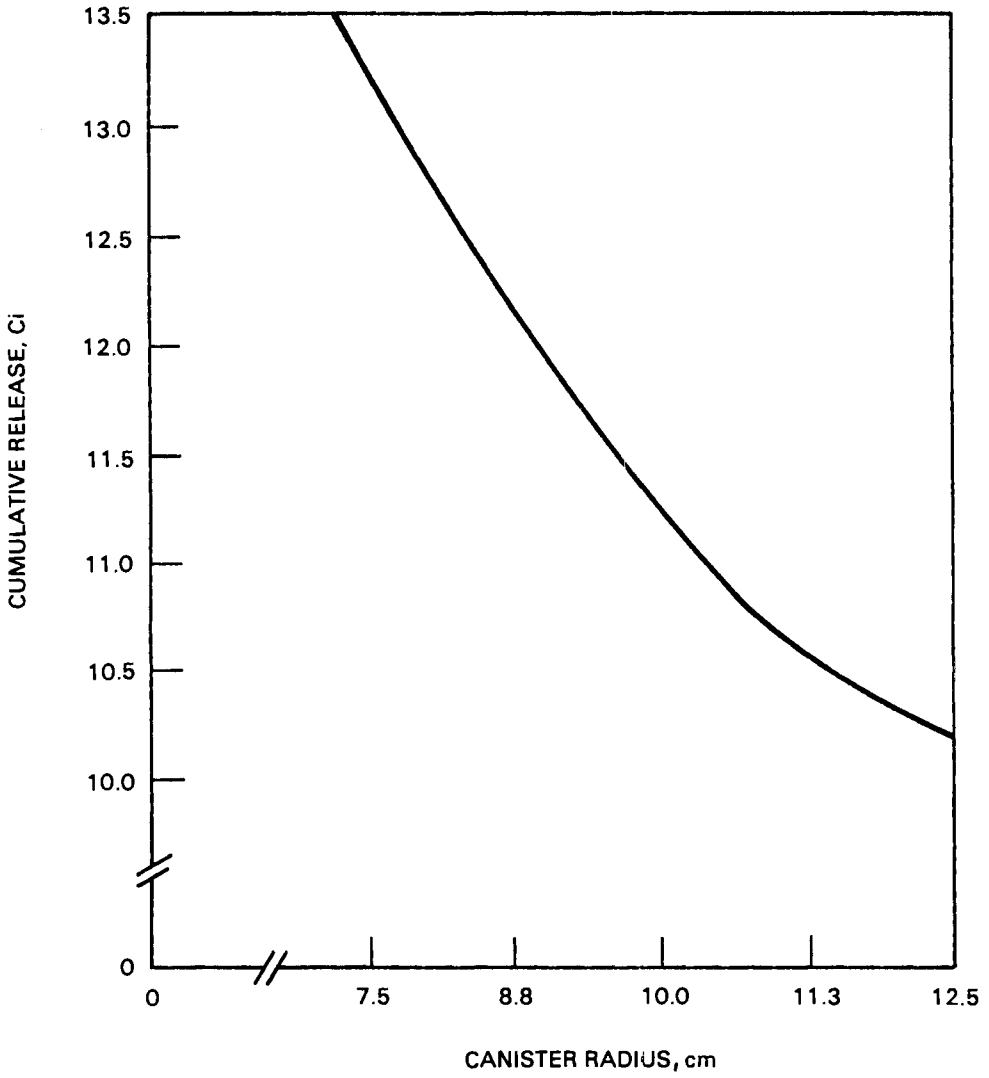

FIGURE D.2. Plot of Cumulative Release Versus Canister Radius for ^{241}Am

Cumulative releases for all isotopes are presented in Table D.41. As expected, the other isotopes exhibit the same release to canister radius relationship as does ^{241}Am. For perspective, these releases are compared to EPA release limits. All individual isotopes in Table D.41 are within their corresponding release limits. In addition, the sum of the ratio of releases for each isotope divided by its cumulative release limit is less than one.

TABLE D.41. Cumulative Releases from Drilling Events Occurring Over 10,000 Years at a Basalt Repository[a] (Ci)--Alternative B

Radionuclide	Subcases a, b	Subcase c	Subcase d	EPA[b]
^{241}Am	1.3×10^{1}	1.1×10^{1}	1.0×10^{1}	5.1×10^{2}
^{243}Am	7.7	6.3	5.9	2.1×10^{2}
^{14}C	8.2×10^{-2}	6.8×10^{-2}	6.3×10^{-2}	1.0×10^{4}
^{135}Cs	7.7×10^{-2}	6.3×10^{-2}	5.9×10^{-2}	1.0×10^{5}
^{137}Cs	2.8×10^{1}	2.3×10^{1}	2.2×10^{1}	2.5×10^{4}
^{237}Np	2.6×10^{-2}	2.2×10^{-2}	2.0×10^{-2}	1.0×10^{3}
^{238}Pu	3.4×10^{-1}	2.8×10^{-1}	2.6×10^{-1}	2.0×10^{4}
^{239}Pu	4.2×10^{-1}	3.5×10^{-1}	3.2×10^{-1}	5.0×10^{3}
^{240}Pu	3.5	2.9	2.7	5.0×10^{3}
^{242}Pu	5.2×10^{-3}	4.2×10^{-3}	3.9×10^{-3}	5.0×10^{3}
^{226}Ra	7.1×10^{-4}	5.8×10^{-4}	5.4×10^{-4}	1.6×10^{2}
^{90}Sr	1.5×10^{1}	1.2×10^{1}	1.1×10^{1}	4.0×10^{3}
^{99}Tc	3.2	2.6	2.4	1.0×10^{5}
^{126}Sn	1.3×10^{-1}	1.1×10^{-1}	1.0×10^{-1}	4.0×10^{3}
^{129}I	8.7×10^{-3}	7.2×10^{-3}	6.6×10^{-3}	5.1×10^{2}

(a) Assume Environmental Protection Agency's (EPA) first estimates of drilling rates.
(b) Based on information in EPA (1982) and assuming the 50,000 metric tons equivalent (MTE) repository contains 8.7×10^{5} Ci of alpha-emitting transuranic (TRU) waste.

Releases for Subcases a and b (under Alternative B) are similar to releases under the Reference Case. This is because separating or fractionating wastes into components should not affect the expected release[a] of waste from a repository as a result of multiple random events. Releases for Subcases a through d (under Alternative B) are similar to releases for Subcases a through d (under Alternative A), with the exception of Cs and Sr values. As mentioned previously, the larger the canister radius, the smaller the average fraction of canister removed to the surface, and the smaller the cumulative release. The Cs/Sr canister has a larger radius than the aged-HLW canisters and, therefore, release of Cs and Sr under Alternative B would be expected to exceed that under Alternative A.

(a) Expected release is used here in the same manner "expected value" is used in statistics. Expected release is the mathematical product of the likelihood of an event occurring multiplied by the consequences of occurrence.

REFERENCES

Altenhofen, M. K. 1981. Waste Package Heat Transfer Analysis: Model Development and Temperature Estimates for Waste Packages in a Repository Located in Basalt. RHO-BWI-ST-18, Rockwell Hanford Operations, Richland, Washington.

Bechtel National, Inc. 1979. National Waste Terminal Storage - Conceptual Reference Repository Description. ONWI/SUB/79/E512-01600.16. Prepared for the Office of Nuclear Waste Isolation by Battelle-Columbus Laboratories, Columbus, Ohio.

Brown, R. W. 1980. Standardized Repository and Encapsulation Facility Cost Estimates for Comparative Evaluation and Pricing Study. ONWI-110. Prepared for the Office of Nuclear Waste Isolation by Battelle-Columbus Laboratories, Columbus, Ohio.

Clark, L. L., et al. 1983. RECON: A Computer Program for Analyzing Repository Economics. PNL-4465, Pacific Northwest Laboratory, Richland, Washington.

Crane, R. A., and R. I. Vachon. 1977. "A Prediction of the Bounds on the Effective Thermal Conductivity of Granular Materials." Int. J. of Heat and Mass Transfer. 20:711-723.

Daling, P. M. 1983. Analysis of Near-Term Spent Fuel Transportation Hardware Requirements and Transportation Costs. PNL-4575, Pacific Northwest Laboratory, Richland, Washington.

Dove, F. H., et al. 1982. AEGIS Technology Demonstration for a Nuclear Waste Repository in Basalt. PNL-3632, Pacific Northwest Laboratory, Richland, Washington.

Eckert, E. R. G., and R. M. Drake, Jr. 1972. Analysis of Heat and Mass Transfer. pp. 535-541. McGraw-Hill, New York.

Exxon Nuclear Company, Inc. 1978. Final Report for Study of the Separation and Recovery of Select Radioisotopes from Commercial Nuclear Fuel Wastes. Richland, Washington.

Hebert, J. A., et al. 1978. Non-Technical Issues in Waste Management: Ethical, Institutional, and Political Concerns. PNL-2400, Battelle Human Affairs Research Centers, Seattle, Washington.

Hill, O. F., et al. 1981. Preconceptual Design Study for Solidifying High-Level Waste: Appendices A, B, C, West Valley Demonstration Project. DOE/TIC-11433, PNL-3608-2, Pacific Northwest Laboratory, Richland, Washington.

Kuehn, T. H., and R. J. Goldstein. 1973. "An Experimental Study of Natural Convection Heat Transfer in Concentric and Eccentric Horizontal Cylinderical Annuli." J. Heat Transfer. 100:635-640.

Kuehn, T. H., and R. J. Goldstein. 1976a. "An Experimental and Theoretical Study of Natural Convection in the Annulus Between Horizontal Concentric Cylinders." J. Fluid Mechanics. 74:695-719.

Kuehn, T. H., and R. J. Goldstein. 1976b. "Correlating Equations for Natural Convection Heat Transfer Between Horizontal Circular Cylinders." Int. J. Heat Mass Transfer. 19:1127-1134.

Kwon, S. S., T. H. Kuehn and T. S. Lee. 1982. "Natural Convection in the Annular Between Horizontal Circular Cylinders With Three Arial Spacers." Trans. ASME. 104:118-124.

McCallum, R. F., et al. 1982. Waste Mixes Study for Space Disposal. ONWI-422, Office of Nuclear Waste Isolation, Columbus, Ohio.

McCann, R. A. 1980. HYDRA-I: A Three-Dimensional Finite Difference Code for Calculating the Thermal Hydraulic Performance of a Fuel Assembly Contained Within a Canister. PNL-3367, Pacific Northwest Laboratory, Richland, Washington.

Mendel, J. E., et al. 1981. A State of the Art Review of Materials Properties of Nuclear Waste Forms. PNL-3802, Pacific Northwest Laboratory, Richland, Washington.

Northrup, C. J., L. J. Jardine and M. J. Steindler. 1982. "An Alternate Strategy for Commercial High-Level Radioactive Waste Management." IAEA Symposium on the Conditioning of Radioactive Wastes for Storage and Disposal, Utrecht, the Netherlands, 21-25 June 1982.

Parsons, Brinkerhoff, Quade and Douglas (PBQ&D). 1978. Technical Support for GEIS: Radioactive Waste Isolation in Geologic Formations. Y/OMI/TM-36, Vol. 18. Prepared for and available from the U.S. Department of Energy, Washington, D.C.

Peterson, P. L., and R. E. Rhoads. 1978. Conceptual Design of a Shipping Container for Transporting High-Level Waste by Railroad. PNL-2244, Pacific Northwest Laboratory, Richland, Washington.

Platt, A. M., and E. A. Eschbach. 1981. "Rethinking the Management of High-Level Nuclear Waste: The Need for Fractionation." Proceedings, Waste Management '81, ANS Topical Meeting, Tuscon, Arizona.

Projahn, U., H. Reiger and H. Beer. 1981. "Numerical Analysis of Laminar Natural Convection Between Concentric and Eccentric Cylinders." Numerical Heat Transfer. 4:131-146.

Scientific Applications, Inc. 1978. Technical Support for GEIS: Radioactive Waste Isolation in Geologic Formation. Vol. 19, Thermal Analysis, Y/OWI/TM-36119. Oak Ridge, Tennessee.

Slate, S. C., W. A. Ross and W. L. Partain. 1981. Reference Commercial High-Level Waste Glass and Canister Definition. PNL-3838, Pacific Northwest Laboratory, Richland, Washington.

Sweet, J. N., and J. E. McCreight. 1980. Thermal Conductivity of Rocksalt and Other Materials. SAND-79-1665, Sandia National Laboratory, Albuquerque, New Mexico.

Taylor, R. E., H. Groot and R. L. Shoemaker. 1979. Thermophysical Properties of Glass - A Report to Battelle Pacific Northwest Labs. TPRL-191, School of Mechanical Engineering, Purdue University, West Lafayette, Indiana.

Thadani, M. 1980. A Depth Optimization Study for Geologic Isolation of Radioactive Wastes. PNL-3079, Prepared by Teknekron, Inc., for Pacific Northwest Laboratory, Richland, Washington.

U.S. Department of Energy. 1979a. Technology for Commercial Radioactive Waste Management. DOE/ET-0028, Washington, D.C.

U.S. Department of Energy. 1979b. Environmental Aspects of Commercial Radioactive Waste Management. DOE/ET-0029, Washington, D.C.

U.S. Department of Energy. 1980. Final Environmental Impact Statement - Management of Commercially Generated Radioactive Waste. DOE/EIS-0046F, Washington, D.C.

U.S. Department of Energy. 1981. The Monitored Retrievable Storage Concept. DOE/NE-0019, Washington, D.C.

U.S. Department of Energy. 1982. National Plan for Siting High-Level Radioactive Waste Repositories and Environmental Assessment. DOE/NWTS-4 and DOE/EA-151, Public Draft, Office of NWTS Integration, Battelle Memorial Institute, Columbus, Ohio.

U.S. Environmental Protection Agency. 1980. Technical Support of Standards for High-Level Radioactive Waste Management. EPA 520/4-79-007D, Washington, D.C.

U.S. Environmental Protection Agency. 1982. Environmental Standards and Federal Radiation Protection Guidance for Management and Disposal of Spent Nuclear Fuel, High-Level and Transuranic Radioactive Wastes. (Working Draft No. 21). Washington, D.C.

U.S. Nuclear Regulatory Commission. 1981a. Code of Federal Regulations. Title 10, Part 20, "Standards for Protection Against Radiation," Appendix, Table II, Washington, D.C.

U.S. Nuclear Regulatory Commission. 1981b. Code of Federal Regulations. Title 10, Part 60, "Disposal of High-Level Radioactive Wastes in Geologic Repositories," Washington, D.C.

Wallace, R. W., et al. 1980. Topical Report on Release Scenario Analysis of Long-Term Management of High-Level Defense Waste at the Hanford Site. PNL-3363, Pacific Northwest Laboratory, Richland, Washington.

Westinghouse Electric Corporation. 1981a. Engineered Waste Package Conceptual Design: Defense High-Level Waste (Form 1), Commercial High-Level Waste (Form 1), and Spent Fuel (Form 2) Disposal in Basalt. AESD-TME-3113, Westinghouse Electric Corporation, Pittsburgh, Pennsylvania.

Westinghouse Electric Corporation. 1981b. Engineered Waste Package Conceptual Design: Defense High-Level Waste (Form 1), Commercial High-Level Waste (Form 1), and Spent Fuel (Form 2) Disposal in Salt. AESD-TME-3131. Westinghouse Advanced Energy Systems Division, Pittsburgh, Pennsylvania.

DISTRIBUTION

No. of Copies

OFFSITE

27 DOE Technical Information Center

2 Division of Waste Management
U.S. Nuclear Regulatory Commission
Washington, D.C. 20555
ATTN: J. B. Martin
R. F. Cook

3 Office of Waste Disposal and Remedial Action
U.S. Department of Energy
Washington, D.C. 20545
ATTN: W. W. Ballard
F. E. Coffman
J. R. Coleman

4 Office of Defense Waste and Byproducts Management
U.S. Department of Energy
Washington, D.C. 20545
ATTN: J. J. Jicka
G. K. Oertel
W. C. Remini
G. H. Daly

2 Plans and Evaluations Division
Office of Nuclear Energy
U.S. Department of Energy
Washington, D.C. 20545
ATTN: J. P. Thereault
E. F. Mastal

K. O. Laughon
Office of Spent Fuel Management and Reprocessing Systems
U.S. Department of Energy
Washington, D.C. 20545

Raymond Cooperstein
Office of Environmental Protection, Safety and Emergency Preparedness
U.S. Department of Energy
Washington, D.C. 20545

No. of Copies

4 Nuclear Waste Policy Act Project Office
U.S. Department of Energy
Washington, D.C. 20545
ATTN: C. R. Cooley
D. Z. Kaufman
J. W. Bennett
M. J. Lawrence

J. Neff
U.S. Department of Energy
Columbus Program Office
505 King Avenue
Columbus, OH 43201

3 Oak Ridge National Laboratory
P.O. Box Y
Oak Ridge, TN 37820
ATTN: K. Notz
T. Low
J. O. Blomeke

K. R. Braziel
Los Alamos Scientific Laboratory
P.O. Box 1663
Los Alamos, NM 87544

T. B. Hindman
DOE Savannah River Operations Office
P.O. Box A
Aiken, SC 29801

2 DOE Oak Ridge Operations Office
P.O. Box E
Oak Ridge, TN 37830
ATTN: S. Ahrends
D. E. Large

No. of Copies

3 DOE Albuquerque Operations Office
P.O. Box 5400
Albuquerque, NM 87185
ATTN: R. Y. Lowrey
D. T. Schueler
K. Carlson

J. B. Whitsett
DOE Idaho Operations Office
550 2nd Street
Idaho Falls, ID 83401

S. A. Mann
DOE Chicago Operations Office
Crystalline Rock Project Office
9800 South Cass Avenue
Argonne, IL 60439

D. L. Veith
DOE Nevada Operations Office
Las Vegas, NV 89114

3 Allied-General Nuclear Services
P.O. Box 847
Barnwell, SC 29812
ATTN: J. A. Buckham
W. L. Godfrey
A. K. Williams

2 Argonne National Laboratory
9700 South Cass Avenue
Argonne, IL 60439
ATTN: M. J. Steindler
L. E. Trevorrow

3 Battelle Memorial Institute
Office of Crystalline Repository Development
505 King Avenue
Columbus, OH 43201
ATTN: T. L. Anderson
M. Kehnemuyi
W. M. Pardue

No. of Copies

6 Battelle Memorial Institute
Office of Nuclear Waste Isolation
505 King Avenue
Columbus, OH 43201
ATTN: S. H. Basham
W. Carbiener
J. O. Duguid
S. Goldsmith
P. L. Hofmann
Beverly Rawles

R. E. De Wames
Rockwell International
8900 DeSoto Avenue
Canoga Park, CA 91304

2 E. I. du Pont de Nemours Company
Savannah River Laboratory
Aiken, SC 29801
ATTN: J. L. Crandall
E. J. Hennelly

R. Williams
Electric Power Research Institute
3412 Hillview Avenue
P.O. Box 10412
Palo Alto, CA 94304

George Dix
266619 Haney Avenue
Damascus, MD 20750

R. K. Brown
Westinghouse Electric Corp.
Advanced Energy Systems Div.
WIPP Library
P.O. Box 40039
Albuquerque, NM 87196

2 Lawrence Livermore Laboratory
P.O. Box 808
Livermore, CA 94550
ATTN: J. H. Campbell
W. G. Sutcliff

No. of Copies

3 Sandia Laboratories
Albuquerque, NM 87185
ATTN: D. R. Anderson
C. J. Northrup
W. Weart

R. G Post
College of Engineering
University of Arizona
Tucson, AZ 85721

W. Tope
Westinghouse Electric Corp.
Mail Stop 23
Box 3912
Pittsburgh, PA 15230

Technological Assessment Division
Office of Radiation Programs
U.S. Environmental Protection Agency
Washington, D.C. 20460

2 Roy F. Weston Associates
2301 Research Blvd.
Rockville, MD 20850
ATTN: A. Metry
E. J. Ziegler

R. Roy
202 Materials Research Laboratory
University Park, PA 16802

F. K. Pittman
3508 Sagecrest Terrace
Ft. Worth, TX 76106

W. Hannum
DOE West Valley Demonstration Project Office
West Valley, NY 14171

J. L. Knabenschuh
West Valley Nuclear Services
West Valley, NY 14171

No. of Copies

ONSITE

6 DOE Richland Operations Office

P. F. X. Dunigan, Jr.
O. J. Elgert
O. L. Olson
H. E. Ransom
J. J. Schreiber
M. W. Shupe

10 Rockwell Hanford Operations

M. K. Altenhofen
H. Babad
R. A. Deju/R. J. Gimera
L. R. Fitch
R. N. Gurley/R. T. Wilde
M. J. Smith
D. A. Turner
B. A. Wolfe
T. Woods
J. W. Patterson

Westinghouse Hanford Company

A. G. Blasewitz/R. E. Lerch

55 Pacific Northwest Laboratory

W. F. Bonner
L. A. Bray
J. B. Brown
T. D. Chickalla
L. L. Clark
P. M. Daling
D. A. Dingee
H. K. Elder
E. A. Eschbach
V. F. Fitzpatrick
R. M. Fleischman
C. R. Hann
J. H. Jarrett/D. J. Bradley
D. E. Knowlton
M. R. Kreiter/J. M. Latkovitch

No. of
Copies

ONSITE (contd)

Pacific Northwest Laboratory (contd)

D. E. Larson
R. C. Liikala/J. L. McElroy
R. F. McCallum
R. W. McKee (10)
G. B. Mellinger/H. H. Hollis
J. E. Mendel
J. E. Minor
R. E. Nightingale
D. R. Payson
A. M. Platt (2)
J. V. Robinson (2)
W. A. Ross
K. J. Schneider
D. J. Silviera
J. L. Swanson
G. L. Tingey/G. A. Jensen
D. S. Trent
R. P. Turcotte
H. H. Van Tuyl
M. K. White/G. W. McNair
L. E. Wiles
L. D. Williams
Technical Information (5)
Publishing Coordination (2)